3-20-2008

Three Models of Anthrax Toxin Effects on the MAP-Kinase Pathway and Macrophage Survival

Daniel J. Schneider

THREE MODELS OF ANTHRAX TOXIN EFFECTS ON THE MAP-KINASE PATHWAY AND MACROPHAGE SURVIVAL

THESIS

Daniel J. Schneider, Captain, USAF, BSC

AFIT/GIH/ENV/08-M02

DEPARTMENT OF THE AIR FORCE
AIR UNIVERSITY
AIR FORCE INSTITUTE OF TECHNOLOGY

Wright-Patterson Air Force Base, Ohio

AFIT/GIH/ENV/08-M02

THREE MODELS OF ANTHRAX TOXIN EFFECTS ON THE MAP-KINASE PATHWAY AND MACROPHAGE SURVIVAL

THESIS

Presented to the Faculty

Department of Systems and Engineering Management

Graduate School of Engineering and Management

Air Force Institute of Technology

Air University

Air Education and Training Command

In Partial Fulfillment of the Requirements for the

Degree of Master of Science in Industrial Hygiene

Daniel J. Schneider, BS

Captain, USAF, BSC

March 2008

AFIT/GIH/ENV/08-M02

THREE MODELS OF ANTHRAX TOXIN EFFECTS ON THE MAP-KINASE PATHWAY AND MACROPHAGE SURVIVAL

Daniel J. Schneider, BS
Captain, USAF, BSC

Approved:

//signed//	20 March 2008
Major Jeremy Slagley (Chairman)	Date
//signed//	20 March 2008
Dr. Peter Robinson (Member)	Date
//signed//	20 March 2008
Dr. Charles Bleckmann (Member)	Date

AFIT/GIH/ENV/08-M02

Abstract

Lethal factor (LF), a component of anthrax toxin, is the primary virulence factor that allows *Bacillus anthracis* to evade the immune response by blocking the activation of mitogen-activated protein kinase (MAPK) enzymes. This research modifies three published MAPK models to reflect this signal inhibition and to estimate a first-order reaction rate by fitting the models to published viability data for two macrophage cell lines cultured with the LF-producing *Bacillus anthracis*-Vollum1B strain. One model appears to be ill-suited for this purpose because not all relevant MAPK components could be integrated into the inhibition equations. Despite different underlying parameters and values, the remaining two models display consistent behavior, due to the highly conserved signal pathway structure, and provide approximately equal rate constants and measures of the relative sensitivity between cell lines. The results demonstrate model robustness and an ability to guide experimental design toward quantifying the LF reaction rate and estimating the sensitivity of human alveolar macrophages. The models serve as a first step toward an inhalation dose-response model and, by providing a measure of differential susceptibility, can lend increased confidence in extrapolation between cell types *in vitro* or between species *in vivo*.

To my wife,

To our children,

To the moon and back.

Acknowledgments

I want to acknowledge the assistance and never-ending patience of my advisor, Major (Dr.) Jeremy Slagley, who has been persistently positive and a true academic enthusiast through the full term of this graduate program and the thesis process. My gratitude is also extended to Dr. Peter Robinson, who introduced me to this subject, eagerly 'took me in,' and listened patiently as a novice struggled to piece the toxicology and biochemistry together. To Dr. Charles Bleckmann, thank for your instruction over the last year and a half and for helping me bridge the gap between chemistry and biology. I am eternally thankful to my wife – my high school sweetheart and my best friend – for her love, support and constant encouragement and, though she seems unaware that she possesses it, for her strength which has provided us with four brilliant children, moved us all over the world, and sustained our family each day. Thank you for enduring the long days and late nights here and throughout our time in the Air Force. I am grateful to my children for helping me play when I needed it and for their constant prayers that "daddy will get his work done." Finally, I would like to thank my father, a 1972 AFIT graduate, and my mother for their support while our family has been back home in Ohio.

Daniel J. Schneider

Table of Contents

Page

List of Figures

Figure Page

List of Tables

THREE MODELS OF ANTHRAX TOXIN EFFECTS ON
THE MAP-KINASE PATHWAY AND MACROPHAGE SURVIVAL

I. Introduction

Motivation

Centuries before the role of pathogenic microorganisms was discovered, the impact of disease on a community was well understood by those wishing to kill and demoralize an enemy. In the mid-fourteenth century, forces surrounding the walls of Caffa, a coastal city on the Crimean Sea, suddenly took heavy losses from plague and, hoping "that the intolerable stench would kill everyone inside," began catapulting the "mountains" of victims into the city (Derbes, 1966:180; Wheelis, 2002:973). After enduring three years of siege, the defenders were quickly overcome by pestilence and fled by sea; their destination ports became the initial sites of the Black Death that killed over one quarter of Europe in just six months (Derbes, 1966:181-182). Despite occurring 600 years ago, the Great Plague remains the public's ideation of a pathogen's potential for devastation. The anthrax letters that infected 23 and killed 5 in late 2001 (USAMRIID, 2005:10) and continuous news reports about severe acute respiratory syndrome (SARS), avian flu pandemic, and weapons of mass destruction (WMD) have heightened public awareness of the threat posed by microorganisms. Motivated by this threat, this research aims to advance knowledge of inhalational anthrax pathogenesis by developing a model of a critical biomolecular reaction exerted by anthrax toxin on alveolar macrophages.

Biological Weapons History and Increasing Threat.

The biological weapons threat is very real. Japan had an aggressive research program during World War II that included disseminating plague infected fleas from aircraft, causing epidemics in villages in China and Manchuria (USAMRIID, 2005:4). According to a 1994 study by Meselson, as relayed by U.S. Army Medical Research Institute for Infectious Diseases (USAMRIID), "an accidental aerosol release" of anthrax spores from a Soviet military facility in 1979 caused "66 fatalities in the 77 patients identified" in Sverdlovsk, the town downwind from the compound (USAMRIID, 2005:7). Under United Nations scrutiny in 1991, Iraq confirmed running an extensive offensive bio-weapons program; over 6,500 liters of anthrax and 11,500 liters of toxins had been loaded into munitions and deployed throughout Iraq earlier that year (USAMRIID, 2005:8). Today "at least 17 nations are believed to have offensive biological weapons programs" (Inglesby and others, 1999:1736), but the modern biological weapons threat does not come only from nation states with established laboratories.

Examples of terrorists using or planning to use biological weapons are recorded with increasing frequency over the last 25 years. In 1984 the Rajneeshee cult sprayed salmonella on food in Oregon restaurants in an attempt to influence local elections (Shea, 2004:CRS-2). Aum Shinrikyo gained notoriety by attacking Tokyo subways with sarin nerve agent, killing 12 and injuring over 6,000 (Cronin, 2003:CRS-1). Investigation also revealed at least eight unsuccessful anthrax and botulism aerosol attacks in the streets of Tokyo from 1993 to 1995 (Inglesby and others, 1999:1736; USAMRIID, 2005:10). The anthrax mail attacks in the U.S. brought the threat into sharp focus and resulted in

increased biodefense efforts by law enforcement and public health agencies across the United States and perhaps the world. Subsequently, authorities thwarted a terrorist cell's plan to put cyanide in the water supply to the U.S. Embassy in Rome in 2002 (Cronin, 2003:CRS-4). Between January 2003 and February 2004, "terrorist plots to use ricin were uncovered in England," and "ricin was found in a South Carolina postal facility…and in the Dirksen Senate Office building in Washington, D.C." (USAMRIID, 2005:11). These examples are only a few of the bio-terror incidents in recent years.

Reasons for this increased usage are addressed in *Terrorist Motivations for Chemical and Biological Weapons Use: Placing the Threat in Context*, a March 2003 Congressional Research Service (CRS) Report For Congress by Audrey Kurth Cronin, a terrorism expert for the CRS. The terrorist chemical and biological weapons (CBW) threat has increased because the "internationalization of terrorism" has all but erased the moral and political boundaries observed by *traditional* terrorists like the Irish Republican Army (IRA) and the Basque National Party in Spain (Cronin, 2003:CRS-3). Religious militants are willing to kill large numbers of "heretics or infidels" and sacrifice their own members, such as by suicide bombing in public gathering areas (Cronin, 2003:CRS-3). Unconventional weapons, information and expertise are more available due to unaccounted-for former Soviet program assets (and possibly Iraqi assets). Finally, terrorists have demonstrated "clear indications of interest in CBW," such as when Osama bin Laden "spoke of acquiring weapons of mass destruction being a 'religious duty'" and when al Qaeda dedicated a volume to producing CBW in the "Encyclopedia of Jihad" (Cronin, 2003:CRS-3–CRS-4). USAMRIID's *Medical Management of Biological*

Casualties Handbook, commonly known as *The Blue Book*, aptly emphasizes to medical providers that the reality of the threat should not be eschewed:

> The threat of the use of biological weapons against U.S. military forces and civilians is more acute than at any time in U.S. history, due to the widespread availability of agents,…knowledge of production methodologies, and potential dissemination devices. …Therefore, awareness of and preparedness for this threat…is vital to our national security. (USAMRIID, 2005:12)

Anthrax Threat.

Anthrax is a zoonotic disease caused by *Bacillus anthracis* (BA), a gram-positive, encapsulated, rod-shaped bacterium (USAMRIID, 2005:34; Heymann, 2004:20). BA exists in the environment in a metabolically inactive spore form, which results when nutrients are no longer available and which, unlike vegetative bacteria, lead to disease upon bodily uptake (Liu and others, 2004:164). Layers form an "armored external shell," depicted in Figure 1, to protect the dormant bacterium in the core where the DNA is preserved in a crystalline form for later reanimation by rehydration (Driks, 2003). While active bacteria survive only briefly outside a host or for 24 hours in water (Inglesby and others, 1999), the shell layers protect the spore from changes in humidity, temperature, and pH, solar radiation, and other environmental conditions for decades or possibly longer (Driks, 2003; Nicholson and others, 2000). BA spores germinate in a moist, nutrient-rich environment like the human body; then the vegetative bacteria multiply rapidly and cause anthrax disease in three unique forms: cutaneous, gastrointestinal, and inhalational. Cutaneous anthrax occurs naturally among those working with animals or their skins and has a mortality rate of less than 1% when treated (USAMRIID, 2005:36). Insufficiently cooked meat from infected animals can cause rare cases of gastrointestinal

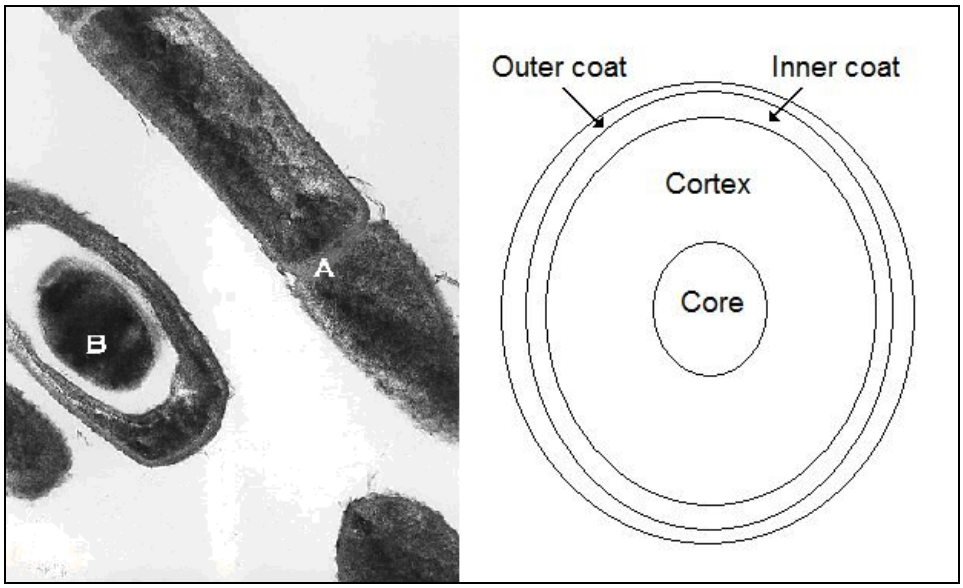

Figure 1: Image of *Bacillus anthracis* by transmission electron micrograph, showing cell division (A) and spore (B), left (http://phil.cdc.gov/phil/bt.asp, photo ID #1813); and detail of protective layers of a *Bacillus* spore, right (after Driks, 2003).

anthrax, which may result in pharyngeal ulcers or flu-like symptoms that can progress to sepsis, resulting in a high mortality rate of 50%. Because spores can be dispersed in an aerosol and because mortality may reach 85% with treatment, inhalational anthrax is the "primary concern for intentional infection" in humans (USAMRIID, 2005:36-37). The ability of a naturally occurring disease to cause such high morbidity and mortality is not sufficient for a disease to be suitable for use as a biological warfare agent.

For application as a bio-warfare agent, a microorganism must also be able to be mass produced, be stable enough to survive dissemination and the environment, and be reasonably quick to cause disease or death; and the resultant disease must be preventable or treatable (van Aken and Hammond, 2003:S58). The latter requirement applies primarily to a nation state using bioagents against an enemy while not wanting to harm

friendly forces. However, this requirement may not apply to modern terrorist groups willing to sacrifice their own people and cross international borders to conduct the attack far from home, where risk to their countrymen is reduced. Regarding the four other requirements, "anthrax is of course the first choice because the causative agent, *B anthracis*, fulfils nearly all of these specifications," where the only specification not met is in the ability to successfully treat anthrax victims "even several days after infection" (van Aken and Hammond, 2003:S58). However, the 2001 anthrax letters did not have a large quantity or a technical dissemination device; though a slow-acting pathogen, the covert nature of the attacks resulted in delayed diagnosis and widespread fear. Law enforcement, laboratories, and the military have embarked on developing greater defense against such terrorist attacks.

In an effort to prioritize biodefense efforts, CDC led a risk assessment of sixteen potential bioagents. Anthrax ranked higher than or equal to the other threat agents in five of the six categories: infection rate, death rate, ease of production and dissemination, public perception of risk, and need for specialized planning and logistical preparations. Only smallpox was given higher priority due to a maximum score in the sixth category of person-to-person transmissibility, whereas anthrax received a score of zero because anthrax is not communicable between people (Rotz and others, 2002). A significant number of lives would still be lost from a large scale anthrax attack. The dissemination of 100 kg of weaponized anthrax outside a major metropolitan area such as Washington D.C. could result in 130,000 to 3,000,000 deaths, where the numbers increase with dissemination under more ideal weather conditions (OTA, 1993:54). Comparatively, the

combined deaths from the World War II fire bombing of Tokyo, Japan and Dresden, Germany was approximately 300,000 (OTA, 1993:2). A major anthrax attack would equal or surpass the lethality of a one megaton (TNT-equivalent) hydrogen bomb and dwarf a 1,000-kilogram sarin attack by three orders of magnitude (OTA, 1993:53). The significant public health risks, when combined with increased threat, motivate microbiological research to better elucidate the pathogenesis of inhalational anthrax and to identify biomolecular mechanisms that may lead to advances in defense or treatment.

Background

Intracellular Signaling and Anthrax Toxin.

Just as some multicellular organisms use hormones to signal between organs and systems to trigger growth, reproductive development, or metabolic changes, all eukaryotic cells use highly-selective, internal signaling pathways to implement proliferation, differentiation, movement, enzymatic changes, gene expression, or cell death (Downward, 2001:759). This intracellular communication network is extremely complicated, like a three-dimensional, interdependent and interactive spider web of biochemical relationships spanning the cytoplasm between the cell membrane and the nucleus. An alveolar macrophage (AM) is a highly phagocytic leukocyte serving as the innate immune system's first-responder, responsible for clearing the lungs of respired particles, for recruiting other immune cells, and for triggering antibody (Ab) production by stimulating lymphocytes (Dörger and Krombach, 2002:47). (Terms like leukocyte, antibody and lymphocyte, as well as acronyms and abbreviations like AM, are defined in Appendix A.) An AM is dependent on its internal molecular communication network for

up- and down-regulating gene expression that mediates macrophage activation, defensive factors, inflammation, and apoptosis, to facilitate combating an infection. Recent research shows that interruption of critical signal transduction pathways changes the macrophage and immune system responses and allows the survival of many pathogens: *Brucella abortus*, a bacterium that causes brucellosis (Jarvis and others, 2002:7162); *Leishmania donovani*, a parasitic protozoan that causes leishmaniasis (Junghae and Raynes, 2002:5034); all three pathogenic *Yersinia* species of bacteria (Zhang and others, 2005:7946-7948); *Plasmodium falciparum*, the parasite that causes malaria (Zhu, Krishnegowda and Gowda, 2005:8623); and the biological threat agent *Bacillus anthracis* (Park and others, 2002:2048).

In inhalational anthrax, aerosolized spores are respired into the alveoli of the lungs, where vigorously phagocytic alveolar macrophages (AM) rapidly ingest the foreign particles. Normally the key executor of early bactericidal action, the AM instead serves as the primary site of the BA spore's germination into a vegetative bacterium (Guidi-Rontani and others, 1999:13). The reanimated bacterium must quickly begin to produce anthrax toxin (AT) to suppress the macrophage's production of cytotoxic reactive oxygen intermediates and of cytokines, proteins that would recruit additional innate and adaptive immune cells to the site of infection (Guidi-Rontani, 2001:935; Chakrabarty and others, 2006:4430). AT is composed of three parts: protective antigen (PA), lethal factor (LF) and edema factor (EF). The binding of a factor with PA results in the correlating toxin, lethal toxin (LF + PA = LT) or edema toxin (EF + PA = ET). PA binds to receptors on cell membranes and forms a complex with LF and EF; the complex is then endocytosed

into the cytosol (Park and others, 2002:2048; Singh and others, 1999:1857-1858). ET increases the cytoplasmic concentration of cyclic adenosine monophosphate (cAMP), which causes the edema (Leppla, 1991:3164). The critical mechanism is the interruption of the cell's signal network when LF, a proteinase, cleaves enzymes in one of the most common (and most frequently studied) signal path families, the mitogen-activated protein kinase (MAPK) cascade. By eliminating intermediate enzymes in a series of enzyme activations, LF prevents downstream enzymes' activation (the signal output), inhibiting subsequent nuclear transcriptions required for normal immune response and facilitating programmed cell death (Park and others, 2002:2048). Decades of in vitro and in vivo studies were supported by a study in which mice were injected with BA clones able to produce only two of the three toxin components; the results "strongly suggest that LF in combination with PA is the key virulence factor" (Pezard, 1991:3476). However, *in vivo* exposure to LT alone is not equivalent to inhalational anthrax due to the difference in immune response mechanisms for injected toxin and inhaled spores.

The macrophage, called a Trojan horse in many journal articles, plays a prominent role in anthrax pathogenesis. Macrophages transport BA from the alveoli, through the mucosal layer that typically bars direct bacterial penetration, and to the mediastinal lymph nodes between the lungs (Guidi-Rontani, 2002:407). The bacteria proliferate, cause lymphadenopathy for which chest a x-ray will show characteristic widened mediastinum (see Figure 2), and cross into the bloodstream, causing respiratory distress, septicemia, shock, and death (USAMRIID, 2005:37). The macrophage has been implicated in toxicity even in the absence of bacteria. For undetermined reasons, mice depleted of their

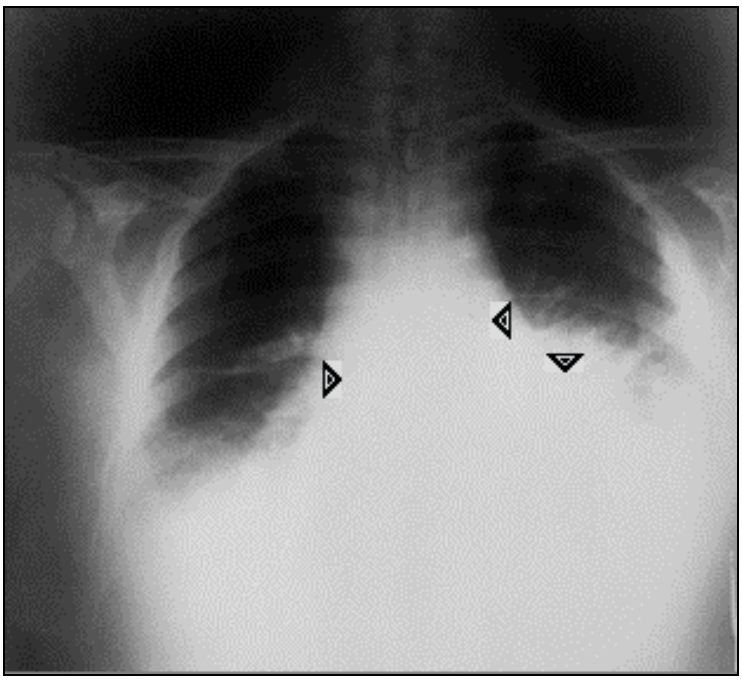

Figure 2: Chest radiograph of inhalational anthrax victim, 22 hours before death (modified from CDC, http://phil.cdc.gov/phil/bt.asp, photo ID #1118)

macrophages before injection with a lethal dose of LT were resistant to the toxin (Hanna and others, 1993:10199). By inhibiting MAPK signaling, BA turns the macrophage's activation signal into "a trigger of rapid cell death," meaning no active macrophages "alert the remainder of the immune system to the presence of the pathogen" (Park and others, 2002:2051). An understanding of macrophage MAPK inhibition by LF and the resultant effects is critical to advancing anthrax treatment and biodefense research. The dynamic nature of the host-pathogen system demands a dynamic investigation method.

Systems Biology.

While advances in genomic research have permitted the cataloguing and analysis of a multitude of cellular components, laboratories are frequently resource limited and thus "concentrate on models that are part of a larger whole" or, in signal transduction,

"individual pathways and usually only a subset of proteins for any particular experimental set-up" (Cho and Wolkenhauer, 2003:1504). Experimental scope is also constrained to facilitate drawing conclusions within the highly variable intracellular environment. Researchers often only investigate the function of individual proteins, genes, or other biomolecules and therefore reveal only associations or covariant relationships while failing to determine causality (Cho and Wolkenhauer, 2003:1503). Volumes of fragmented data do not readily provide understanding of behavior, because in reality:

- One stimulus may activate multiple pathways and cause multiple responses;
- Redundancies exist (so inhibitors may not fully have the intended effect);
- Positive and negative feedback loops are embedded throughout signal pathways;
- Pathway components' kinetic relationships are often non-linear;
- Cells constantly sense and respond to multiple stimuli simultaneously; and
- Signal transduction is both time and space dependent.

"A different approach is necessary to identify causal entailment directly from experimental data"; "a signal- and systems-oriented approach is the way forward in the understanding of gene expression and regulation" (Cho and Wolkenhauer, 2003:1503). An emerging discipline of mathematical modeling known as systems biology (SB) blends microbiology and engineering to bridge the gap between existing, piecemeal experimental data and the "relationships…that give rise to cause and effect in living systems" (Cho and Wolkenhauer, 2003:1503). The goal is a more holistic view of how cells function and what gives rise to behavior. SB models are used to validate current understanding, indentify incongruities, predict behavior, "reveal features not easily recognizable by

examining the constituent parts," and "suggest experimentally testable hypothesis" (You, 2004:169,175). Even highly simplified models based on significant assumptions can be useful, even if unable to predict behavior, by guiding experimental design and by helping "to identify which variables to measure and why" (Cho and Wolkenhauer, 2003:1509).

Although "host-pathogen systems biology is still in its infancy" (Forst, 2006:220), cost reduction and acceleration of therapy and drug discovery has led researchers to use the paradigm to examine signal inhibition for: Group A *Streptococcus* (Musser and DeLeo, 2005); *Plasmodium* parasites that cause murine (rodent) malaria (Fraunholz, 2005); *Helicobacter pylori*, the bacteria that cause ulcers (Franke and others, 2008); and macrophage activation by an endotoxin (Tegner and others, 2006). *In vivo* and *in vitro* MAPK research has already been integrated into 'dry lab' experiments performed *in silico*, a term coined to describe the computer chips in which the computations occur. However, based on review of the literature, it is believed that no host-pathogen SB study has examined the signal interactions of a macrophage and *Bacillus anthracis* or its toxin.

Research Objectives

As expressed by various authors in the SB discipline, even a simple model may prove useful for predicting intracellular interactions and, therefore, for establishing hypotheses toward tailored laboratory investigation. The purpose of this research is to develop a model that depicts the effect of anthrax lethal factor on the macrophage MAPK signaling pathway by comparison to *in vitro* data for macrophage cell death. The model will also provide estimates of the MAPKK cleavage reaction rate constant. Published and fully parameterized signaling models are used as the model foundation to which the

equations for the host-pathogen interaction are added. A basic model of the key host-pathogen intracellular activities is the first step in developing more detailed cell signaling models that may include combined toxin effects, multiple signal path effects, gene transcription and cytokine secretion, or toxin effects in other immune and non-immune cells. Models of increasing scale, such as macrophage migration to the lymph nodes or system-level immune response, may also follow. Ultimately, though a human infection model is "still in the realm of science fiction" (Forst, 2006:227), an airborne spore concentration-dependent dose-response model is needed for a more accurate health risk assessment following an anthrax attack. Modeling may also progress to drug discovery or investigation of prophylaxis options. This initial model of the root pathologic mechanism should aid in designing experiments that will facilitate advancing the model.

Scope and Limitations

The models developed here are specific to the macrophage and do not consider other leukocytes, evasion of the immune response, or systemic disease. The models are limited to the interactions of lethal factor with the MAPK cascade. The models exclude the potential effects of edema factor and protective antigen and do not address toxin interaction with other pathways as possible contributions to virulence and pathogenesis. Each model investigated here is assumed to be an accurate representation of the underlying data, referenced in the respective work, and to be properly parameterized. The cascade kinetics and constants are assumed to be applicable to the activated macrophage, and those values are assumed to be unaffected by phagocytosis of *B anthracis* by the macrophage. The cleavage of MAPK signal intermediates by LF is assumed to be

catalytic and first-order. Further, despite the existence of a number of molecular variations (isoforms), target intermediates are treated as a group because LF reacts with nearly all forms at the same level in the cascade. Finally, the active MAPK concentration is assumed to be linearly related to the cell viability data from "Differential susceptibility of macrophage cell lines to *Bacillus anthracis*-Vollum 1B," published in *Toxicology in Vitro* by Gutting *et al* in 2005, in which macrophage cells were cultured in tandem with a LT-producing strain of BA. The limitations and assumptions collectively result in limitations on the application of the models. The models cannot be used as predictive tools for detailed cell or system response, for cells other than macrophages, or as dose-response models. While the models are expected to perform qualitatively as representations of system behavior, the limited cell viability data and inability to accomplish stronger validation tests also result in limited confidence in quantitative output of the models.

II. Literature Review

Chapter Overview

For over a century *Bacillus anthracis* (BA), the causative bacterial agent leading to anthrax disease, has been to microbiologists what the fruit fly has been to traditional (macro) biologists. Before biologists observed inheritance of genetic traits in fruit flies, microbiologists were developing theories on pathogenic disease transmission using BA. Research has since been conducted into the effects of anthrax on numerous animals, immune cell types, epithelial cells, and even nerve cells. The components of anthrax toxin have been purified and used for *in vivo* and *in vitro* research for many years. More recently, the effect of anthrax toxin on immune cell MAPK signaling has been investigated *in vitro* and *in vivo*. This literature review begins by providing more detail on the MAPK signaling enzyme family and the MAPK-mediated cellular immune response. The topics of pathogenesis and biomolecular effects of inhalational anthrax on the immune cells follow. Finally, the systems biology modeling approach is introduced, and the selection of published MAPK cascade models built upon for this analysis will be covered with respect to their unique attributes.

Signaling and Immunity

Mitogen-Activated Protein Kinases.

It is necessary to simplify signal transduction from "the impenetrable soup of acronyms that it might at first appear to be" into key functional roles or sequential steps seen in most signaling pathways (Downward, 2001:759). First, as a form of sensory

perception that allows information about the extracellular environment to be internalized, cell membrane surface receptors bind with specialized stimulus molecules called ligands on the external side of the membrane, often resulting in changes in structure or orientation of the surface receptor molecules. Second, a change at the intracellular end of the receptors initiates the cell's internal signaling, commonly by activation of enzymes. Third, the active enzymes recognize certain proteins; an enzyme will bind with a target protein to form a complex or will catalytically activate other proteinaceous enzymes. A series of enzyme activations, known as a cascade, may occur. Finally, whether by one or many steps in series, the signal's chain reaction commonly ends with a product protein entering the nucleus and altering gene transcription activities by either activating or inhibiting proteins known as transcription factors that mediate generation of messenger ribonucleic acid (mRNA), a protein synthesis template that facilitates information transfer from the DNA to the cytoplasm (Downward, 2001:759-760). Signal strength can be affected by interaction of enzymes with upstream mediators in the same reaction chain, resulting in either a positive or negative feedback loop. "Some pathways work as on/off switches": a signal does not complete the path from surface receptor to transcription factor unless the intensity of the input signal at the surface receptors reaches a threshold level, at which point "positive feedback results in full activation of downstream targets" (Downward, 2001:762). Kinases are perhaps the most common and, therefore, the most represented enzymatic messengers in research.

A kinase is an enzyme which transfers a phosphate group from a donor such as adenosine triphosphate (ATP), the key supplier of energy to cells for various biochemical

processes, to a target molecule. This process, known as phosphorylation, has the effect of either activating or inhibiting the receiving target. Naming of a kinase is based on the substrate: a protein kinase targets a protein for phosphorylation; similarly, a kinase kinase is a kinase that phosphorylates another kinase. The term mitogen-activated protein kinase (MAPK) was originally the name for a specific phosphoprotein in the early 1980s, but research has since revealed dozens of enzymes with similar structure and biological functions (Pearson and others, 2002:154). A mitogen is an extracellular stimulus that signals for the initiation of mitosis; however, just as multiple MAPKs with different terminal functions have been identified, various cytokines (non-antibody proteins released as intercellular mediators of immune response to an antigen), thermal stress, and osmotic shock have been identified as MAPK cascade stimuli (Pearson and others, 2002:158). MAPK thus became a term for a family of enzymes and then, after analysis showed multiple isoforms of each MAPK type, a "superfamily" (Nick and others, 2001). "All eukaryotic cells possess multiple MAPK pathways, which coordinately regulate diverse cellular activities running the gamut from gene expression, mitosis, and metabolism to motility, survival and apoptosis, and differentiation" (Roux and Blenis, 2004:321).

The biochemical stages that apply to each MAPK pathway can also be simplified as seen on the left half of Figure 3. At the cell membrane, a MAP kinase kinase kinase (MAPKKK, also herein denoted as generic enzyme E3 for simplicity) is activated by cell surface receptors in response to external stimuli. MAPKKKs in turn activate a MAP kinase kinase (MAPKK, or E2) by phosphorylating two amino acid sites via two separate reactions. Finally, MAPK (E1) is also activated by MAPKKs by two reactions (Roux and

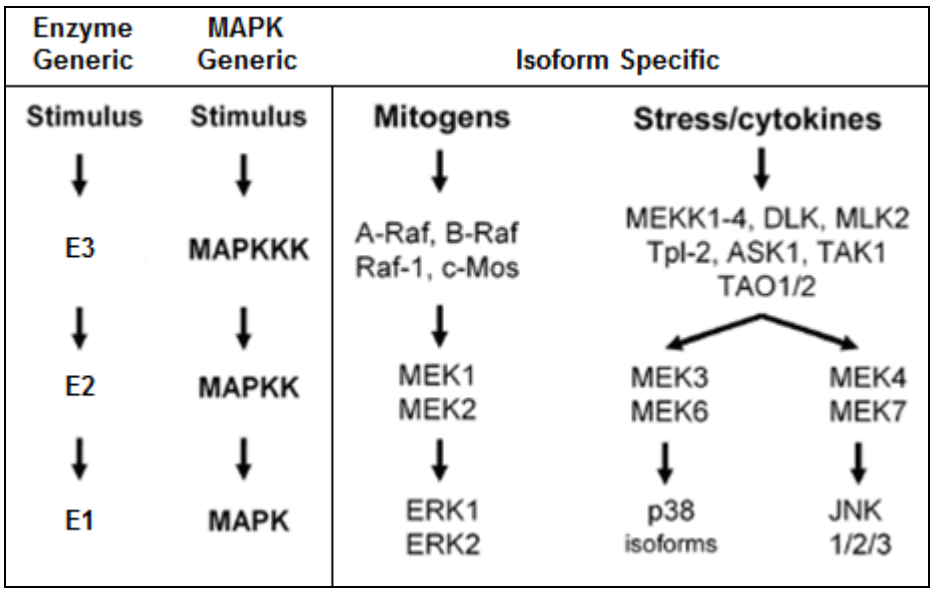

Figure 3: Steps of the MAPK cascade (modified from Roux & Blenis, 2004)

Blenis, 2004:321). On the right, Figure 3 depicts the three main subfamilies of terminal MAPKs: extracellular signal-regulating kinase (ERK), p38, and c-Jun N-terminal kinases (JNK). Multiple isoforms exist within each of the three main modules and are typically designated by a number, as in ERK1, or with a Greek character, such as p38α. As the final tier in the cascade (not shown in the figure), the active MAPKs either activate regulatory biomolecules in the cytoplasm or migrate into the nucleus to activate transcription factors for production of various isoform-dependent cytokines. Some of the cytokines are specialized chemoattractants called chemokines that are released during inflammation to mobilize and activate phagocytes and lymphocytes. Table 1 lists some of the cellular sources and immune functions of some cytokines related to macrophages. Blocking a signal through inhibition or reaction with MAPK or an upstream kinase may disrupt intracellular homeostasis or regulatory mechanisms through excess or insufficient

Table 1: Cytokine sources and immunoregulatory functions

Cytokine	**Source(s)**	**Physiologic Actions**
Interleukin-1 (IL-1)	Macrophages B cells Many non-immune cells	Activation and proliferation of T cells Proinflammatory Induces fever and acute-phase proteins Induces synthesis of IL-8 and tumor necrosis factor-alpha (TNF-α)
IL-6	Macrophages Activated T cells B cells Fibroblasts Endothelial cells	Enhances B cell differentiation and Ab secretion Proinflammatory Proliferation of T cells, increased IL-2 receptor expression
IL-8	Macrophages Platelets Natural killer (NK) cells Endothelial cells	Activation and chemotaxis of monocytes, neutrophils, and T cells Proinflammatory
IL-10	Macrophages T cells B cells	Inhibits macrophage cytolytic activity and activation of T cells Inhibits cytokines in helper T cells Enhances cytotoxic T cell activity Enhances activated B cell proliferation Anti-inflammatory
IL-12	Macrophages B cells	NK cell proliferation and cytolytic action Cytotoxic T cell activation, proliferation Stimulates production of IFN-γ Proliferation of activated T cells
IL-15	Activated monocytes Macrophages Many non-immune cells	NK cell activation T cell proliferation
Interferon-α/β (IFN-α/β)	Leukocytes Epithelial cells Fibroblasts	Induction of class I expression Antiviral activity Stimulation of NK cells
Tumor necrosis factor-α (TNF-α) and lymphotoxin (TNF-β)	Macrophages Lymphocytes	Induces inflammatory cytokines Increases vascular permeability Activates macrophages and neutrophils Tumor necrosis action Primary mediator of septic shock
Transforming growth factor-β (TGF-β)	Macrophages	Enhances macrophage chemotaxis Enhances wound healing Inhibits T and B cell proliferation Inhibits macrophage cytokine synthesis Inhibits Ab secretion

(adapted from Klaassen and Watkins, 2003: 181)

cytokine production, which in turn can lead to apoptosis, necrosis, or a failure to respond to exoteric substances.

A pathogen that can alter gene transcription can thus alter the immune cell's response. One study analyzed five different bacteria that were phagocytosed by neutrophils, which are highly microbicidal phagocytes that constitute the largest fraction of leukocytes, also known as polymorphonuclear (PMN) leukocytes, granulocytes or professional antigen presenting cells (APC). The neutrophils subsequently experienced up- and down-regulation of common sets of genes leading "to resolution of bacterial infection" followed by apoptosis (Kobayashi and others, 2003:10951). Phagocytosis of a sixth bacterium, *Streptococcus pyogenes*, affected transcription of the same gene sets in the same manner as the other five, but also simultaneously down-regulated 21 additional genes that control immunoregulatory factors known as interferons (IFN). Neutrophil apoptosis was highly accelerated and then, unlike the other five, followed by necrosis. The change in gene transcription uniquely "alters the apoptosis differentiation program in neutrophils, resulting in pathogen survival and disease" (Kobayashi and others, 2003:10951). Though these effects on gene expression may not have been caused by MAPK signal inhibition, the MAPK cascade is responsible for regulating the expression of cytokines involved in cellular and systemic immune response.

MAPKs and Immunity.

The cytokine tumor necrosis factor-alpha (TNF-α) is a "proinflammatory cytokine that acts as a mediator of host defense against…infection and is principally expressed in macrophages" at up to 10,000 times normal levels upon bacterial challenge (Zhu and

others, 2000:6349). TNF-α regulates immune cell inflammatory response and apoptosis, but release of TNF-α is first regulated through MAPK signaling. In an investigation of the relationship between the MAPK signal, TNF-α, and immunity, murine alveolar macrophages and neutrophils were treated with "the most highly selective and potent inhibitor of p38 MAPK described to date" and then stimulated by lipopolysaccharide (LPS), an endotoxin derived from Gram-negative bacteria and commonly used as a macrophage activator (Nick and others, 2000:2152). "Rapid accumulation of neutrophils to the lung in response to a proinflammatory stimulus is one of the first recognizable events in the pathogenesis of many pulmonary diseases" (Nick and others, 2000:2151). Inhibition of p38 *in vitro* blocked LPS-induced secretion of TNF-α and the murine-homologues of IL-8, a neutrophil-specific chemoattractant; and administration of the p38 inhibitor by gastric intubation resulted in a 50% drop in TNF-α secretion and failure of the neutrophils to migrate to the lungs *in vivo* (Nick and others, 2000:2152). Neutrophil recruitment may have failed *in vivo* because the p38-inhibited neutrophils could not mobilize toward the chemoattractant, because the p38-inhibited macrophages and epithelial cells could not produce adequate chemoattractant, or due to a combination of both. Regardless, the results show that MAPK inhibition causes the immune cells and system to respond in a significantly reduced capacity.

MAPK activation and inhibition has been studied for a number of diseases, as was briefly summarized in the introduction. MAPK cascades have been investigated by neurologists searching for the molecular basis of memory formation (Sharma and Carew, 2004) and have even been researched in heavy metal toxicity and thermal stress response

in mollusks (Kefaloyianni and others, 2005). The cytokine-inducing roles ERK, p38 and JNK pathways were examined in murine bone-marrow derived macrophages exposed to *Plasmodium falciparum*, a parasite that causes malaria in rodents. *In vitro* testing with targeted inhibitors revealed that all three pathways are activated by the pathogen and that each correlates to the expression of a different set of cytokines. A demonstration of specificity and redundancy between pathways occurs between the two JNK isoforms. JNK1 and JNK2 both trigger secretion of TNF-α by macrophages stimulated with the parasite's proinflammatory factors, but only activation of the JNK2 MAPK path results in interleukin-12 (IL-12) production (Zhu, Krishnegowda and Gowda, 2004:8624-8625). Similar to some anthrax studies, rapid apoptosis of macrophages has been found to facilitate survival of *Yersinia pseudotuberculosis*. A protease (an enzyme that catalytically breaks down proteins, also called a proteinase) associated with the pathogen inhibits activation of the JNK, p38, and ERK pathways (Zhang and others, 2005:7947). The result is a lack of enzyme-mediated gene expression of anti-apoptotic factors that would allow the macrophage time to respond to the ingested pathogen, and instead the macrophage experiences rapid apoptosis. As mentioned above, anthrax LF is also a protease and inhibits nearly all MAPK cascades. Interestingly, another study of MAPK signaling, in relation to the disease leishmaniasis, showed that "a specific inhibitor of p38…increases *Leishmania donovani* survival in human peripheral blood mononuclear macrophages" and that treatment with a p38 and JNK activator actually reduced parasite survival while decreasing the macrophage infection rate by 50% (Junghae and Raynes, 2002:5026). Hijacking the macrophage's internal communication network, and often

times the MAPK cascades specifically, presents pathogenic microorganisms the opportunity to breach the barrier of early immune response and go on to cause systemic infection. Yet the reverse is also true: "MAPK activation may have a potential therapeutic value" (Junghae and Raynes, 2002:5026).

Differential Responses.

Despite the findings of Nick *et al* on MAPK-mediated TNF release in relation to neutrophil recruitment, the unique roles of the three primary MAPK groups in cytokine production are still unclear. A 1999 article in the *Journal of Surgical Research*, "Macrophage TNF Secretion in Endotoxin Tolerance: Role of SAPK, p38, and MAPK" by Kraatz *et al*, investigated the effects of repeated stimulation and appears to agree with the findings of Nick *et al*. Testing peritoneal murine macrophages pre-treated with LPS 24 hours prior to LPS activation and analysis, Kraatz *et al* indicate that LPS activates stress-activated protein kinase (SAPK, called JNK here), p38, and MAPK (called ERK here); that "partial blockade of p38 alone results in decreased TNF" in a dose-response relationship; and that, though the role of ERK is unclear, JNK does not appear to be required for TNF-α release (Kraatz and others, 1999:163). However, in the June 2000 edition of *The Journal of Immunology*, Zhu *et al* published "Regulation of TNF Expression by Multiple Mitogen-Activated Protein Kinase Pathways," in which they found that LPS activates all three main MAPK modules in the RAW264.7 macrophage cell line, and that all three are necessary for full TNF-α production. A similar study with the same cell line only identified p38 and JNK as being activated by LPS stimulation; that study also found that treatment of cells to dephosphorylate p38 and JNK resulted in "a

substantial decrease in TNF-α production" without a significant decrease in active ERK (Chen and others, 2002:6414). *In vitro* analysis of Group B Streptococci (GBS) activation of monocytes, which are macrophage precursors, resulted in a dose-dependent activation of all three main MAPK subgroups; however, MAPK activation by GBS was more delayed and of longer duration that LPS-induced MAPK activation. The effect of JNK inhibition was not tested, but inhibiting either the ERK or p38 MAPK pathways did partially inhibit TNF-α expression. The simultaneous inhibition of ERK and p38 was required to completely block TNF-α release (Mancuso and others, 2002:1401-1402). The p38 inhibitor used by Nick *et al* blocked TNF-α release effectively, like anthrax LT does, whereas the p38-specific inhibitor used by Park *et al* in "Macrophage Apoptosis by Anthrax Lethal Factor Through p38 MAP Kinase Inhibition," published in *Science* in 2002, did not prevent TNF secretion (Park and others, 2002:2050), and the p38 inhibitor used on the GPS-activated monocytes caused significant but partial TNF-α expression. Interestingly, Park *et al* and Kraatz *et al* used the same inhibitor (SB202190) but obtained very conflicting results, with the former finding no TNF-α inhibition and the latter finding dose-dependent inhibition (supporting Nick *et al*). One possibility is that repeated stimulation affects the macrophages' response; but the underlying biological variation among cells and animals is generally known to make a difference in cell response.

Bonni *et al* described the pro-survival, anti-apoptotic functions of ERK in "Cell survival Promoted by the Ras-MAPK Signaling Pathway by Transcription-Dependent and –Independent Mechanisms" from the 12 November 1999 issue of *Science*. When activated in neurons, ERK "promotes cell survival by a dual mechanism" in which ERK

phosphorylates one pro-apoptotic protein, deactivating it and thereby suppressing apoptosis, and phosphorylates one anti-apoptotic transcription factor, suppression of which "triggers apoptosis" (Bonni and others, 1999:1358,1361). Logically, though ERK may not directly affect TNF secretion, inhibition of the ERK pathway would, in turn, result in inhibition of the anti-apoptotic factor and lead to apoptosis as seen in macrophages treated with LF (Park and others, 2002). However, Bonni *et al* studied neurons, not macrophages. Park *et al* specify that LF inhibits both the p38 and JNK MAPK paths, the two paths associated with inflammatory response and apoptosis (Herlaar and Brown, 1999:439); those results represent anthrax LF treatment of the J774A.1 cell line and bone marrow-derived macrophages. In "MAP kinase activation in macrophages" from the January 2001 *Journal of Leukocyte Biology*, Krishna Rao states that "the activation of MAPKs seems to be different in cell lines compared with primary cells," or even between macrophages from different tissues. This is a possible reason for the differential susceptibilities observed in different species. Rao recommends against extrapolation from cell lines, such as RAW264.7, to primary cells, such as the human AM (Krishna Rao, 2001:3). However, data for signal transduction and cytokine secretion by the human alveolar macrophage are rare.

Each investigator used a different experimental set-up. Nick *et al* used murine alveolar macrophages, while Kraatz *et al* used murine peritoneal macrophages and seems to support Nick *et al*. Park *et al* and Zhu *et al* studied cell lines and conflicted with Nick *et al* and Kraatz *et al*. It is possible that Park's p38 inhibitor did not successfully inhibit all p38 isoforms (Nick *et al* claimed theirs to be the "most selective and potent" to date);

or Nick's inhibitor may also inhibit redundant MAPK pathways, such as JNK (nearly three years later, Park's may be more selective), leading to TNF-α gene expression. Park *et al* and Kraatz *et al* used the same inhibitor and may have observed different effects due solely to the difference between cell types. Factors such as repeat stimulation used by Kraatz *et al* or simple methods of treatment may have also influenced the results. Zhu *et al* and Chen *et al* stimulated the same macrophage cell line using LPS, but only one found that ERK was activated. "All three MAPKs have been shown to undergo activation in several macrophage cell types using a variety of stimuli, [and] the response appears to be context-specific" (Krishna Rao, 2001:7). Anthrax lethal factor has been widely accepted as the main virulence factor of BA, and though the complete mechanism is not understood, the main cytotoxic activity is the non-selective cleavage of nearly all MAPKK isoforms. Adding that all terminal MAPKs have the potential to affect human AM microbicidal response, all forms of MAPKs should be considered when modeling cell response.

Anthrax Evasion of Immune Response

Inhalational anthrax in the U.S. has historically had a mortality rate of over 85%, but many cases included in this figure occurred prior to development of modern medical facilities and antibiotics available during the intentional 2001 postal attacks, which resulted in five deaths among the eleven inhalational cases, or a 45% mortality rate (USAMRIID, 2005:37). The majority of natural inhalational infections during the twentieth century were from occupational activities, occurring among wool sorters in textile mills, goat hide and hair processing workers, and tannery workers (Inglesby and

others, 1999:1736). Unique from the long-recognized cutaneous form, inhalational anthrax was even known historically as Woolsorters' disease due to its prevalence among this high-risk population (USAMRIID, 2005:36). As described in the introduction, respirable spores are quickly bound and phagocytosed by AMs, which begin transferring the spores from the lung to the mediastinal lymph nodes. Despite the microbicidal attacks of the leukocytes, BA spores may survive for up to 60 days before they germinate into vegetative bacteria and may possibly multiply inside the macrophages (Chakrabarty and others, 2006:4430; Park and others, 2002:2048; Guidi-Rontani and others, 1999:13). In the lymph nodes, the vegetative bacteria proliferate and produce anthrax toxin (AT), "leading to hemorrhage, edema, and necrosis" in the infected tissue (Inglesby and others, 1999:1737-1738; Heymann, 2004:20-22). After an incubation period generally lasting one to six days, a generic illness manifests with flu-like symptoms of fever, fatigue, headache, mild cough, and nausea. A correct diagnosis is further complicated due to an examination of the lungs typically being normal in this early stage. However, once the disease progresses victims exhibit the characteristic mediastinal widening (Figure 2), often also with pleural effusion (USAMRIID, 2005:37). After approximately two to five days, the non-specific symptoms may improve briefly only to be followed abruptly by severe respiratory distress. "Septicemia, shock and death usually follow within 24-36 hours after onset of respiratory distress unless dramatic life-saving efforts are initiated" (USAMRIID, 2005:37). In Figure 2, a radiograph from the CDC Public Health Image Library, the white areas indicated by the arrows show the classic signs of mediastinal

widening and pleural effusion in an inhalational anthrax victim less than a day before succumbing to the systemic bacterial infection and toxins.

Instead of preventing the infection, macrophages play the critical role of facilitator by allowing a BA bacterium to evade the immune response and progress to a systemic, lethal disease. The ability of BA to effectively subvert a macrophage's normal protein, enzyme or genome functions to evade the cellular immune response are not unique to the macrophage. BA also exerts MAPK pathway inhibition in dendritic cells, vigorous phagocytes and antigen presenting cells (APC) like the macrophage but with a smaller population, better ability to migrate to the lymph nodes, and a more potent T-cell priming ability; in T-cells, adaptive immune lymphocytes that promote the overall immune response, kill exogenic microorganisms through specialized antigen recognition, and provide long-term immunity; and B-cells, adaptive lymphocytes that produce antibodies in response to antigens (Baldari and others, 2006:437-439).

- In a dendritic cell (DC), anthrax toxin up- and down-regulates the production of different interleukins, which are cytokines secreted to mediate lymphocyte response, and inhibits the production of TNF-α (Tournier and others, 2005:4938-4940). When MAPK signaling is disrupted by LT, DCs "do not upregulate co-stimulatory molecules, secrete greatly diminished amounts of proinflammatory cytokines, and do not effectively stimulate antigen-specific T cells in vivo" (Agrawal, 2003:329). The DC response is effectively dampened such that it is unable to respond to stimuli.

- Two studies recently showed that T-cells fail to produce IL-2 due to LT inhibition of MAPK signals. One study found that LT caused inhibition of T-cell proliferation; LT was so selective in its attack on MAPK intermediates that the researchers even proposed LT be used as a MAPK signal inhibitor in investigating other signal pathways (Fang and others, 2005:4970-4971). Using a mouse (murine) model *in vitro*, the second T-cell study showed that IL-2 inhibition directly resulted in failure of cell activation and identified two of the three main MAPK sub-families, which are discussed below, as the primary targets of the toxin (Comer and others, 2005:8278-8279).
- "Anthrax LT treatment causes severe B cell dysfunction" at "picomolar concentrations *in vivo* and sublethal doses *in vitro*"; LT causes "markedly diminished capacity to proliferate and produce" immunoglobulin-M (IgM) in response to stimuli (Fang and others, 2006:6155).

While recent work has shown that DCs also transport anthrax spores to the lymph nodes (Cleret, 2007:7994), activated AMs have been shown to inhibit the migration of DCs to the lung (Jakubzick, 2006:3582) and the antigen presenting function of naïve and mature resident pulmonary DCs (Holt and others, 1993:404). Further, analysis has shown that a threshold particle exposure must first be reached to induce phagocytosis of particulates by pulmonary DCs; and AMs that engulf respired particulates still outnumber DCs by more than two orders of magnitude (Jakubzick, 2006:3578,3581). While macrophages may be less efficient at transport to the lymph nodes, DCs are outnumbered and depend on macrophages for chemotaxis and activation. The focus in anthrax pathogenesis research

centers on the effects of LT or LF on macrophage MAPK signal transduction because macrophages fill this significant role in the early response to and transportation of the inhaled spores and in initiating the full innate and adaptive immune response.

"In order to understand how anthrax evades the innate immune response and to gain insight into why inhalation anthrax is so lethal, it is critical to dissect the complex interactions between *B anthracis* and macrophages" (Banks and others, 2005:1180). The article by Park *et al* reported on the "causal relation between dismantling of MAPK signaling and LT-mediated toxicity" (Park, 2002:2048). Macrophage cell lines were treated with LPS or with lipoteic acids, an activator derived from Gram-positive bacteria. Both activators induce multiple MAPK pathways, including the three main sub-families: ERK, p38 and JNK. Protective antigen was added to facilitate LF entry into the cells. At a 200 ng/mL concentration, LF caused rapid apoptosis in LPS-activated macrophages and no observed apoptosis in non-activated cells. At the same concentration, LF was also found to inhibit p38 and JNK1 MAPKs. "Using inhibitors that are selective for each MAPK cascade," a portion of this LT-induced inhibition was simulated for each of the three MAPK modules individually (Park and others, 2002:2049). The p38 inhibitor was the only one to cause LPS-activated macrophage apoptosis similar to LF. Macrophage mutants were then designed to express p38-activating MAPKKs (E2) that are not recognized for cleavage by LF. LPS-treatment of these mutants showed "considerable resistance to LF-induced apoptosis" but no resistance to the p38-specific inhibitor, leading to the conclusion that apoptosis following introduction of lethal toxin is dependent the ability of the macrophage to produce p38 (Park and others, 2002: 2049).

Polymerase chain reaction (PCR) DNA analysis determined that p38 MAPK inhibition by both LT and the p38-specific inhibitor resulted in failure of the macrophages to express genes for IL-1 isoforms α and β. IL-1 cytokines trigger production of IL-2 in T cells as well as the general inflammatory response. Further, PCR revealed that LT suppressed TNF-α gene transcription and, unlike Kraatz *et al*l and Nick *et al*, that the p38-specific inhibitor did not suppress expression of TNF-α genes (Park and others, 2002:2050). The majority of studies indicate that TNF-α is the product of multiple MAPK pathways, of which p38 is only one, but all of which are inhibited by LT. Further, in tests that were able to insert LF into cells without the use of PA, LF alone "was cytolytic for the sensitive macrophages while resistant cells were unaffected," leading to the conclusion that "lethal factor by itself possesses the toxic activity of lethal toxin" (Friedlander and others, 1993:245). Echoing most current literature, Park and others conclude that *Bacillus anthracis* uses MAPK inhibition to manipulate a macrophage activation signal into "a trigger of rapid cell death," thereby preventing "the secretion of chemokines and cytokines that alert the remainder of the immune system to the presence of the pathogen" and releasing vegetative bacteria into the lymph and circulatory systems to proliferate and cause systemic toxigenic effects and bacteremia (Park and others, 2002:2051).

The biochemical mechanism by which the MAPK cascades are inhibited is very well documented in the literature. LF is a protease, or proteinase, that cleaves the MAPKK (E2) near the amino-terminus of the protein with such catalytic efficiency that "proteolysis of MAPKK1 was observed within 15 min with as little as 2 ng of LF per 200 ng MAPKK1" (Duesbery and Vande Woude, 1999:291). The MAPK/ERK kinases

(MEKs) MEK1 and MEK2, which activate the ERK family; MEK3 and MEK6, which activate p38 MAPKs; and MEK4 and MEK7, which activate JNK isoforms, have all been confirmed as targets of the proteolytic action of LF (Pellizzari and others, 1999:199; Vitale and others, 2000:739; Bardwell and others, 2004:574-575). Interestingly, two potential cleavage sites exist for MEK4 and MEK7, one of which resembles but is not a docking site for MAPK recognition and phosphorylation (Bardwell and others, 2004:576). The regions of MAPKKs recognized by LF have even been identified via testing cells with engineered point mutations in MEK1 and MEK6. The cleavage of the MEK1 "was found to reduce not only the affinity of MEK1 for its substrate…but also its intrinsic kinase activity" (Chopra and others, 2003:9402). The E1-level terminal kinases that regulate cell function and cytokine expression can no longer be phosphorylated because lethal factor's "removal of the amino terminus of MAPKKs eliminates the 'docking site' involved in the specific interaction with MAPKs" (Vitale and others, 1998:706). The strong evidence of LF-induced apoptosis has led to research on the use of LF as a therapeutic agent. A study funded by the National Cancer Institute showed melanoma cell apoptosis via treatment with both LT and MAPKK inhibitors and even documented "tumor regression without apparent side effects" in mice (Koo and others, 2002:3052). The literature is thus found to support this effort of developing an initial host-pathogen systems biology model based on MAPKK cleavage by anthrax LF resulting in alveolar macrophage apoptosis.

System Biology and the Host-Pathogen Model

"The emergence of systems biology signals a shift of focus away from molecular characterization of the components in the cell to an understanding of functional activity through the interactions in molecular dynamics" (Cho and Wolkenhauer, 2003:1503). Though systems biology (SB) literature has increased significantly in the last decade, the application to the doubly-dynamic host-pathogen system is still a nascent, novel approach within the microbiology and systems disciplines (Musser and DeLeo, 2005:1461). However, recognizing the uniqueness of modeling infectious diseases, the term host-pathogen systems biology already appears to be well established in the SB community. Of course, though traditional microbiological studies of pathogens have occurred for more than a century, much more modern laboratory research on all the relevant biomolecular components and their individual relationships is still necessary to provide an adequate aggregate of data for increasingly detailed computational biological models. Until then, a number of assumptions must be made to turn disjointed, limited and possibly disparate data on molecular mechanisms into testable predictions of system (organism) behavior. In a 2005 review from the *American Journal of Pathology* titled "Toward a Genome-Wide Systems Biology Analysis of Host-Pathogen Interaction in Group A *Streptoccoccus,*" Musser and DeLeo state:

> Analysis of the molecular pathogenesis of infectious disease by a systems biology approach is especially complicated, in part because pathogens are highly diverse genetically, multiple phases of the infectious process can be prolonged and anatomically distinct (e.g. multiple organs), and host immune responses are multiphasic. (Musser and DeLeo, 2005:1463)

As previously discussed, the benefits of SB modeling include the identification of possibly incorrect theories on causality or recognition of dynamic features that cannot otherwise be observed. While the process may seem unwieldy, Musser and DeLeo assure researchers that each iterative step of model building and experimentation will provide new insight. The understanding of gene expression and biomolecular associations can be increased simultaneously with and through understanding the underlying, mechanistic biological behavior.

As implied by the title of the article by Musser and DeLeo, a focus on genome-wide analysis using massive data sets exists in the SB literature from research institutes and established laboratories. Made possible by advances in genomics and proteomics over the last decade, such models are built from the gene up and tested to see which genes or proteins might have a role in pathogenesis. Several reviews on this type of SB application to drug discovery have been published in the last few years (Cho an others, 2006; Davidov and others, 2003; Apic and others, 2005). A model of signaling in cancer cells contained 326 molecular components, referred to as nodes in the model, and 892 chemical relationships between the components. Despite high genetic variability in cancer cells, the researchers were able to conclude that "clear patterns of oncogene-signaling collaborations emerge recurrently at the network level" by applying the holistic SB approach to the signal transduction data (Cui and others, 2007:1). An even larger modeling effort investigated apoptosis through signaling, using multiple stimuli as input and cytokine production as output for the model, and integrated a massive 7980 signals with 1440 apoptosis-related responses. By varying two extracellular stimulants, the JNK

MAPK path was found to have a dynamic "four-dimensional signal-response" relationship to apoptosis. Three stimulants and nearly 8,000 signals results in 660 dimensions and an unsolvable matrix of coefficients (Janes and others, 2005:1647-1649). The model was simplified through partial least squares regression and still maintained the ability to predict 12 apoptosis outputs with multiple stimuli. Combining *in vitro* lab experimentation with a "data-driven" systems approach revealed two opposing signal clusters, one pro-death and one pro-survival, that "capture the dynamic intracellular signal processing of diverse stimuli, including autocrine-feedback circuits" (Janes and others, 2005:1653). The previously unknown involvement of autocrine signaling is an excellent example of how using a holistic systems approach can identify features that otherwise could not be observed within such a dynamic system. These research efforts, combined with continuing advancement in genomics and proteomics technologies that facilitate faster and more accurate data collection, provide a positive outlook for the future of SB modeling. Unfortunately, at this time they are still limited in application due to limits in available data and computational methodologies.

However, host-pathogen models can take a "top down" approach that focuses on a specific signal or cell of interest, addresses a specific problem, and does not demand intensive data collection (Forst, 2006:221). To advance knowledge signal transduction in a dynamic network, instead of traditional, linear, non-dynamic statistical correlations, mechanistic analysis of reaction kinetics by nonlinear ordinary differential equations is the preferred quantitative modeling method (Cho and Wolkenhauer, 2003:1405; Forst, 2006:222; Smith, 2005:53; You, 2004:172). Top-down, kinetic models are often simple

and based on a number of assumptions such as the 'mixed model' where an enzyme's chemical concentration within the cell is considered homogeneous throughout, though in reality concentrations vary by compartment and by location within a compartment. Such simplifications do have precedent in successful, widely-accepted toxicological modeling applications such as the systems dynamics-based physiologically-based pharmacokinetic (PBPK) modeling, in which the instant mixing and homogeneous chemical concentration assumptions are made at the tissue scale. To achieve a more accurate dose-response model, toxicologists should shift away from the paradigm of linear regression of dose-response data and toward integrating increasing details of signal and biochemical interaction. To do this, toxicologists must work toward understanding "the underlying biology prior to evaluating the perturbation of the system following chemical exposure" (Andersen and others, 2005:328-329). This report attempts to develop the understanding of biomolecular pathogenesis in inhalational anthrax by implementing a host-pathogen systems biology model using published, parameterized mathematical models of the MAPK cascade as the foundation.

Published MAPK Models

As one of the most significant signal path families, the MAPK cascade has been thoroughly studied in both wet and dry laboratories, *in vivo*, *in vitro*, and *in silico*. A number of authors have published SB models of MAPK signal transduction with varying levels of complexity. The models were selected for review and implementation based, first, on availability of completely parameterized models in the BioModels Database and, second, on variation presented in the model. BioModels Database is repository of

mathematical biological models that are intended to be shared through the Internet (http://www.ebi.ac.uk/biomodels) for the promotion of research. The database is administered by the European Molecular Biology Laboratory's European Bioinformatics Institute (EMBL-EBI) in England. EBI is an academic non-profit member of the EMBL group, an international organization established in 1974 that now includes five research centers throughout Europe. Previously, EBI has also been funded in part by the Defense Advance Research Projects Agency (DARPA) of the U.S. Department of Defense.

As with most modeling of dynamic systems, models should not be too large in scope so as to encompass components irrelevant to the feature being investigated. Thus, the selection begins with early, more simple models that identify unique characteristics of MAPK signaling such as ultrasensitivity, which allows a very quick and strong output response to a very small stimulus, and oscillatory behavior in the signal output, activated MAPK. The third model includes the relationship between MAPK enzymes and scaffold proteins, which bind enzymes in a signal sequence to increase selectivity and decrease 'cross-talk' interference between different pathways. Scaffold proteins may exist to decrease system nonlinearity and thereby "lead to elimination of sustained oscillations" (Kholodenko, 2000:1587).

Ultrasensitivity Model.

Huang and Ferrell may have been the fist to apply computational modeling to the MAPK cascade in their paper "Ultrasensitivity in the mitogen-activated protein kinase cascade," which was published in the September 1996 *Proceedings of the National Academy of Sciences*, now simply known as *PNAS*. The ultrasensitivity model follows the simplified

MAPK cascade structure, as shown in Figure 4. The figure includes added annotations -P and -PP, which represent the singly and doubly phosphorylated MAPKK and MAPK, and P'ase, an abbreviation for the phosphotases that dephosphorylate both the singly and doubly phosphorylated forms of MAPKK and MAPK (Huang and Ferrell, 1996:100078). The kinetic equations in this model explicitly depict the double phosphorylation for activation of the intermediate and terminal kinases. This is accomplished, for instance, by including the bound MAPK/MAPKK-PP complex that produces MAPK-P, the MAPK-P/MAPKK-PP complex that produces the fully active MAPK-PP, and each of the singly and doubly phosphorylated kinases formation in the bound state with its respective

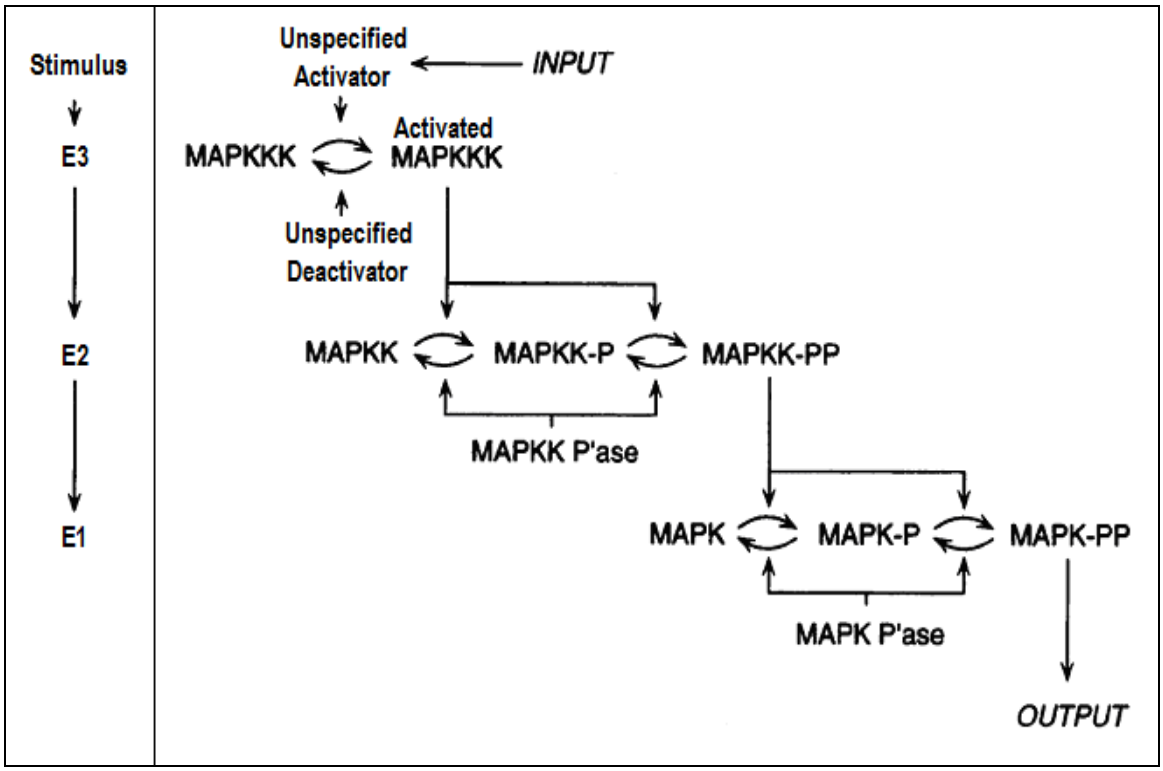

Figure 4: Schematic of MAPK cascade for ultrasensitivity model
(after Huang and Ferrell, 1996)

phosphotase, such as the MAPK-PP/MAPKP'ase complex that results in deactivation of the kinase to MAPK-P. The stoichiometric, chemical equations listed in Huang and Ferrell (1996) show the detailed association and disassociation reactions for each enzyme-substrate pairing; the article also includes the time-dependent differential equations. Huang and Ferrell were able to predict that MAPK would "behave like a highly cooperative enzyme, even though it was not assumed that any of the enzymes in the cascade were regulated cooperatively" (Huang and Ferrell, 1996:100078). Cooperative behavior arises from having multiple binding sites, for which binding of one affects activity of another, and results in a sigmoidal or S-shaped curve, meaning behavior does not follow Michaelis-Menten (MM) kinetics (Figure 5). Ultrasensitivity in cooperative enzymes is measured by the Hill coefficient, n_H. The Hill coefficient equals one for the MM kinetic model and approximately five for the ultrasensitive MAPK cascade (Ferrell and Machleder, 1998:896). As the term implies, an ultrasensitive signal is able to react to much smaller changes in the concentration of ligands, the extracellular molecules that bind with membrane receptors to initiate the signal. For Michaelian enzymes where $n_H = 1$ "there must be an 81-fold change in ligand" concentration to increase "from 10%...to 90% maximal enzyme activity," whereas a non-MM, "cooperative enzyme with a Hill coefficient of 4 can give the same enzyme activity change with only a 3-fold variation in ligand concentration" (Goldbeter, 1981:6444). Huang and Ferrell were subsequently able to validate the model's prediction of ultrasensitivity via an *in vitro* experiment in which the MAPK activity was measured in *Xenopus* (frog) oocytes. Like the predicted curve, the empirical sigmoidal curve for

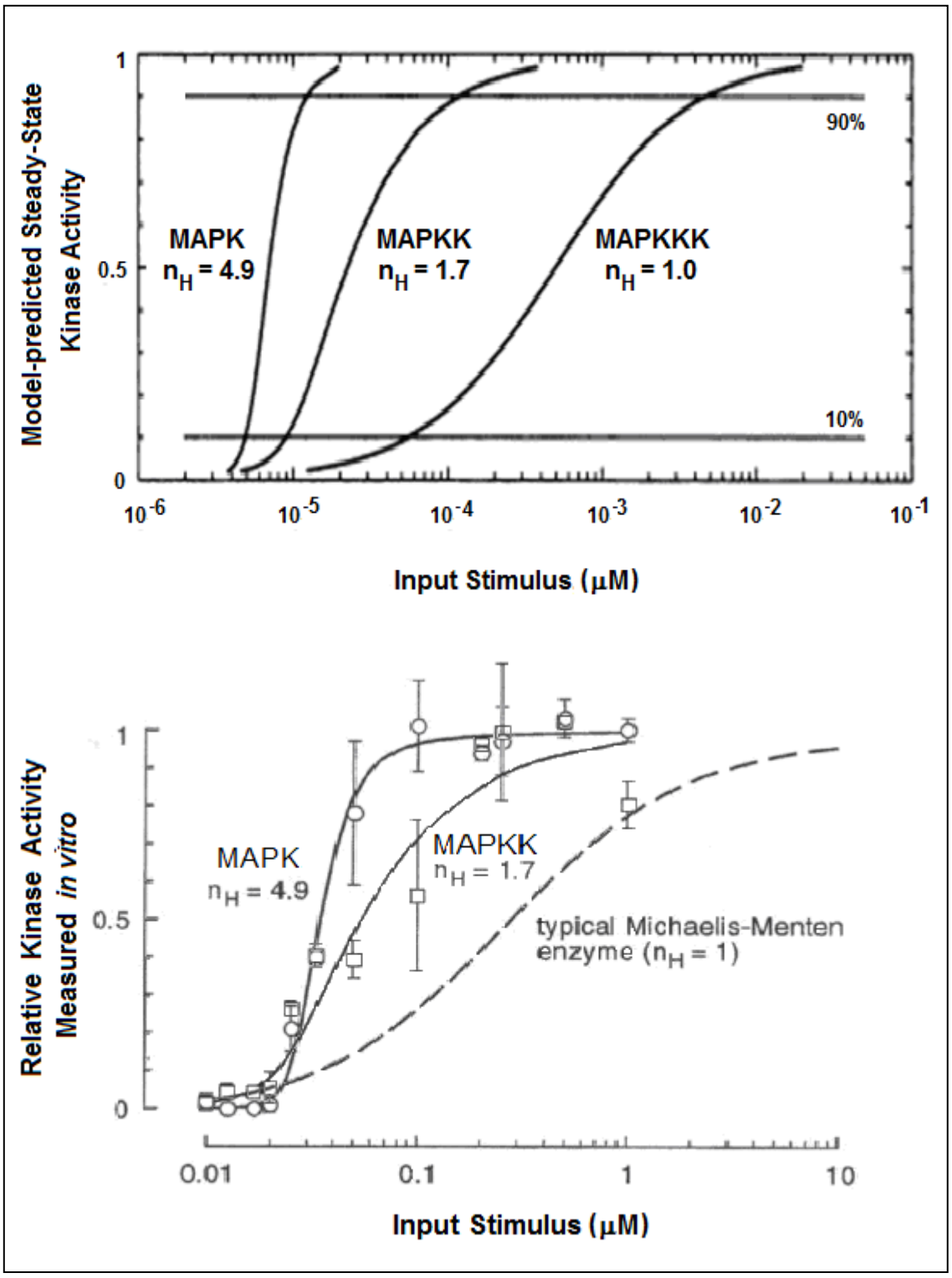

Figure 5: Ultrasensitivity model-predicted and observed kinase activation levels (*in vitro* data from *Xenopus* oocyte extracts) (modified from Huang and Ferrell, 1996)

MAPK was found to be much steeper than for an enzyme following normal Michaelis-Menten kinetics. The authors predicted and then confirmed the all-or-none, switch-like behavior known as ultrasensitivity in the MAPK cascade. The kinase activity levels presented in Figure 5 represent the steady-state activity at varied concentrations of a cascade stimulant. The time-dependent active MAPK output of the ultrasensitivity model is shown in Figure 6, in which it can be seen that the steady-state activation is reached in only 60 seconds. Ultrasensitivity increases with the number of intermediates in the cascade. This may explain why MAPKs have more steps in the activation chain than most other signal pathways and why MAPK signaling is "particularly appropriate for mediating processes like mitogenesis…where a cell switches from one discrete state to another" (Huang and Ferrell, 1996:100078). Because a macrophage would be activated during the process of binding and engulfing the spore, LF-induced inhibition of MAPK

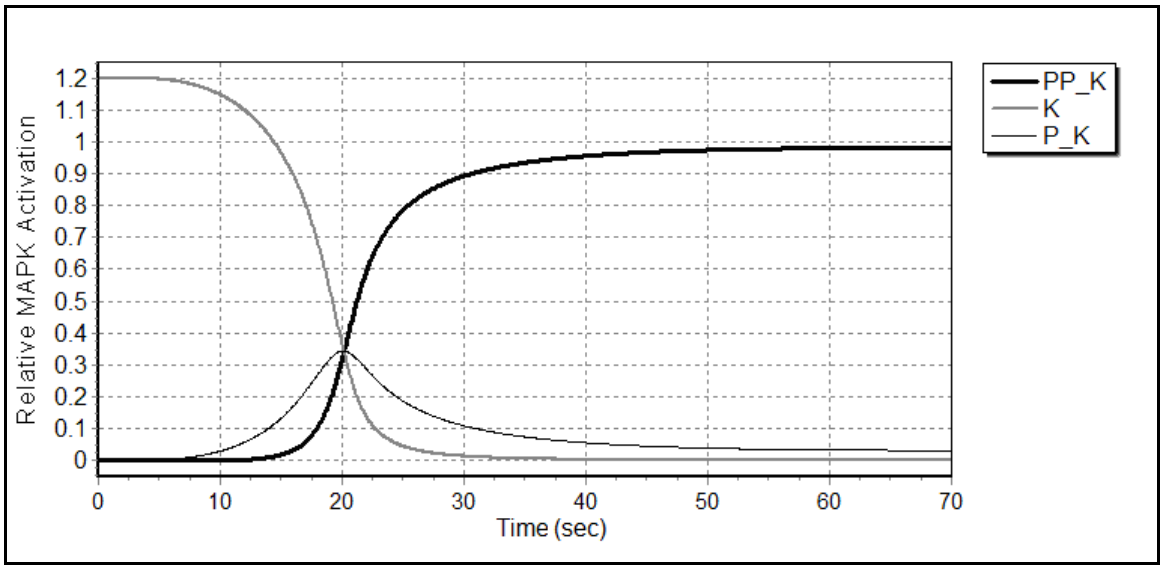

Figure 6: Ultrasensitivity model output
(PP_K is MAPK-PP, P_K is MAPK-K, and K is MAPK)

activation would likely not affect response sensitivity but would slowly 'switch off' the activation signal as MAPKKs are depleted.

Oscillating Negative Feedback Model.

In "Negative feedback and ultrasensitivity can bring about oscillations in the mitogen-activated protein kinase cascades" from the 2000 *European Journal of Biochemistry*, Kholodenko demonstrated that the MAPK signal would oscillate due to ultrasensitivity combined with a negative feedback loop in which the terminal MAPK (E1) inhibits activation of the MAPKKK (E3). Kholodenko refers to Huang and Ferrell as having a similar cascade structure; the schematic, shown in Figure 7, also uses the

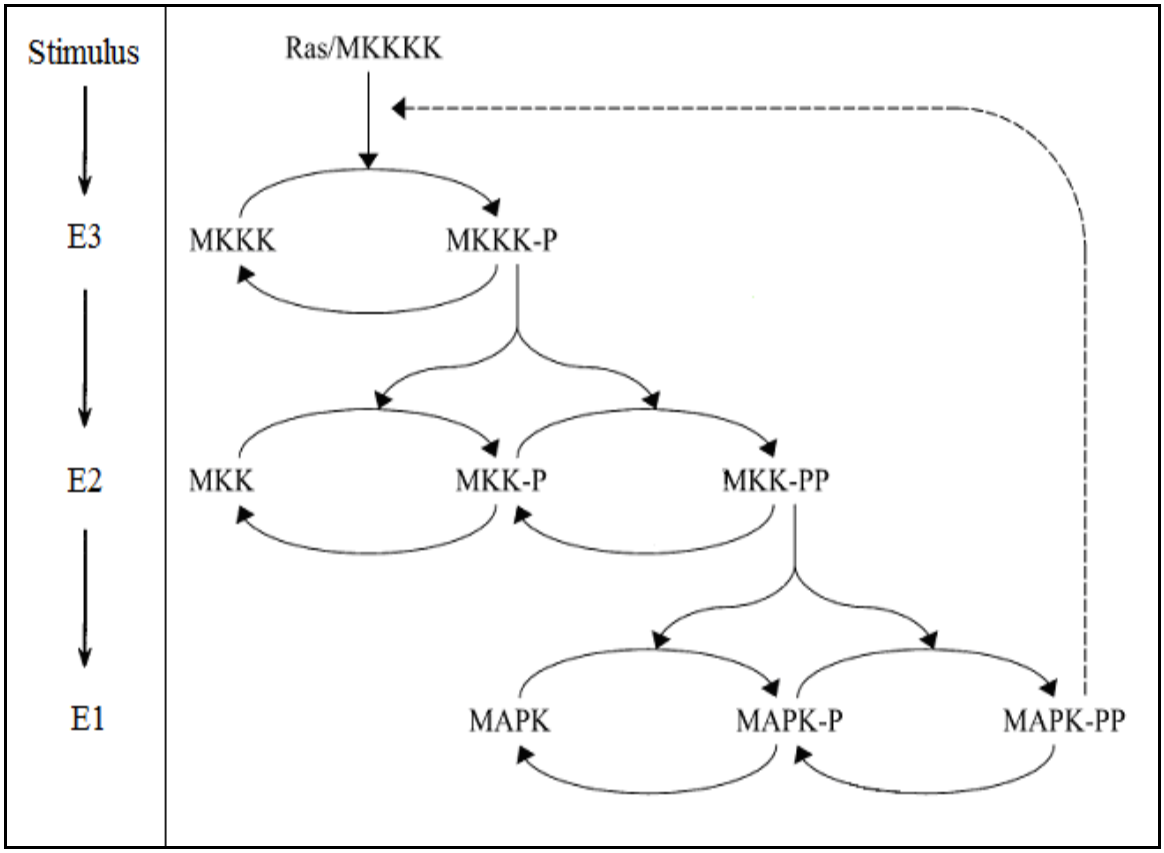

Figure 7: Schematic of MAPK cascade with feedback loop (after Kholodenko, 2000)

same annotations for the enzyme activation states. However, this schematic denotes MAPKKK (E3) as MKKK and shows MAPKKK to be activated at the cell membrane by one phosphorylation from Ras, which is otherwise termed MKKKK by the kinase naming convention. While adding the negative feedback relationship between activated MAPK (MAPK-PP) and Ras, Kholodenko excludes the phosphotases that were included in the kinetic equations by Huang and Ferrell. Because "*in vitro* enzymatic studies have shown that dual-specificity kinases (MEK1) follow the Michaelis-Menten mechanism," Kholodenko applied MM kinetics in his differential equations (Kholodenko, 2000:1584). In another deviation from Huang and Ferrell's model, the kinetic equations are developed without regard to the transient kinase-to-kinase and kinase-to-phosphotase intermolecular complexes experienced during kinase activation and deactivation, respectively. Robinson and others developed and implemented a first attempt to model the LF-MAPKK interaction using Kholodenko's model, which was selected for being the most simple model available (Robinson and others, 2007). That initial anthrax host-pathogen model, which was presented in the poster session of the 5th Annual American Society for Microbiology (ASM) Biodefense and Emerging Diseases Research Meeting in 2007, provided the precedent for this research effort.

Kholodenko's significant contribution is the negative feedback loop in which the active MAPK inhibits Ras activation through phosphorylation. As a result, an increasing concentration of active MAPK results in decreased production of more active MAPK. As MAPK then decreases in concentration, stimulation at the cell membrane overcomes the inhibition; this causes MAPK-PP concentrations to begin to increase again. Eventually,

the concentration again affects inhibition, and the oscillatory cycle repeats as depicted in Figure 8. The oscillation of MAPK-PP levels was a model-derived prediction by Kholokenko, and that prediction has been reported as being observed in the laboratory by other researchers (Sauro and Kholodenko, 2004:26). The removal of the stimulus that generates the switch-like response would result in damped oscillations, until steady-state is reached by the system output. Of course, due to phosphotase activity on the active MAPKs, LF would continue to inhibit active MAPK such that, unlike a cessation of stimulation, it falls below baseline levels required for cell function regulation.

MAPK Model with Scaffold Proteins.

In the same year as the publication of the oscillatory model in the Europe, Levchenko, Bruck and Sternberg published a MAPK model in the United States under the

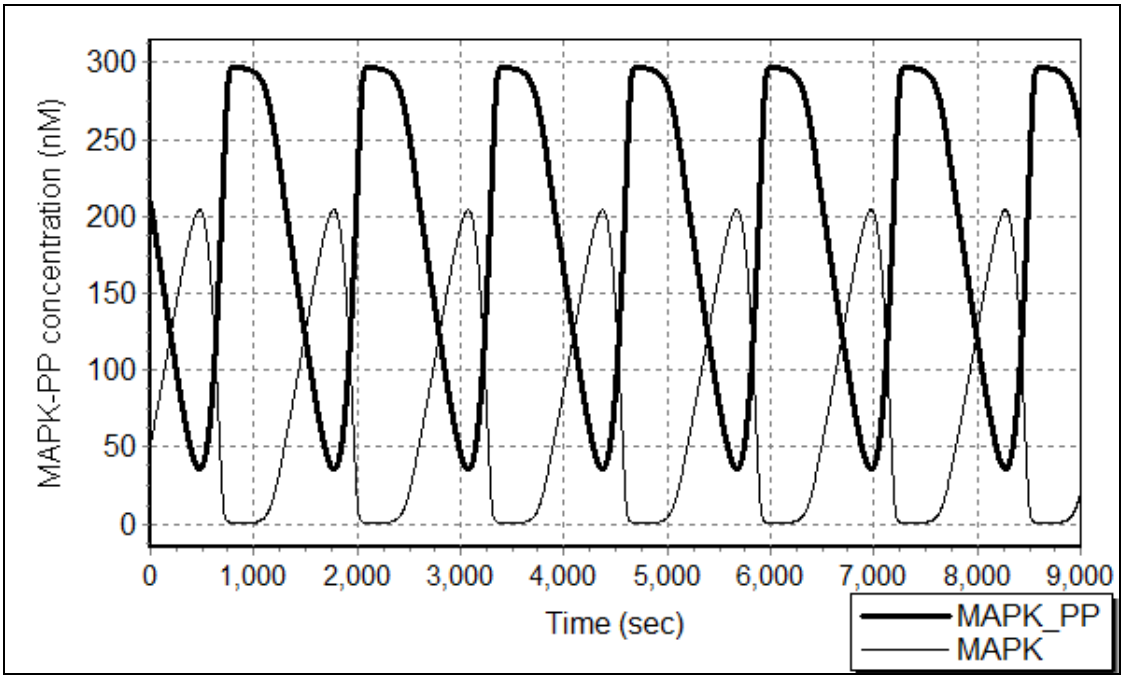

Figure 8: Feedback model output showing MAPK-PP oscillations (after Kholodenko, 2000)

title “Scaffold proteins may biphasically affect the levels of mitogen-activated protein kinase signaling and reduce its threshold properties” in *PNAS*. Scaffold proteins “serve as organizing centers for signal transduction because they can bind several members of a signaling cascade to form a multimolecular complex” (Levchenko and others, 2000:5818). The model was built to demonstrate that “formation of scaffold–kinase complexes can be used effectively to regulate the specificity, efficiency, and amplitude of signal propagation” (Levchenko and others, 2000:5818). The bound complexes of scaffold proteins and kinases are in the model equations as unique chemical species, but in a non-transient form, unlike the kinase-phosphotase complexes used by Huang and Ferrell. Simplified diagrams of the postulated scaffold-kinase complexes are shown in Figure 9; only the transitions for the unbound scaffold are shown (solid arrows) for clarity. The scaffold-facilitated reactions are denoted on the bottom of Figure 9 by the dashed arrows. Some MAPKKs (the E2 level) have even been found to act in both the role of a kinase and a scaffold protein. Due to the high number of nodes (86 kinases, kinase-kinase complexes, kinase-phosphotase complexes, and scaffold complexes, with three states of kinase phosphorylation) and reactions (300), a schematic of the scaffold model is too large and intricate to be presented here.

The scaffold model includes the kinase-deactivating phosphotase components like Huang and Ferrell, but referencing early works on biochemical ultrasensitivity and MM kinetics (Goldbeter and Koshland, 1981, 1984), Levchenko *et al* instead apply M-M kinetics like Kholodenko. Modeling MAPK complexes with a generic scaffold protein shows that scaffold proteins “can substantially increase the signaling output”; but

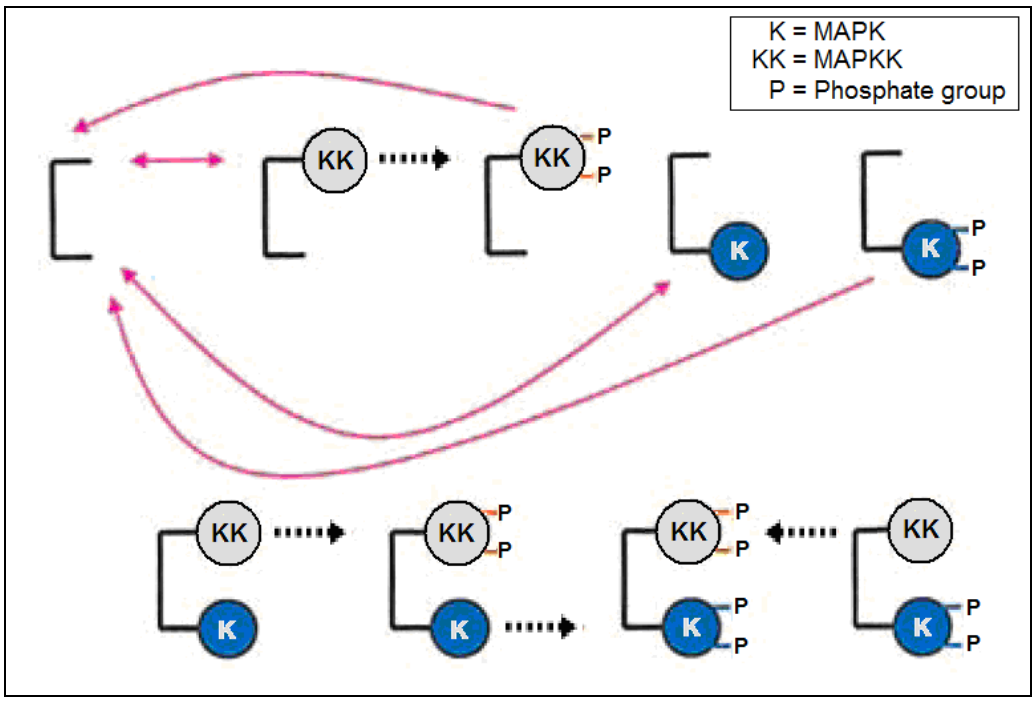

Figure 9: Examples of kinase-scaffold protein complexes and transitions
('K' is MAPK, 'KK' is MAPKK, and 'P' is a phosphate group on a kinase)
(modified from Levchenko and others, 2000)

alternatively "if the scaffold concentration is greater than optimal, a significant decrease in signaling can occur" (Levchenko and others, 2000:5818). Figure 10 reflects the output of MAPK-PP concentration over time using the scaffold protein model as downloaded from BioModels Database. Figure 11 demonstrates this optimization concept through a graph of the model output with different concentrations of the two-kinase scaffold complex, where increasing two-member concentration increases kinase activity. At some point a threshold is crossed and the 1 micromolar (μM) concentration results in a significant drop in MAPK-PP concentration that is lower than activity without scaffold proteins. This may present a reason why analysis of some kinases in scaffold complexes within the cytoplasm appear to be inhibited, perhaps because the scaffold limits kinase

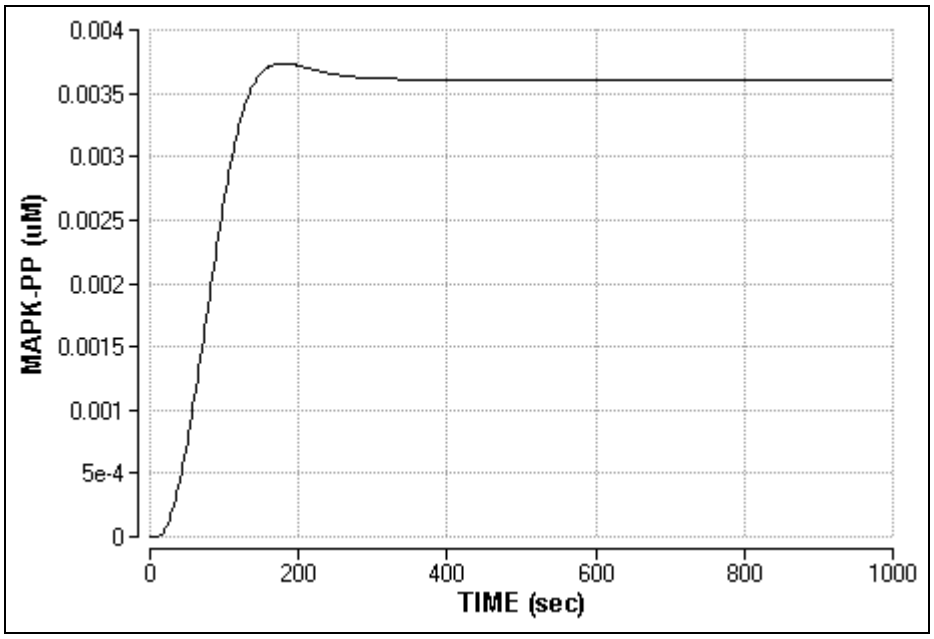

Figure 10: Scaffold protein model output for active MAPK levels

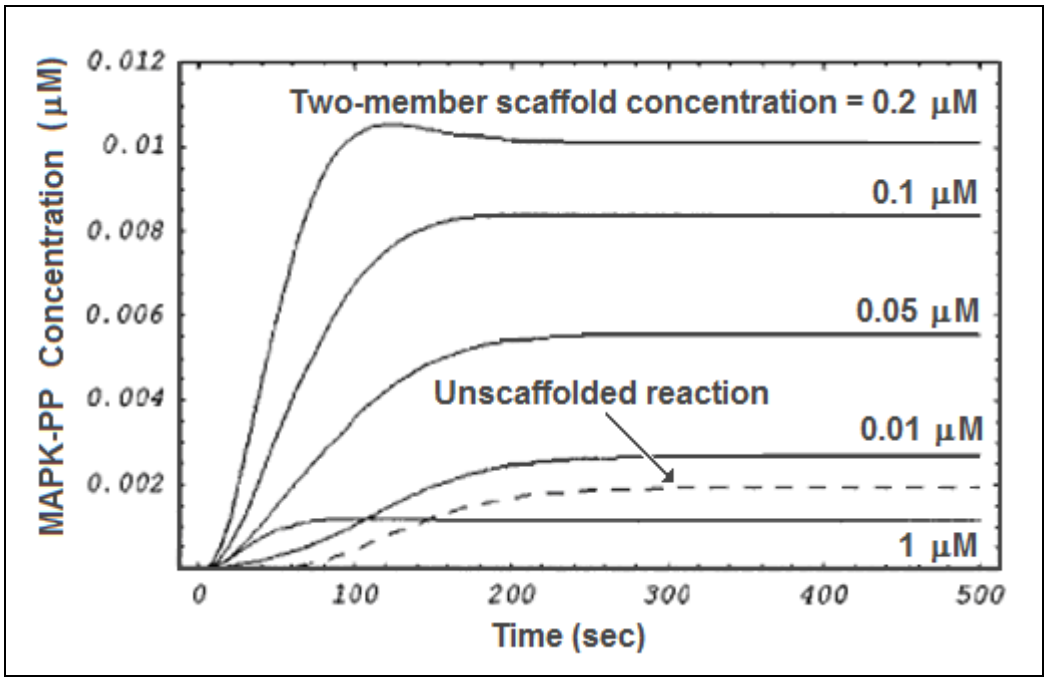

Figure 11: MAPK activation as a function of fully-bound scaffold concentration (modified from Levchenko and others, 2000)

enzyme mobility in the cytoplasm, compared to tests with purified, unbound enzymes. If the concentration of the scaffold protein in the cytoplasm is over the optimal level, then the signal response is reduced below its potential; a reduction in the expression of the scaffold protein could increase the output beyond that possible in tests with unbound enzymes.

Summary

Macrophages eagerly ingest anthrax spores but, upon spore germination, are disabled by the LF inhibition of MAPK signal transduction, resulting in accelerated programmed cell death and a failure to activate the full immune response. Though variation exists between MAPK activations and subsequent effects, macrophage apoptosis depends on multiple pathways, and LF is known to inhibit nearly all MAPK pathways by cleaving MAPKKs, the E2 intermediates. Combining published systems biology models of the MAPK cascade with laboratory data for cell viability of macrophages cultured with LT-producing strain of anthrax, a model of the host-pathogen dynamic system is feasible.

III. Methodology

Overview

All models have been developed from published, fully-parameterized MAPK cascade models obtained through BioModels Database (http://www.ebi.ac.uk/biomodels), which facilitates systems biology research through the sponsorship of EMBL-EBI. The following procedure, mostly derived from the procedure for a first attempt to model the LF-MAPK interaction by Robinson and others, was used to modify three models to include LF-induced cleavage of MAPKKs and to translate software-specific code for the parameters and equations (Robinson and others, 2007). By varying the kinetic reaction rate constants defining the cleavage of MAPKKs by LF, the model output, which is the MAPK-PP concentration or MAPK activation level, was adjusted to fit empirical macrophage cell viability data for two LT-sensitive murine macrophage cell lines co-cultured with a LT-producing strain of *B anthracis.*

Model Development

The models were downloaded from BioModels in Standard Biological Mark-up Language (SBML), an XML-based computer language developed explicitly for computational modeling of biological processes. The SBML code was imported into JDesigner (version 2.0.41), a free, open-source program that was developed for systems biology modeling with the support of DARPA and the U.S. Department of Energy. Within JDesigner, each model was modified to add the chemical reactions accounting for the cleavage of MAPKKs (the E2 intermediate from Figure 1). The catalytic reaction was

assumed to possess first-order linear kinetics; the kinetic constants for the reactions were initially approximated using the values from the initial effort by Robinson and others. The code of each model was then exported from JDesigner and modified, using the procedure described in Appendix B, to allow the code to be imported into Berkeley Madonna (version 8.3.11). Berkeley Madonna is a general purpose differential equation solver developed by faculty at the University of California at Berkeley through the sponsorship of the National Science Foundation and National Institutes of Health. Thought not explicitly a systems biology modeling tool, Berkeley Madonna was selected for model implementation because it is a significantly faster ordinary differential equation (ODE) solver and because it allows variables to be more easily manipulated than JDesigner. Berkeley Madonna is also the modeling program in use by the research sponsor, AFRL/RHPB. The edited code that was run in Berkeley Madonna for each model is provided in Appendix C. Though parameter values were varied in determining the effective reaction rate constants, the code reflects only one value per parameter.

Chemical Reaction Kinetics.

All models were used in their published form, as downloaded from BioModels Database. One exception occurred in the MM kinetic equations established by Kholodenko for the oscillating negative feed back model with regard to strength of the negative feedback. The power in the first reaction rate equation in the oscillating model's code, provided in Appendix C, determines the level of negative feedback, where n = 2 is approximately equivalent to cooperative inhibition (Kholodenko, 2000:1586). (The

variable is ‘n’ in the published equations and is coded in the rate equation as the kinetic parameter ‘J0_n.’) Both presentations of negative feedback power were investigated.

As discussed in Chapter II, the literature is clear in statements that LF cleaves all MAPKK isoforms, with the one exception of MEK5. However, nothing could be found in the literature regarding the possibility of LF reacting differentially with the three phosphorylation states of the E2 intermediate. The phosphorylations occur at two amino acids among hundreds in the polypeptide chain, whereas LF recognizes a specific site adjacent to the N-terminus of the protein (Bardwell and others, 2004:576). Each subsequent phosphorylation may affect the affinity and reactivity of LF with its substrates, via changes in diffusive or electrophoretic mobility of MAPKKs within the cytoplasm, but the available literature contains no analysis or even suppositions regarding proteolysis being dependent on phosphorylation or activation state.

When a macrophage is challenged, the macrophage is activated, signaling initiates, and MAPKs are rapidly phosphorylated. In the case of the ultrasensitivity model, biphosphorylation becomes the predominant state for MAPKKs; logically, LF would have to cleave the biphosphorylated, active MAPK in order to accomplish cytolysis via pathway inhibition. In the negative feedback model output seen in Figure 8, the concentration of biphosphorylated MAPK, MAPK-PP, varies over a significant range of concentration (approximately 40 to 300 μM). As a consequence of the negative inhibition exerted by MAPK-PP on activation of the initial, E1 level of the cascade, the concentrations of the three phosphorylation states of MAPKK also oscillate. Within the third model, in which MAPKKs are bound to scaffold proteins, the mobility as a function

of the number of phosphorylations is presumably insignificant compared to mobility restrictions as a result of the scaffolds. It is therefore assumed herein that LF reactivity is inclusive of all unphosphorylated, monophosphorylated and biphosphorylated MAPKK isoforms. Because the rapid switch-like nature of MAPK activation and deactivation shows that all forms of kinases are readily accessed within the cytoplasm, and in the absence of data indicating otherwise, kinetic values for the three phosphorylation states of MAPKK were assumed to be equal. Finally, one study has shown that MAPKKs continue to interact with and be phosphorylated by MAPKKKs at the start of the cascade. Active MAPKKs may also behave normally in other cellular interactions outside the MAPK cascade, but are only unable to recognize and bind with MAPKs due to the loss of the amino-terminus, which is part of the docking site (Paccani and others, 2005:329). As suggested in the literature review, studies have shown reduced intrinsic kinase activity in addition to significant loss of interaction between MAPKK and its substrates as a result of proteolysis (Chopra and others, 2003:9402). The models thus assume that all incomplete forms of MAPKK, regardless of activation state, are chemically no longer functionally MAPKKs due to the inability to activate MAPKs.

All models were treated similarly with regard to implementing the first-order reaction kinetics for catalytic cleavage of MAPKKs by anthrax lethal factor. Being produced by a bacterium in a phagosome within the macrophage, the chemical concentration of lethal factor was assumed to be sufficient for sustained catalytic reaction (Park and others, 2002:2049), therefore LF was not included in the models as a chemical species. The equations for the three models all followed the same structure for a time-

dependent ordinary differential equation, which is represented here using the traditional brackets around chemical species to denote concentration and using k as the variable for the reaction rate constant (Engel, 1977:15):

$$d[\text{Cleaved MAPKKs}]/dt = [\text{Cleaved MAPKK}] + [\text{Cleaved MAPKK-P}] + [\text{Cleaved MAPK-PP}] \quad (1)$$

where,

$$[\text{Cleaved MAPKK}] = k_{KK}\,[\text{MAPKK}] \quad (2)$$

$$[\text{Cleaved MAPKK-P}] = k_{KKP}\,[\text{MAPKK-P}] \quad (3)$$

$$[\text{Cleaved MAPK-PP}] = k_{KKPP}\,[\text{MAPKK-PP}] \quad (4)$$

Again, the three rate constants (k) for LF cleavage are assumed equal. Each model applies different initial concentrations for the three MAPKK phosphorylation states based on the sources referenced in each respective publication. A model node was added in JDesigner to represent the accumulated products of the three cleavage reactions, and the initial parameter value was assigned at the estimated 2.5e-4 s^{-1} established in previous model work (Robinson and others, 2007). Following basic functional testing to ensure operability of the model in JDesigner, models were translated for import into and parameterization in Berkeley Madonna.

In Berkeley Madonna, each model was manipulated and evaluated using procedures described in model-specific detail within the results. The output for all models was the active terminal MAPK (MAPK-PP), for which concentration was plotted against time. The behavior of the output was compared to data on the viability of two standard, LT-sensitive murine macrophage cell lines, RAW264.7 and J774.1, which were cultured for at least 15 hours with *Bacillus anthracis*-Vollum 1B (V1B), a virulent strain

of BA that produces LT and a "capsule that inhibits phagocytosis of vegetative BA" (Gutting and others, 2005). The graphs in Figure 12 represent two separate experiments to assess cell death in two macrophage cell lines cultured with and without *Bacillus anthracis*-Vollum 1B. While the two cell types shown are differentially susceptible to LT, the overall behavioral trend is similar, especially when considering error. Fitting to the data for the two cell lines, each model was parameterized for first-order reaction constants for lethal factor's catalytic reaction with MAPKKs.

Ultrasensitivity Model.

The ultrasensitivity model includes MAPKKs in a bound complex form ("BIOMD0000000009- Huang1996_MAPK_ultrasens," 2007). For instance, MAPKKK

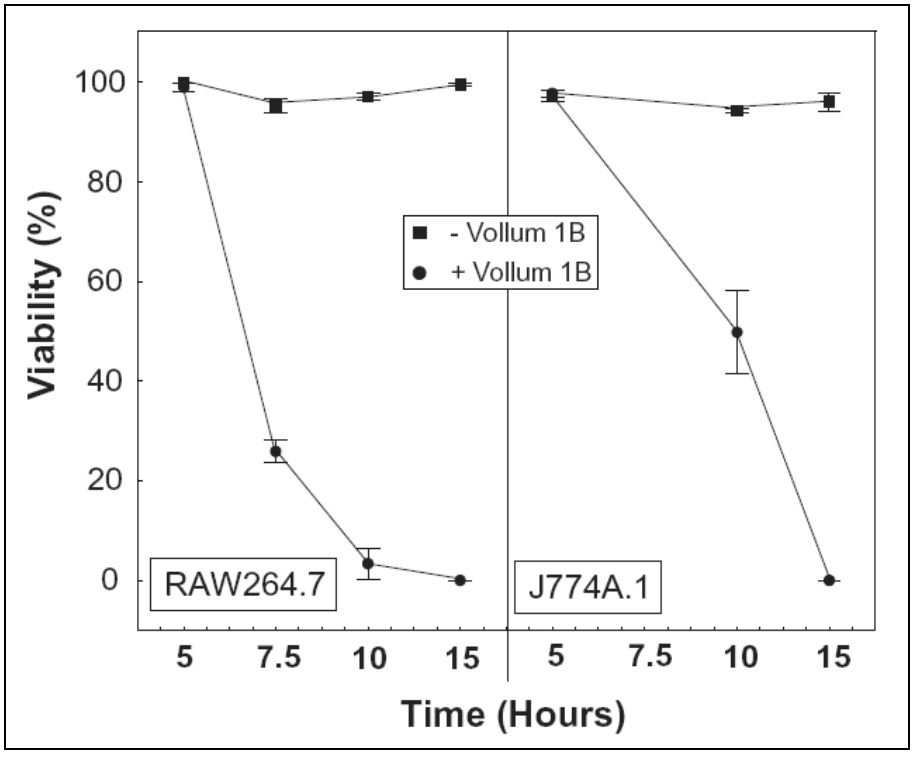

Figure 12: Macrophage viability when cultured alone or with V1B (modified from Gutting and others, 2005)

(E3) interfaces with MAPKK (E2) to activate it; and this interaction is explicitly represented as a transient multi-molecular species (node) within the model. Cleavage of LF substrates while bound to other macromolecules presented a problem: without a more complex kinetic model, a first-order reaction with MAPKK while bound would have also subtracted from the pool of the other complex member. These transient species exist only during the recognition and phosphorylation of the kinase substrate or the dephosphorylation of the phosphotase substrate. The available concentration and time for LF proteolysis of a MAPKK while in such a kinase-kinase or kinase-phosphotase complex are assumed to be minimal; therefore it was assumed that LF did not actively cleave the bound MAPKKs. This assumption was validated after tuning the LF/MAPKK reaction kinetics to fit the J774A.1 cell line data. Only doubly phosphorylated MAPKK exists in complexes at appreciable concentrations: the MAPKK-PP/MAPK complex peaks under 0.05 μM, and the MAPKK-PP/MAPK-P complex peaks under 0.09 μM (Figure 13). For comparison, unbound MAPKK begins at 1.2 μM and is quickly activated, resulting in slightly over 0.8 μM MAPK-PP. Thus, LF interaction with the transient MAPKK (E2) complexes was ignored.

Oscillating Negative Feedback Model

Minor modifications have been made for application of the negative feedback model and for comparison to the macrophage viability data. The oscillation model downloaded from BioModels Database starts with an initial (t = 0) MAPK-PP concentration of 10 μM, so the absence of phosphotases in the model would result in a steady-state 10 μM concentration after damping of the oscillation via depletion of

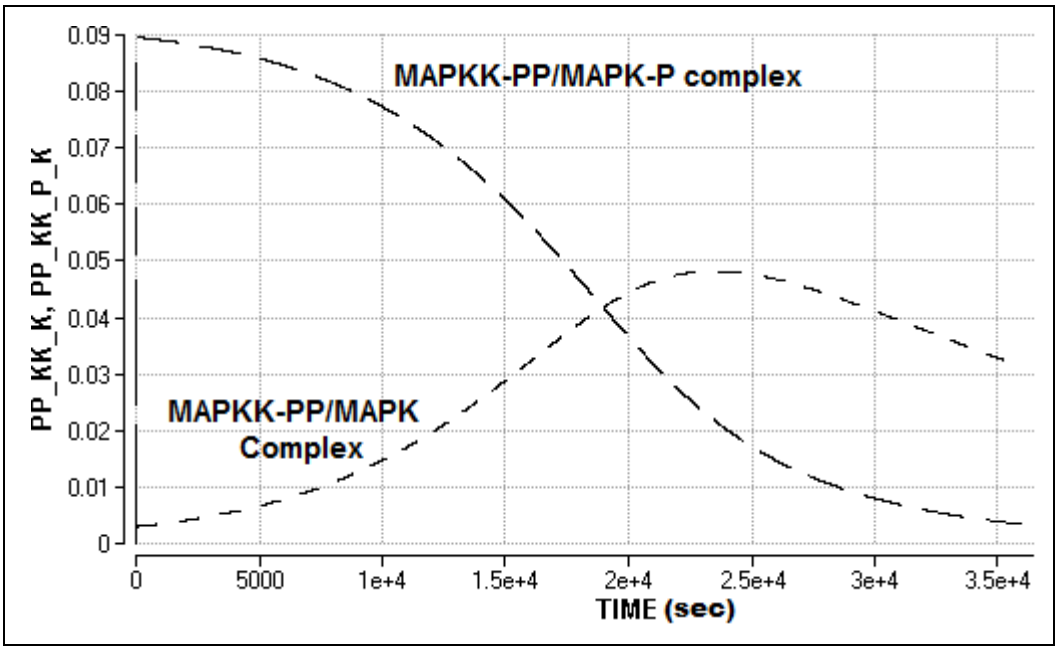

Figure 13: Ultrasensitivity model's low bound MAPKK complex concentrations

MAPKKs ("BIOMD0000000010 – Kholodenko2000_MAPK_feedback," 2007). This may not be optimal for simulating inducement of apoptosis if the baseline value is sufficient to sustain inhibited functions to be modeled later. The model output published by Kholodenko, shown Figure 8, shows an initial MAPK-PP concentration of zero; another published figure (not shown) related to evaluation of the effect of cooperative inhibition does show an initial concentration of 10 μM for MAPK-PP. To permit full deactivation of the active MAPK pool by phosphotases, the initial MAPK-PP concentration was changed to zero (coded as "init MAPK-PP = 0" as shown in Appendix C). Second, the cell viability data from Figure 12 have been time-shifted by 5 hours to take into account the time required for germination and gene expression prior to the production of LT. The first data point at the five-hour point has a cell viability of 100% and, for the purposes of the model, is reset to t = 0 because LT-induced inhibition of

MAPKs begins immediately. Finally, as stated above, the MM kinetic parameter for power of the negative feedback loop, n, was varied as shown in publication.

The presence of oscillations had to be accounted for in the process so that the average MAPK-PP concentration could be fit to the data. The model was run as a MAPK signal model without the presence of LF so that the natural oscillations could be observed. Because the active MAPK effectively 'spends more time' at the oscillation peaks than at the minimums, the average is weighted toward the peaks. The numerical output was exported from Berkeley Madonna; the peak, minimum, and average active MAPK concentrations were determined using Microsoft Excel 2003. The average MAPK without LF-induced MAPKK cleavage was graphed as equivalent to the 100% macrophage viability. As seen in the results, respective fractions of the average were applied as appropriate for each cell line and negative feedback loop strength combination.

MAPK Model with Scaffold Proteins

Like the ultrasensitivity model, the scaffold facilitated model involves biomolecular complexes between kinases, phosphotases, and scaffold proteins ("BIOMD0000000014 – Levchenko2000_MAPK_scaffold," 2007). The scaffold protein complexes, however, are not assumed to be transient and limited in concentration relative to unbound targets of the toxin. Following the same argument for the ultrasensitivity model, where reaction with bound kinases would also deplete the scaffold proteins, the interaction of LF with the bound MAPKKs was ignored. This presents a significant limitation in applying this model to LF cleavage of MAPKKKs due to the model focusing on the promotion of kinase activation via these sustained complexes. Because the

catalysis cannot be applied to a significant portion of the MAPKK population in the model, the kinetic constants applied to the unbound forms will be overestimated to compensate.

IV. Analysis and Results

Chapter Overview

Each MAPK cascade model was modified to include LF proteolysis of MAPKKs via a first-order reaction. The model output, active MAPK, was plotted, and the kinetic reaction rate constants for the cleavage of MAPKKs was parameterized to fit the *in vitro* data for the RAW264.7 and J774A.1 macrophage cell lines (Figure 12). The models designed around the ultrasensitivity and negative feedback characteristics were able to be manipulated to fit the cell viability data, and for the latter the strength of the feedback loop was evaluated in relation to the laboratory results. Unfortunately, the scaffold protein model proved to be a poor model for investigating LF-induced inhibition of the MAPK cascade. The model was only unable to provide a fit for the J774A.1 viability data and resulted in a high cleavage rate estimate for the RAW macrophage cell data; both are likely due to the limitations of the model imposed by the binding of MAPKKs to scaffold proteins.

Results of Simulation Scenarios

Ultrasensitivity Model

The ultrasensitivity model results in an S-curve of the MAPK activation and quickly approaches steady-state (Figure 6). Though still present, the switch-like response to the bacterial stimulus is not perceptible in the output due to the time scale of the anthrax incubation (15 hr). At first glance, the 'reverse' S-curve showing inhibition of MAPK activation appears to match the behavior of the J774A.1 macrophage viability plot

better than the inverse shape of the RAW264.7 viability plot. However, it should be noted that the RAW viability at 10 hr in Figure 12 shows a lower bar of the range or error at approximately zero; this indicates that the actual behavior of the RAW cell line when incubated with LT-producing BA may be closer to that of J774A.1 cells than implied by the simple linear data point connectors in Figure 12. Additionally, the error bars plotted represent the standard error of the mean (SEM) instead of standard deviation (SD) with a confidence interval. According to a report on misuse of the SEM in biomedical research:

> Authors often use the [SEM] to describe the variability of their sample… As the SEM is always smaller than the SD, the unsuspecting reader may think that the variability within the sample is much smaller than it really is… The SD tells us the distribution of individual data points around the mean, and the SEM informs us how precise our estimate of the mean is. It is therefore inappropriate and incorrect to present data only as the mean (SEM)… The use of the SEM should be limited to inferential statistics where the author explicitly wants to inform the reader about the precision of the study. (Nagele, 2001:514)

Given that the SEM range is very near to zero and that an SD-derived confidence interval would likely result in a larger range, a viability of zero is therefore assumed to be within the confidence interval. With parameters set according to the code in Appendix C and with all three reaction constants for LF cleavage assumed equal, parameterizing to fit the *in vitro* data for RAW264.7 results in a reaction rate of 2.95e-4 s^{-1} (Figure 14). The curve has 25% activation at 2.5 hours (9,000 s), per the *in vitro* analysis, and near-zero activation at 5 hours (18,000 s), which is within the range of error.

The kinetic parameters for LF reactivity in the J774A.1 cell line were more easily obtained. The range of error for the 5-hour data point (10-hour point in Figure 12, minus the 5-hour shift), using SEM, is approximately 40% to 60%. This corresponds to first-order constants of 1.2e-4 s^{-1} to match 50% viability at 5 hr (18,000 s), with a range of

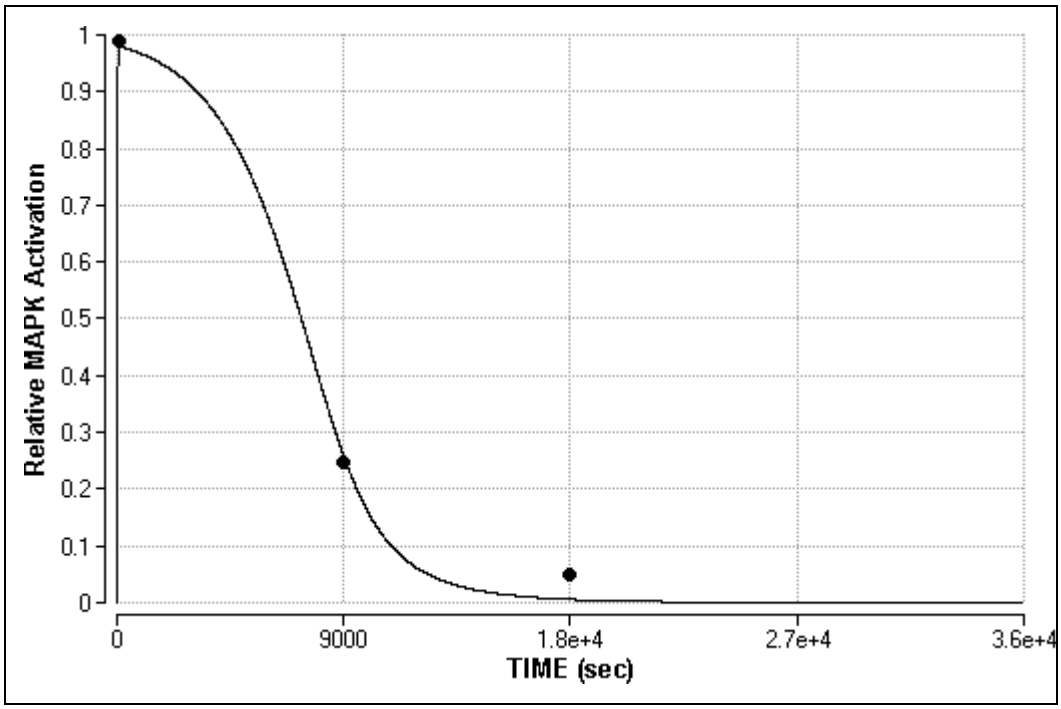

Figure 14: Ultrasensitivity model parameterized to fit RAW264.7 *in vitro* data (dots)

1.1e-4 s^{-1} for 60% viability up to 1.3e-4 s^{-1}, for 40% viability. Corresponding to the *in vitro* data, the fit for 40% viability at 5 hours (18,000 s) also corresponds to a near-zero, 1% viability at 10 hours (36,000 s) (Figure 15). The data for both cell lines is provided in Table 2 following discussion of the results for the other models.

Oscillating Negative Feedback Model

The negative feedback model presents a challenge in that the average of the oscillations must be fit to the empirical cell line data. Figures 16 and 18 illustrate the results of fitting the data using the non-competitive inhibition model where n=1, for which results in an oscillation peak at about 287 μM and a minimum around 36 μM, giving an initial amplitude of 125 and, due to the oscillation spending more time at the peaks than the valleys, an average of about 184 μM prior to MAPK inhibition. The

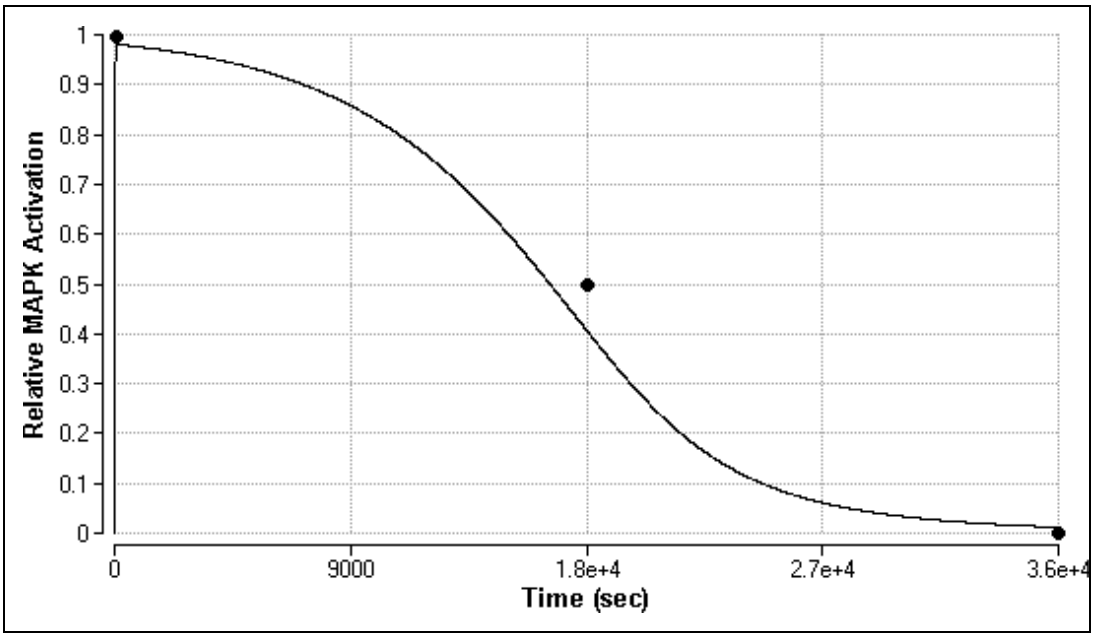

Figure 15: Ultrasensitivity model parameterized to fit J774A.1 *in vitro* data (dots)

rate constant for the RAW264.7 data (Figure 16) with n=1 is 2.9 e-4 s^{-1}, and the rate is 1.2 e-4 s^{-1} for J774A.1 macrophages (Figure 17). The stronger negative inhibition (n = 2) is applied in Figures 17 and 19 to give an oscillation peak near 288 μM and a minimum of about 9 μM, for an amplitude of approximately 140 and an average of 175 μM. For n=2, the rate constant for the RAW264.7 viability data (Figure 18) is 2.3 e-4 s^{-1}, and the rate is 9.5 e-5 s^{-1} for J774A.1 macrophages (Figure 19). At a glance, Figures 17 and 19 appear to demonstrate a better match to the data behavior due to having full loss of MAPK-PP (0% cell viability) at a later time point. One might expect the stronger inhibition of the cascade's initial activation step via the negative feedback loop to result in a more rapid loss of active MAPKs, but both outputs for increased negative feedback show more oscillations at 5 hours (18,000 s) and a later x-axis intercept. Kholodenko

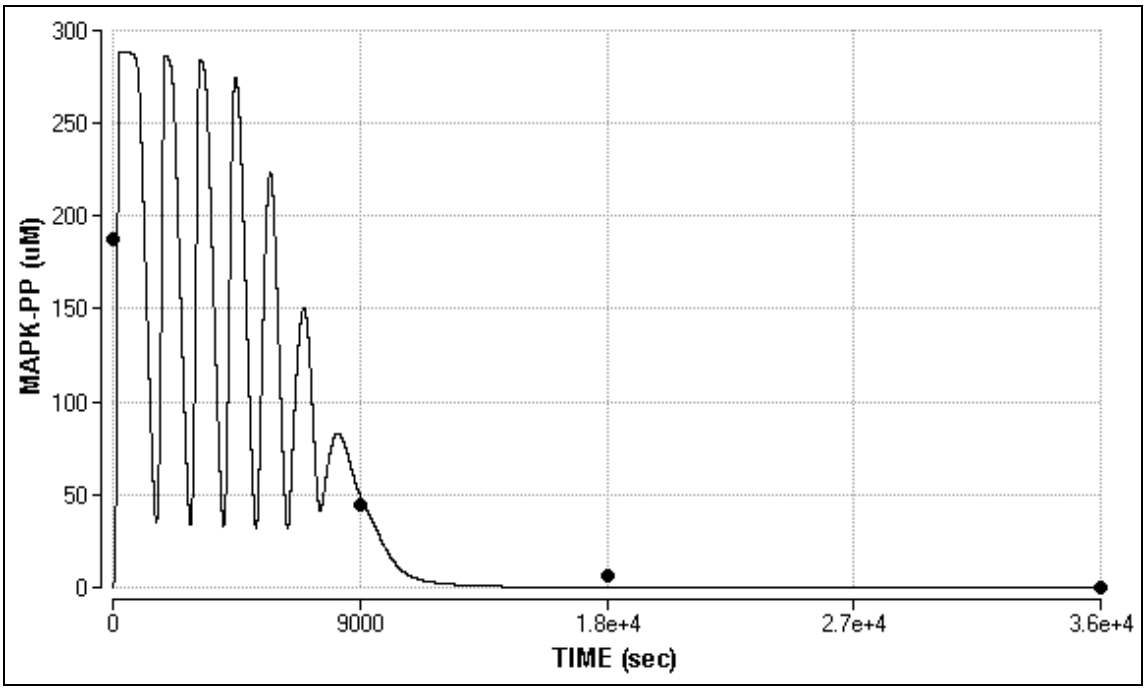

Figure 16: Negative feedback model (n=1) fit to RAW264.7 data (dots)

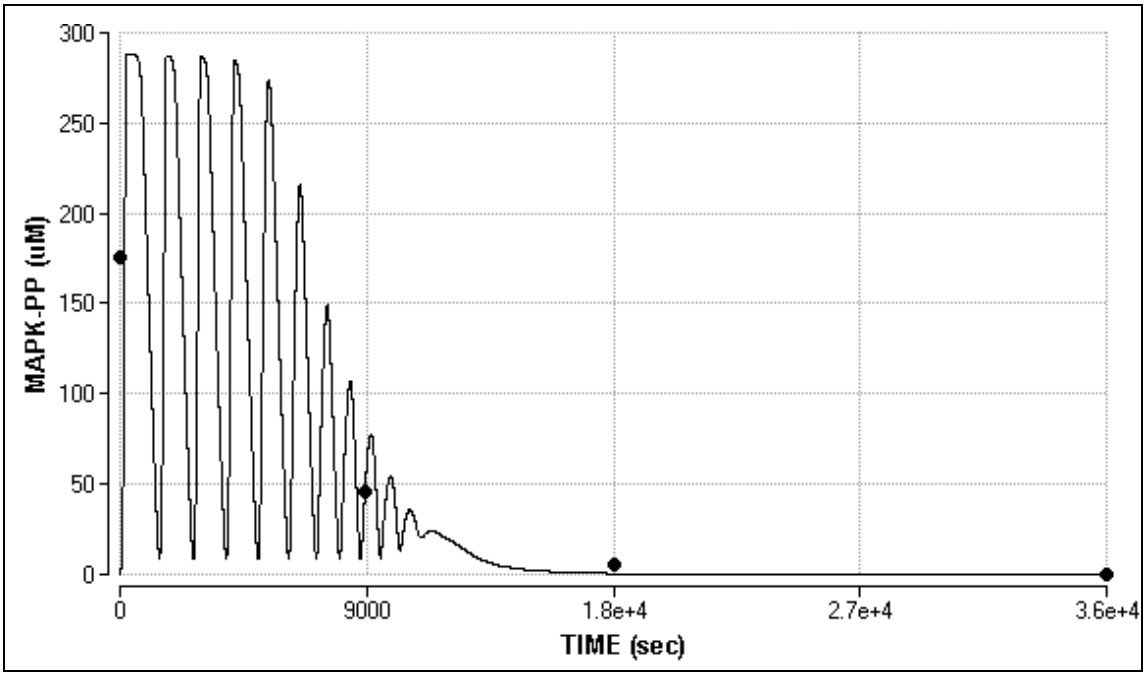

Figure 17: Negative feedback model (n=2) fit to RAW264.7 data (dots)

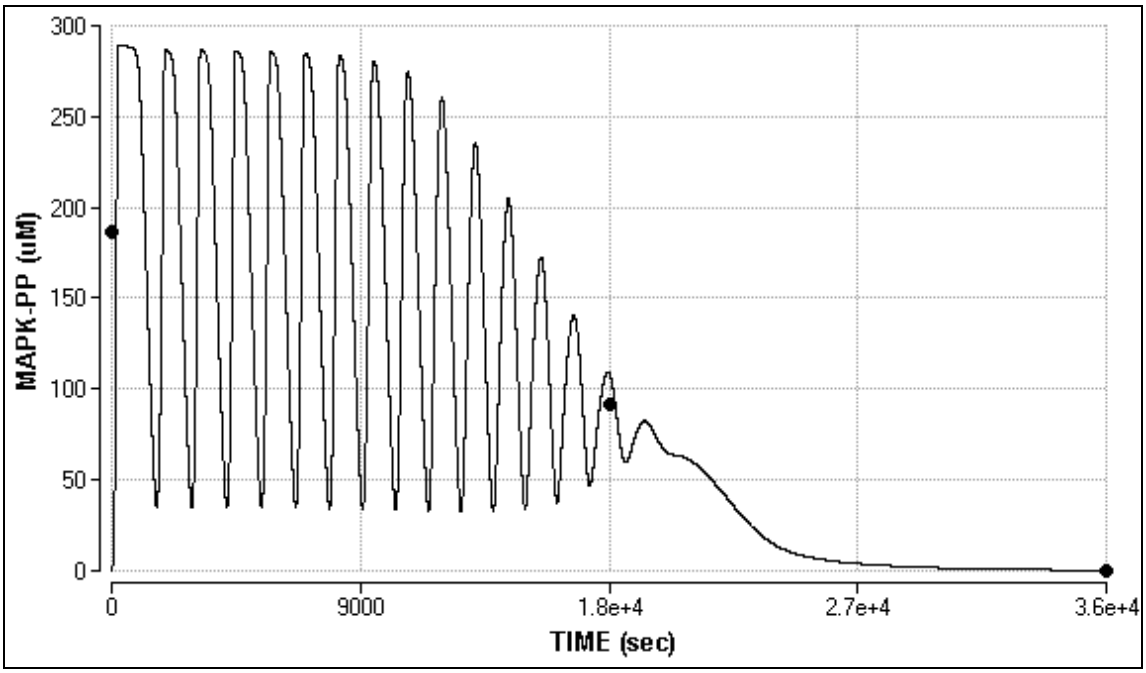

Figure 18: Negative feedback model (n=1) fit to J774A.1 data (dots)

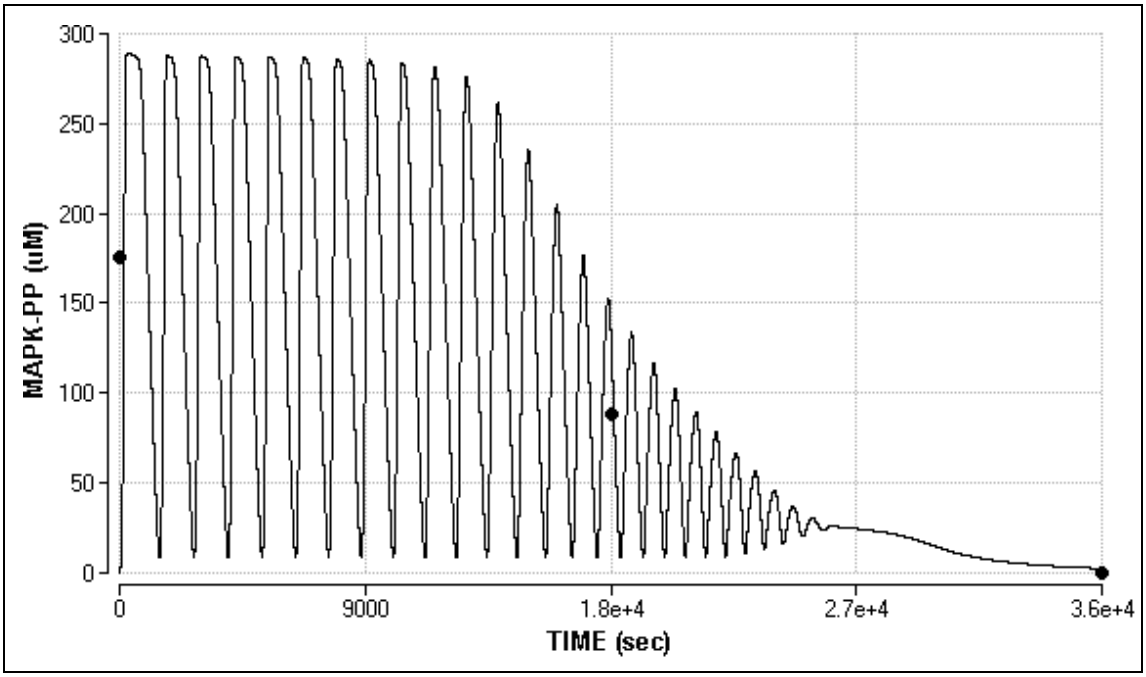

Figure 19: Negative feedback model (n = 2) fit to J774A.1 data (dots)

notes that an increase in kinase concentrations or in the MM kinetic parameter KM could cause the oscillations to transition to a stable state, but increased negative feedback allowed oscillations to reemerge (Kholodenko, 2000:1586). This suggests that SOS (effectively an MKKKK) may be inhibited via double phosphorylation from MAPK (Kholodenko, 2000:1586), but the fit appears better for the confidence in the models, having been qualitatively fit to the data to determine the parameters, do not allow any conclusion regarding whether MAPK cooperatively inhibits SOS/MKKKK through double phosphorylation.

MAPK Model with Scaffold Proteins

The scaffold protein model was not well suited for the modeling of LF cleavage of MAPKs resulting in macrophage cell death. The RAW264.7 cells could be adequately fit with a high reaction rate constant of 5.9e-4 s^{-1}, which is twice that of the other models for this cell type (Figure 20). Unfortunately, the behavior of the J774A.1 macrophages could not be reflected in the model. Dropping the rate constant to a value of 1.0 e-4 did increase the MAPK activation sufficiently to reach the lower SEM limit of 40% viability at five hours, but the 10-hour activation was elevated well above zero (Figure 21). Assuming that the rate constants are equal for all three activation states of unbound MAPKKs, no single number can be found to fit the *in vitro* MAPK activity levels observed in the J774A.1 cell line. As discussed previously, this is likely due to the high proportion of MAPKK bound in complexes with scaffold proteins.

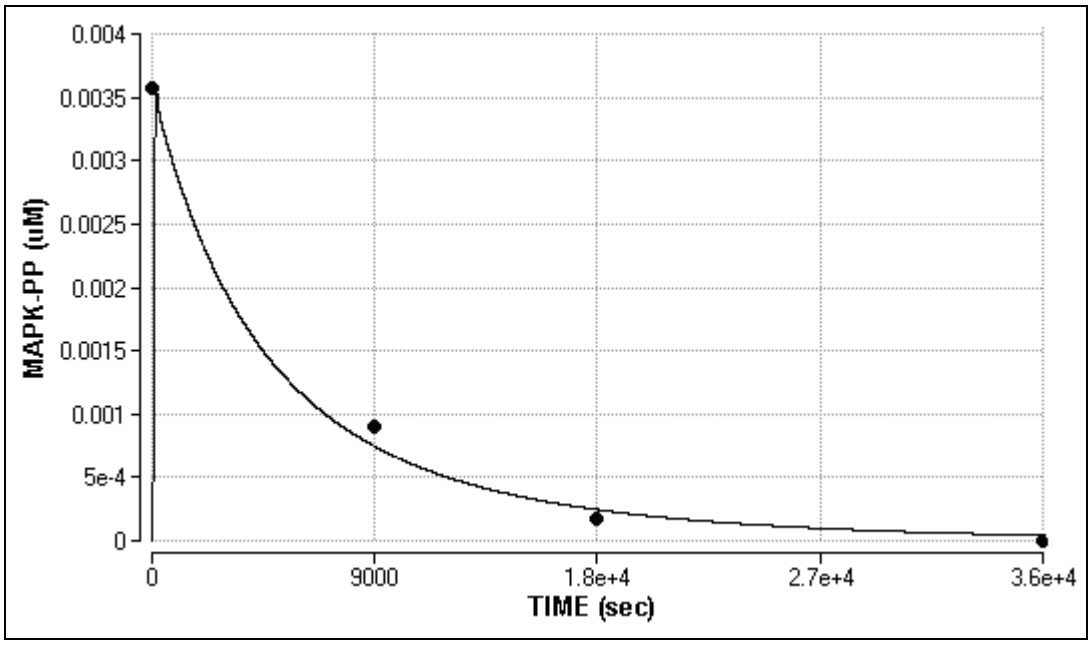

Figure 20: Scaffold protein model fit to RAW264.7 data (dots)

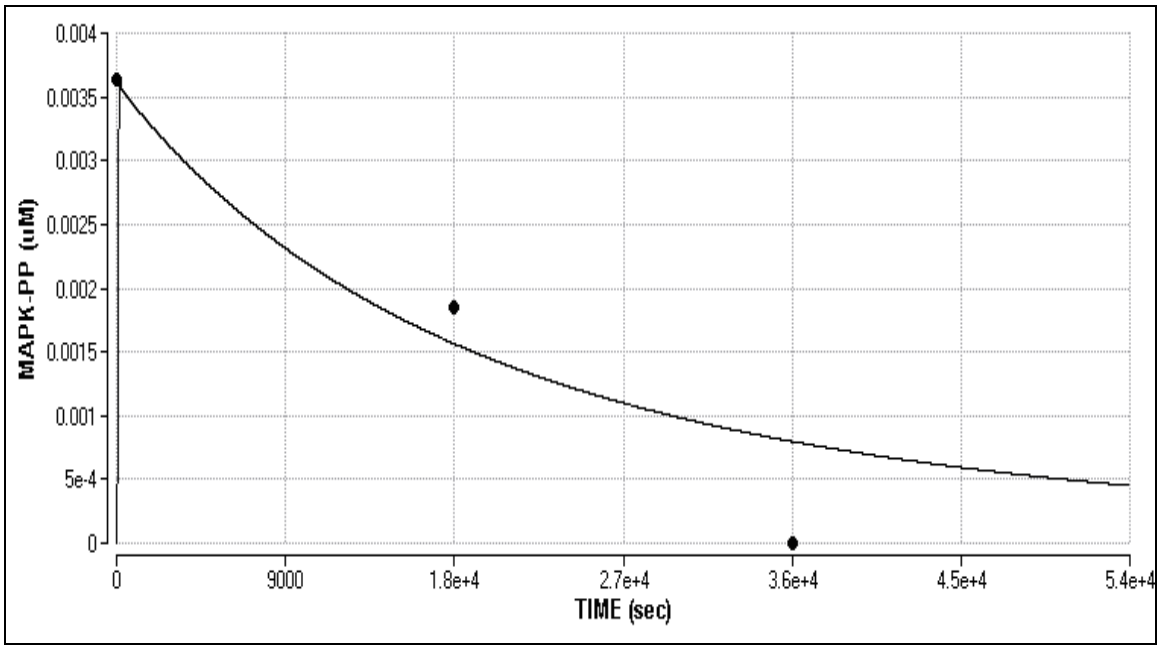

Figure 21: Scaffold protein model showing poor fit to J774A.1 data (dots)

Summary

The ultrasensitivity and negative feedback models were able to be parameterized to fit the *in vitro* data for the co-culturing of macrophage cell lines RAW264.7 and J774A.1 with *Bacillus anthracis*. The model in which MAPKKs are bound to scaffold proteins was unable to fit the data for J774A.1, possibly due to the exclusion of the bound substrates of LF. No data whatsoever could be found in the literature for kinetic reaction rate constants for the cleaving of kinases by LF. The reaction rate constants for the cleavage of all isoforms of bi-, mono- and unphosphorylated MAPKKs by the protease LF were thus estimated for the three published models. The estimated rate constants, which are summarized in Table 2, show a reasonably consistent performance by the models in estimating a LF-MAPKK reaction rate parameter for each macrophage type. Additionally, ratio of the rate constants is approximately the same, around 2.3 to 2.4, for the three simulations fit to both cell lines. While the two versions of negative feedback loop intensity resulted in different estimates for the kinetic constant, the relative sensitivity of the two macrophage cell lines was about the same for both n=1 and n=2 feedback mechanisms. This consistency demonstrates the robustness of the models.

Table 2: Kinetic constants for LF cleavage of MAPKKs

Macrophage Cell Line	**Ultrasensitivity**	**Negative Feedback (n=1)**	**Negative Feedback (n=2)**	**Scaffold Proteins**
RAW264.7	2.95e-4 s^{-1}	2.9e-4 s^{-1}	2.3e-4 s^{-1}	5.9e-4 s^{-1}
J774A.1	1.3e-4 s^{-1}	1.2e-4 s^{-1}	9.5e-5 s^{-1}	*no fit*
Ratio	2.3	2.4	2.4	*n/a*

V. Discussion and Conclusions

Discussion

The mitogen-activated protein kinase (MAPK) pathways mediate critical intracellular communication to enable regulatory functions such as gene expression, survival and apoptosis. The broad capability of *Bacillus anthracis* to suppress cellular and system-wide immune response hinges first on the pathogen's ability to use the macrophage as a Trojan horse in its attack on the immune system. While decades of laboratory analysis have advanced the general understanding of the pathogenesis of inhalational anthrax, the role of the toxin components, and the cytotoxic mechanisms resulting in apoptosis are still unclear. Advances in genomic and proteomic technologies led to the mapping of the human genome, and in the post-genome era a plethora of data can be generated on cellular components and their functions. With computer technology and the development of computational methods, these reserves of biochemical data have made mathematical modeling of complete microorganisms a possibility.

Such advanced models must be built in phases. Some systems modelers apply the top-down approach of establishing a far-reaching model and then applying simplifications until the behavior of concern can be seen in the system, enabling them to see what biomolecular components play a role in the behavior. As in the case of the MAPK models, some biologists conduct research using the bottom-up approach of modeling a single signal transduction pathway to study it for unexpected behaviors, form testable hypotheses, and guide laboratory analysis that will facilitate additional improvements to

the modeling process. Within this research, no unique microbiological study was conducted for comparison; these models were developed with previously published *in vitro* viability data for RAW264.7 macrophages and J774A.1 macrophages that were incubated after phagocytosis of LF-producing spores. Models are often based on data collected for a specific MAPK isoform, but stimulants are not generally isoform-specific and inhibitors can have unpredicted effects that influence the results. The various MAPKK isoforms are treated here as a single chemical species because LF acts destructively on nearly all MAPKKs, because the redundancies and cross-over interactions between pathways are not well defined, and because no MAPK models exist that would support a more detailed, isoform-specific model.

The three MAPK models investigated here exhibit specific characteristics (ultrasensitivity, negative feedback and scaffold proteins) and were developed by their respective authors for the purpose of studying these respective aspects of the MAPK pathway. By adding the depletion of MAPKKs by anthrax lethal factor (LF), the known inhibition of the MAPK signal output is be observed, and the reaction rate constant for MAPKK cleavage has been approximated. For the scaffold protein model, only one cell line's viability could be matched, and the resultant approximation of the rate constant from that parameterization is twice that estimated by the other two models. Presumably due to the dominance of bound substrates that are unavailable for cleavage, the model does not adequately capture the behavior of the system. However, the ultrasensitivity and negative feedback models both exhibited similar behavior and ability to match both cell viability data sets. The application of a stronger negative feedback mechanism in the

oscillating models results in a lower minimum active MAPK concentration but does not alter the periodicity of the oscillations. Without more data on cell viability, either more information regarding the error or more time points over the duration of the experiment, both formulations for negative feedback must be considered equally able to reflect system behavior. The negative feedback model does present a challenge because the average of the oscillations must be used to fit the data and because change of curve shape is more difficult to define. In general, the two simple cascade models are equally capable of fitting the data. The application of the model would likely influence selection. A study of the kinetics inside a cell, such as might be used to study the effect of changes in the expression of immunoregulatory genes, may apply the negative feedback model for its more accurate reflection of intracellular interactions. Comparatively, a study using cultures or approximating the effects of cytokines in tissue would observe a multitude of cells signaling and expressing cytokines simultaneously, and may apply the ultrasensitivity model for a better approximation of the overall chemical concentration contributing to the effects observed in the system.

Excluding the scaffold model, the approximations for the kinetic constants are reasonably consistent. For the RAW264.7 cell line, the LF cleavage reaction occurred at a rate of approximately 3.0e-4 s^{-1} using both the ultrasensitivity and the n=1 negative feedback model. These two models resulted in rates of 1.2e-4 s^{-1} and 1.3e-4 s^{-1}, respectively, for the J774A.1 macrophages. (This close agreement between the two models hints that the action by which MAPK inhibits cascade activation may be a single phosphorylation and not equivalent to cooperative inhibition.) The stronger negative

feedback when n=2 resulted in slightly lower estimates of the rate constants (2.4e-4 s^{-1} for RAW264.7, and 9.7e-5 s^{-1} for J774A.1), which is to be expected since stronger self-regulated inhibition by the pathway output reduces the amount of inhibition work that must be done by LF. Specific concentrations used by the authors in the different models did result in different output (MAPK-PP concentration) seen in the results section, but the different parameter values did not appear to significantly affect the estimates of LF reactivity, an aspect of system behavior. While the increased internal negative feedback did not significantly change the oscillations, the increased internal negative feedback does appear to affect the ability of the system to resist interference.

In the third model, the MAPKKs bound with scaffold proteins are a significant pool of the total available MAPKK population. This effectively limits the elimination of MAPPKs by LF, so inhibition in RAW cells could only be achieved by applying a rate constant of 5.9e-4 s^{-1}, which is twice that estimated in the other two models. The inability of the scaffold model to fit the data for the second cell line indicates that the application of the model does not accurately reflect system behavior and makes the rate constant estimate for the first cell line suspect. The complexity of the scaffold model was much greater than that of the other two; the level of detail in the kinetics added should likely be on par with the kinetics of the base model to obtain reliable results. Model accuracy depends on whether a model correctly defines the underlying biochemical relationships, such as the identification of feedback loops, because it is the structure of the model that determines system behavior. The inclusion of structural aspects

(biochemical species and interactions) that are not relevant to the investigative question should be omitted, so as to not overshadow or overpower the behavior being analyzed.

The estimated rate constants for the reaction between LF and MAPKK also exhibit an interesting trend: for the ultrasensitivity and negative feedback models, respectively, the reaction rate is estimated as being 2.3 and 2.4 times higher within the RAW264.7 macrophages than within the J774A.1 macrophages. The use of stronger feedback loop did have a minor effect on the estimated rate constant; but both of the inhibition parameter values (n=1 and n=2) provided a ratio of 2.4 between the two cell lines' reaction rates. The model's consistent estimation of a kinetic parameter's value under differing inhibitory strengths indicates an ability of this systems biology model to predict approximate relative susceptibility of a cell type to anthrax infection or toxin effects. The ultrasensitivity-based host-pathogen model can be used to guide research for inhalational anthrax in cultures of human alveolar macrophages, the cell type of interest in development of a human dose-response model. The ability to predict relative susceptibility between cell types should also apply to cells from different species. Knowing the relative susceptibility of the cells that facilitate the development of disease, the models would then also be able to increase confidence in the extrapolation of *in vivo* animal data regarding pathogenesis as well as therapeutic agents and the manipulation of gene expression as methods to combat infection.

Significance of Research

This research presents what is believed to be the first host-pathogen systems biology model of anthrax infection. Though a great deal of work must first be done to

achieve it, the goal from a toxicologist's or emergency responder's perspective is a human dose-response model that enables accurate health risk assessments following an intentional aerosol release of anthrax spores. Models of transport of the bacteria to the lymph nodes by macrophages and of systemic infection must first be accomplished. For this model, the approximated kinetic parameters may provide guidance in future research to quantify the rate constants for these cell lines and possibly others. As just discussed, the ability of the models to provide consistent approximations of relative susceptibility to infection may promote the use of systems models to increase confidence in extrapolation between cell types, tissue sources, or species. This model can serve as the starting point for expanding the model to include changes in cytokine expression due to MAPK inhibition, to add edema factor and protective antigen interactions, or to integrate the cell surface receptors that are bound by protective antigen and permit the entry of the toxins. LF can be added as a chemical species to develop concentration-dependent dose-response models for evaluation of cellular effects other than apoptosis or necrosis or for evaluation of therapeutic agents, such as those that would bind LF, inhibit MAPKK proteolysis, or up- and down-regulate genes to counteract the effects of MAPK inhibition.

Recommendations for Future Research

More cell viability data is needed to validate the models' predictive power. Biological variability is compounded by analysis being conducted *in vitro*, outside of the actual environment of infection and in the absence of other stimuli and factors that exist *in vivo*. The human alveolar macrophage would be the best model for co-culture of *Bacillus anthracis*. For any cell type tested, more time point analyses are needed to

present a better picture of behavior that can be used to tune and validate models. Because many other stimuli exist and can activate or suppress MAPK signal pathways, cell viability data for macrophages exposed to purified LF or LT would also be beneficial so that the kinetic parameter estimates could be more confidently attributed to the LF-MAPKK interactions rather than signaling effects due to other stimuli or inhibitors.

Within cell signaling work, the complete interactions of the MAPK cascade, such as the negative feedback loop, must be included to correctly predict system behavior. Research should continue to increase understanding of the intra-cascade interactions and identify other possible positive or negative feedback loops. Though nearly all MAPKKs are cleaved by LF, not all MAPKKs have been implicated in immune response regulation. An isoform-specific MAPK model may better be able to predict cell death and other effects, such as cytokine suppression. This effort may be worth a second attempt if such a detailed model becomes available. Also regarding specificity of LF interactions, this paper questioned the possibility of LF reacting differentially with the bi-, mono-, and unphosphorylated forms of MAPKK. Binding can change the shape of a protein, and phosphorylation changes the mass and thereby possibly diffusion, therefore this possibility may require further investigation. Also, a more complete kinetic model that includes the LF interactions with scaffold-bound MAPKKs is needed to more accurately represent the true intracellular signaling mechanisms.

Summary

Host-pathogen systems biology provides a holistic approach to understanding the dynamic response of a cell to pathogenic challenge and, in the case of *B anthracis*, to

toxins that make infection possible by manipulating the intracellular signal network. This work has expanded on the first model by Robinson *et al* by including all of the phosphorylated states of MAPKK as substrates of the proteinase, LF. While attempting to find one 'best' model to reflect the behavior of macrophages, two host-pathogen models have been developed, parameterized and found acceptable for investigating the inhibition of MAPK signaling by anthrax LF. The ultrasensitivity and negative feedback models can now both be used in additional modeling efforts such as adding edema factor interactions, TNF-α inhibition, or LF concentration-dependence to gain a more complete and accurate approximation of the biological system's behavior. Both of these models can be used concomitantly with empirical data to reflect macrophage system behavior and estimate unknown parameters with seeming consistency, even between cell types. The two models can now also be used for aiding *in vitro* experimental design, such as for the determination of a range of enzyme concentrations under which a given behavior can be observed. This work confirms that parameter estimates can generally be made irrespective of the specific chemical species and parameter values applied in the starting model. In conclusion, both parameterized models for inhibition of the MAPK cascade by lethal factor can be used as a foundation for advancing toward a more complete anthrax-macrophage host-pathogen systems biology model.

Appendix A: Glossary of Terms, Acronyms and Abbreviations

Definitions contained in this appendix are blended from two medical dictionaries, *The American Heritage Stedman's Medical Dictionary* (2nd edition) and *Dorland's Illustrated Medical Dictionary,* which is provided on-line through Merck & Co, unless otherwise specifically cited. Other references included and specifically cited, where applicable, include: *Molecular Cell Biology* by Lodish and others; *Immunobiology* (5th edition) by Janeway and others; *The Cell: A Molecular Approach* (2nd edition) by Cooper; and *Casarett & Doull's Essentials of Toxicology* by Klaassen and Watkins. A list of acronyms and abbreviations are also provided after the definitions.

Term/Acronym	Definition
adaptive (acquired) immunity	Immunity obtained from the specialized lymphocytes and resultant antibodies which are activated by innate immune cells in response to an antigen; or obtained from the transmission of antibodies, as from mother to fetus through the placenta; able to protect from and provide increased immune response to future infection by the specific antigen (Klaassen and Watkins, 2003)
alveolar macrophage (AM)	Rounded, mononuclear, vigorously phagocytic macrophage in alveoli that ingests inhaled particulate matter
andenylate cyclase	Membrane-bound enzyme that catalyzes formation of cyclic AMP (cAMP) from ATP; also called adenylyl cyclase. Binding of certain ligands to their cell-surface receptors leads to activation of adenylyl cyclase and a rise in intracellular cAMP (Lodish and others, 2000)
antibody (Ab)	Molecule that reacts with a specific antigen, such as a bacterium or a toxin, that induced its synthesis or with similar molecules; destroys or weakens bacteria and neutralizes organic poisons, forming the basis of immunity; synthesized by B cells that have been activated by the binding of an antigen to a cell-surface receptor; also known collectively as immunoglobulins (Ig)
antigen (Ag)	Any of various substances (such as toxins, bacteria, or cells of transplanted organs) that induce a specific immune response (production of antibodies) when introduced to the body and can react or be bound by that specific antibody; named by their ability to cause **anti**body **gen**eration
antigen-presenting cell (APC)	Cells that can process antigens and present the fragments on the cell surface with molecules required for T-cell activation; dendritic cells, macrophages, and B cells are all capable of serving as APCs for T cells, but dendritic cells are more specialized and often synonymous with the term 'professional antigen-presenting cell' (Janeway and others, 2001)
B cell	A lymphocyte that differentiates into a plasma cell able to synthesize a specific antibody which will react with the specific antigen that stimulated the B cell

Term/Acronym	Definition
cAMP-response element-binding (CREB) protein	A transcription factor activated by the catalytic subunit of PKA, which is activated by cAMP
chemokine	Any of various chemoattractant cytokines produced in inflammatory response that mobilize and activate cells, especially phagocytes and lymphocytes (Janeway and others, 2001)
chemotaxis	Movement or orientation of an organism or cell along a chemical concentration gradient, either toward or away from the stimulus
cyclic adenosine monophosphate (cAMP)	An intracellular signaling molecule that increases in concentration in response to the binding of G protein-coupled receptors, subsequently activating protein kinase A (PKA) (Lodish and others, 2000)
cytokine	Any non-antibody protein released on contact with a specific antigen; acts as an intercellular mediator such as is the generation of an immune response
cytolysis	The destruction of a cell
cytotoxic	Relating to, or producing a toxic effect on cells
cytotoxic T cell	See T cells; sometimes cytotoxic T leukocyte, or CTL
cytotoxicity	Degree of destructive action by an agent on certain cells
cytotoxin	A T-cell produced protein with a specific toxic effect on target cells (Janeway and others, 2001)
dendritic cells (DC)	Immune cells derived from monocytes or from bone marrow precursors to monocytes; present in skin, lungs, stomach and intestines in small numbers; constantly sample their surroundings for pathogens; phagocytose pathogens, digest pathogen proteins, migrate to lymphoid tissues where they present the protein fragments on the cell surface and signal to activate lymphocyte transformation into specific T cells and B cells; mature upon contact with pathogens, developing dendritic arms for increased surface area for lymphocyte interaction; known as professional antigen-presenting cells (APC) (Hart, 1997)

Term/Acronym	Definition
domain	A tertiary protein structure from folds causing dense clusters of secondary structures, forming distinct regions on a protein; often defined by the included amino acids, by a specific motif, or by its function (catalysis or binding) (Lodish and others, 2000)
endocytosis	Uptake of extracellular material into the cytosol through vesicles (pores) formed in the plasma membrane (Lodish and others, 2000)
endotoxic shock	Shock associated with overwhelming infection and subsequent release of endotoxins by gram-negative bacteria that causes sequestration of blood in the capillaries and veins
endotoxin	Toxin existing as part of the cell membrane of bacteria and released upon destruction of the bacterial cell; less potent than exotoxins
fibroblast	Common cell found in connective tissue; secretes collagen and other components of the extracellular matrix; migrates and proliferates during wound healing (Lodish and others, 2000)
helper T cell	Lymphocyte that makes lymphokines to regulate other immune cells, such as B cells and monocytes; "necessary for the differentiating of B cells into antibody-producing cells"; also T-helper cell, T_h cell, or Th1 cell (*The American Heritage Stedman's Medical Dictionary*, 2004)
immunoglobulin (Ig)	See antibody (Ab); divided into five major classes (IgA, IgD, IgE, IgG, and IgM) with unique structures and antigenic functions (Lodish and others, 2000)
inhibitor	Substance that inhibits, reduces or limits physiological, chemical, or enzymatic action (reaction rate, enzyme catalytic activity, growth of microorganisms)
innate immunity	Immunity that occurs naturally via physical and biochemical barriers of the body, such as skin and the mucociliary escalator, as well as nonspecific immune cells, such as monocytes/macrophages, neutrophils, and dendritic cells, and does not arise from an immunologic memory of previous infection or vaccination (Klaassen and Watkins, 2003)

Term/Acronym	Definition
interferon	Antiviral glycoprotein cytokine produced in response stimuli, such as viruses, bacteria or endotoxins, and that binds to receptors on target cells so as to interfere with viral replication in the cells and, in some cases, modulate specific cellular immune functions
interleukin (IL)	"Any of a class of lymphokines that act to stimulate, regulate, or modulate lymphocytes such as T cells" (*The American Heritage Stedman's Medical Dictionary*, 2004)
kinase	Any of various enzymes that transfer a phosphate group from a donor, such as ADP or ATP, to an acceptor; named for the acceptor molecule such that a kinase which catalytically phosphorylates a protein is a protein kinase
leukocyte	Any of various forms of white blood cells, such as lymphocytes, monocytes, macrophages, and neutrophils, that function as protection against infection by microorganisms; capable of amoeboid movement
lipopolysaccharide (LPS)	an endotoxin derived from Gram-negative bacteria and commonly used as a macrophage activator, due to its ability to induce a strong response in immune cells and induce proinflammatory cytokines in macrophages
lymphocyte	Mononuclear, non-granular white blood cell produced in lymphoid tissue (lymph nodes, spleen, thymus, tonsils) and functioning in the development of immunity by transformation to T cells or B cells; make up 22-28% of white blood cells in humans
lymphokine	General term for soluble proteins that are released by sensitized lymphocytes on contact with specific antigens; mediate transformation of additional lymphocytes and play a role in monocyte and macrophage activity
macrophage	Any of large, mononuclear, highly phagocytic cells derived from monocytes that occur in the walls of blood vessels and loose connective tissue; usually immobile but become actively mobile when stimulated by inflammation; interact with lymphocytes to facilitate antibody production
mitogen	Agent that stimulates mitosis and lymphocyte transformation

Term/Acronym	Definition
monocyte	Large, mononuclear, circulating, phagocytic white blood cell with fine granulation in the cytoplasm; formed in the bone marrow, transported to tissues, then develop into macrophages or dendritic cells; make up 3-8% of white blood cells in humans
motif	In a protein, a specific combination of and three-dimensional configuration of secondary structures (where primary structure is the sequence of amino acids in the protein's polypeptide chain, and secondary structure is a molecular shape such as a helix, sheet, turn, or loop that is stabilized by hydrogen bonds) (Lodish and others, 2000; Cooper, 2000)
murine	Of, relating to, or transmitted by a member of the rodent family
natural killer (NK) cells	Large granular, non-specialized lymphocytes (innate immune cells, unlike T and B lymphocytes) that detect and kill pathogen-infected cells and certain tumor cells (Janeway and others, 2001)
neutrophil	Granular, highly phagocytic, highly pathogen-destructive white blood cell playing an important role in killing extracellular pathogens; "the major class of white blood cell in human peripheral blood" and responsible for recruiting macrophages if unable to contain and infection; also known as polymorphonuclear cells (PMNs) or neutrophilic PMNs (Janeway and others, 2001)
phagocytosis	Process by which extracellular materials, particles or pathogens are internalized, usually by macrophages or neutrophils; bacteria are taken up into a vesicle called a phagosome to be destroyed by lysosomal enzymes (Janeway and others, 2001)
phosphorylation	Addition of a phosphate group to a molecule by a phosphorylase or kinase, especially in the case of activation of an enzyme by addition of one or more phosphate groups to specific amino acids
phosphotase	An enzyme that catalytically removes a phosphate group from a substrate; named for the substrate upon which dephosphorylation is performed such that a kinase phosphotase removes the phosphate group from a kinase, thereby deactivating it (Janeway and others, 2001)

Term/Acronym	Definition
platelet	Cytoplasmic body having no nucleus or DNA, but having mitochondria and active enzymes, that is found in blood plasma and that promotes blood clotting; also called a thrombocyte
protein kinase A (PKA)	Any of a family of inactive protein kinases which dissociates and releases two catalytic subunits when bound on regulatory subunits by cAMP; the released catalytic subunits then phosphorylate various proteins, including in the nucleus; also known as cAMP-dependent protein kinase (cAPK) (Lodish and others, 2000)
T cell	A principal lymphocyte developed in the thymus and transported in the blood to lymphoid tissues where they have various adapted immune system roles such as identification of antigens and activation and deactivation of other immune cells; considered naïve T cells until they specialize upon exposure to an antigen, at which time the naive cell can proliferate and differentiate into cytotoxic T cells, which are capable of killing other cells, or helper T cells (see definition)
transcription factor	Non-RNA polymerase protein that initiates or regulates gene transcription (Lodish and others, 2000)
tumor necrosis factor (TNF)	Cytokine that induces programmed cell death, especially in tumor cells, but also makes inflammatory disease worse; most often produced by macrophages in the presence of an endotoxin (Janeway and others, 2001)
TNF-α	Cytokine with multiple immune functions which is produced by macrophages and activated T cells; primary member of the TNF family of cytokines (Janeway and others, 2001)

Ab	Antibody
Ag	Antigen
AM	Alveolar macrophage
APC	Antigen presenting cell
AT	Anthrax toxin

Term/Acronym	Definition
cAMP	Cyclic adenosine monophosphate; also cyclic AMP
CREB	cAMP-response element-binding (CREB) protein
DC	Dendritic cells
EF	See edema factor
ERK	Extracellular signal-regulated kinase
ET	Edema toxin
LF	Lethal factor
LPS	Lipopolysaccharide
LT	Lethal toxin
MAPK	Mitogen-activated protein kinase
MAPKK	MAPK kinase
MAPKKK	MAPK kinase kinase
MAPK-P	Inactive MAPK with a single phosphate group
MAPK-P'ase	MAPK phosphotase, which dephosphorylates (inactivates) MAPK
MAPK-PP	Dual phosphorylated and thus activated MAPK
NK	Natural killer cells
PKA	Protein kinase A
PA	Protective antigen
TNF	Tumor necrosis factor

Appendix B: Method for Translating SBML Models

Translation of SBML and JDesigner models into Berkeley Madonna was achieved by modifying the relevant code using the following procedures. Madonna has help files with basic instructions on editing and application of equations, such as performing integrations and using exposure parameters (concentrations, durations, repetitions). A complete software user guide is also available on the Madonna website.

1. Open a new file in Madonna and, replacing the default code of the new file, paste in the following:

```
;Parameters for simulated experiment
length = 12           ;Length of inhalation exposure (hrs)
interval = 24
method stiff        ;Rosenbrock stiff solver
starttime = 0
stoptime = 24
dtmin = 0.0001        ;minimum (and initial) step size
dtmax=1               ;maximum step size
tolerance=0.0001      ;error tolerance for stiff solver
dtout=0.1           ;communication interval (optional)
deltaT = stepsize   ;allows plotting step sizes used as
                      deltaT(optional)
interval = 24
```

   The last two lines allow repeated exposure scenarios to be modeled, such as daily exposures (24 h interval).

2. In JDesigner, view the model equations (*View -> View Model Equations*). Cut and paste from this window into a newly created text file. If necessary, omit (or comment out) the moiety conservation equations. Changing the equations to comments can be achieved by placing a semicolon at the start of each line.

3. In JDesigner, select the second 'Export…' option from the File drop down menu; select the Jarnac tab in the resulting window. The 'Display Translation' button at the bottom of the window must be selected to display the code. Cut and paste the code related to the parameter initial values (the lines beginning with 'p.', ignore the model equations). The "p.compartment = 1;" equation code should be not be included.

4. Edit the resulting text file according to the following.

    a. Replace // with ; to convert comment lines.

    b. Replace "p.X = x" with "init X = x", where X is a chemical parameter and x is its initial concentration at t = 0. Replace "p.Y = y" with "Y = y", where Y is a kinetic reaction constant and y is the value of the constant.

    c. Replace "dX/dT" with " X' " (using the prime in Madonna to denote a derivative).

    d. Replace "v[X]" with "X".

    e. Some mathematical expressions may also need to be changed. In Michaelis-Menten kinetic models, "pow(X,n)" becomes "X^n".

5. Paste resulting text file into the Madonna file below the code from step one above.

6. Co-ordinate exposure parameters, if necessary.

7. Run the program. By default, Madonna plots the first two variables listed when the program is run. Other variables can be selected for viewing using the buttons in the graph window.

Example Translation

This example is based on the oscillating model (Kholodenko, 2000) downloaded from BioModels and imported into JDesigner for translation into Berkeley Madonna (without the addition of LF-MAPKK cleavage reactions in JDesigner as described in Chapter III).

The model equations as displayed in JDesigner are:

```
// Reaction Rates:
v[J0] = uVol*J0_V1*MKKK/((1+pow(MAPK_PP/J0_Ki,J0_n))*(J0_K1+MKKK))
v[J1] = uVol*J1_V2*MKKK_P/(J1_KK2+MKKK_P)
v[J2] = uVol*J2_k3*MKKK_P*MKK/(J2_KK3+MKK)
v[J3] = uVol*J3_k4*MKKK_P*MKK_P/(J3_KK4+MKK_P)
v[J4] = uVol*J4_V5*MKK_PP/(J4_KK5+MKK_PP)
v[J5] = uVol*J5_V6*MKK_P/(J5_KK6+MKK_P)
v[J6] = uVol*J6_k7*MKK_PP*MAPK/(J6_KK7+MAPK)
v[J7] = uVol*J7_k8*MKK_PP*MAPK_P/(J7_KK8+MAPK_P)
v[J8] = uVol*J8_V9*MAPK_PP/(J8_KK9+MAPK_PP)
v[J9] = uVol*J9_V10*MAPK_P/(J9_KK10+MAPK_P)
```

```
// Differential Equations:
dMKKK/dt = - J0 + J1
dMKK/dt = - J2 + J5
dMKK_P/dt = + J2 - J3 + J4 - J5
dMAPK/dt = - J6 + J9
dMAPK_P/dt = + J6 - J7 + J8 - J9
dMKKK_P/dt = + J0 - J1
dMKK_PP/dt = + J3 - J4
dMAPK_PP/dt = + J7 - J8

// Conservation Laws:
1: MKKK + MKKK_P
2: MKK + MKK_P + MKK_PP
3: MAPK + MAPK_P + MAPK_PP
```

The parameter values (excluding p.compartment) from the exported Jarnac script are:

```
p.uVol = 1;
p.MKKK = 90;
p.MKKK_P = 10;
p.MKK = 280;
p.MKK_P = 10;
p.MKK_PP = 10;
p.MAPK = 280;
p.MAPK_P = 10;
p.MAPK_PP = 10;
p.J0_V1 = 2.5;
p.J0_Ki = 9;
p.J0_n = 1;
p.J0_K1 = 10;
p.J1_V2 = 0.25;
p.J1_KK2 = 8;
p.J2_k3 = 0.025;
p.J2_KK3 = 15;
p.J3_k4 = 0.025;
p.J3_KK4 = 15;
p.J4_V5 = 0.75;
p.J4_KK5 = 15;
p.J5_V6 = 0.75;
p.J5_KK6 = 15;
p.J6_k7 = 0.025;
p.J6_KK7 = 15;
p.J7_k8 = 0.025;
p.J7_KK8 = 15;
p.J8_V9 = 0.5;
p.J8_KK9 = 15;
p.J9_V10 = 0.5;
p.J9_KK10 = 15;
```

The final Madonna file, after editing, looks like the following:

```
; Parameters for simulated experiment
method stiff        ;Rosenbrock stiff solver
starttime = 0
stoptime = 24
dtmin = 0.0001      ;minimum (and initial) step size
dtmax=1             ;maximum step size
tolerance=0.0001            ;error tolerance for stiff solver
dtout=0.1           ;communication interval (optional)

; Reaction Rates:
J0 = uVol*J0_V1*MKKK/((1+(MAPK_PP/J0_Ki)^(J0_n))*(J0_K1+MKKK))
J1 = uVol*J1_V2*MKKK_P/(J1_KK2+MKKK_P)
J2 = uVol*J2_k3*MKKK_P*MKK/(J2_KK3+MKK)
J3 = uVol*J3_k4*MKKK_P*MKK_P/(J3_KK4+MKK_P)
J4 = uVol*J4_V5*MKK_PP/(J4_KK5+MKK_PP)
J5 = uVol*J5_V6*MKK_P/(J5_KK6+MKK_P)
J6 = uVol*J6_k7*MKK_PP*MAPK/(J6_KK7+MAPK)
J7 = uVol*J7_k8*MKK_PP*MAPK_P/(J7_KK8+MAPK_P)
J8 = uVol*J8_V9*MAPK_PP/(J8_KK9+MAPK_PP)
J9 = uVol*J9_V10*MAPK_P/(J9_KK10+MAPK_P)
J10 = J10_KX*MKK

; Differential Equations:
MKKK' = - J0 + J1
MKK' = - J2 + J5 - J10
MKK_P' = + J2 - J3 + J4 - J5
MKK_PP' = + J3 - J4
MAPK' = - J6 + J9
MAPK_P' = + J6 - J7 + J8 - J9
MKKK_P' = + J0 - J1
MAPK_PP' = + J7 - J8
Cleaved_MKK' = + J10

; Initial values
init uVol = 1;
init MKKK = 90;
init MKKK_P = 10;
init MKK = 280;
init MKK_P = 10;
init MKK_PP = 10;
init MAPK = 280;
init MAPK_P = 10;
init MAPK_PP = 10;
init Cleaved_MKK = 0;
J0_V1 = 2.5;
J0_Ki = 9;
J0_n = 1;
```

```
J0_K1 = 10;
J1_V2 = 0.25;
J1_KK2 = 8;
J2_k3 = 0.025;
J2_KK3 = 15;
J3_k4 = 0.025;
J3_KK4 = 15;
J4_V5 = 0.75;
J4_KK5 = 15;
J5_V6 = 0.75;
J5_KK6 = 15;
J6_k7 = 0.025;
J6_KK7 = 15;
J7_k8 = 0.025;
J7_KK8 = 15;
J8_V9 = 0.5;
J8_KK9 = 15;
J9_V10 = 0.5;
J9_KK10 = 15;
J10_KX = 0.00025;
```

Appendix C: Berkeley Madonna Code for Models

Each model was converted to code able to be imported into Berkeley Madonna (version 8.3.11) following the procedures in Appendix B. This appendix includes the code for each model as exported from Berkeley Madonna; while parameter values were varied according to the discussion in Chapters III and IV, the code included here reflects only one value per parameter.

Ultrasensitivity Model

```
; Huang (3 RXN) with LF cleavage of MAPKK, _P, and _PP

; Parameters for simulated experiment
method stiff                ;Rosenbrock stiff solver
starttime = 0
stoptime = 54000
dtmin = 0.1                 ;minimum (and initial) step size
dtmax=5                     ;maximum step size
tolerance=0.0001            ;error tolerance for stiff solver
dtout=5             ;communication interval, optional (included to alleviate insufficient memory errors)

; Initial values
init PP_K = 0;
init Cleaved_MAPKKs = 0;
init E1 = 3E-05;
init E2 = 0.0003;
init KKK = 0.003;
init P_KKK = 0;
init KK = 1.2;
init P_KK = 0;
init PP_KK = 0;
init K = 1.2;
init P_K = 0;
init KPase = 0.12;
init KKPase = 0.0003;
init E1_KKK = 0;
init E2_P_KKK = 0;
init P_KKK_KK = 0;
init P_KKK_P_KK = 0;
init PP_KK_K = 0;
init PP_KK_P_K = 0;
init KKPase_PP_KK = 0;
init KKPase_P_KK = 0;
init KPase_PP_K = 0;
```

```
init KPase_P_K = 0;
r1a_a1 = 1000;
r1a_d1 = 150;
r1b_k2 = 150;
r2a_a2 = 1000;
r2a_d2 = 150;
r2b_k2 = 150;
r3a_a3 = 1000;
r3a_d3 = 150;
r3b_k3 = 150;
r4a_a4 = 1000;
r4a_d4 = 150;
r4b_k4 = 150;
r5a_a5 = 1000;
r5a_d5 = 150;
r5b_k5 = 150;
r6a_a6 = 1000;
r6a_d6 = 150;
r6b_k6 = 150;
r7a_a7 = 1000;
r7a_d7 = 150;
r7b_k7 = 150;
r8a_a8 = 1000;
r8a_d8 = 150;
r8b_k8 = 150;
r9a_a9 = 1000;
r9a_d9 = 150;
r9b_k9 = 150;
r10a_a10 = 1000;
r10a_d10 = 150;
r10b_k10 = 150;
J20_k = 0.000295; MKK cleavage
J21_k = 0.000295; MKK_P cleavage
J22_k = 0.000295; MKK_PP cleavage
compartment = 1;

; Reaction Rates:
r1a = compartment*(r1a_a1*E1*KKK-r1a_d1*E1_KKK)
r1b = compartment*r1b_k2*E1_KKK
r2a = compartment*(r2a_a2*E2*P_KKK-r2a_d2*E2_P_KKK)
r2b = compartment*r2b_k2*E2_P_KKK
r3a = compartment*(r3a_a3*KK*P_KKK-r3a_d3*P_KKK_KK)
r3b = compartment*r3b_k3*P_KKK_KK
r4a = compartment*(r4a_a4*P_KK*KKPase-r4a_d4*KKPase_P_KK)
r4b = compartment*r4b_k4*KKPase_P_KK
r5a = compartment*(r5a_a5*P_KK*P_KKK-r5a_d5*P_KKK_P_KK)
r5b = compartment*r5b_k5*P_KKK_P_KK
r6a = compartment*(r6a_a6*PP_KK*KKPase-r6a_d6*KKPase_PP_KK)
r6b = compartment*r6b_k6*KKPase_PP_KK
r7a = compartment*(r7a_a7*K*PP_KK-r7a_d7*PP_KK_K)
r7b = compartment*r7b_k7*PP_KK_K
r8a = compartment*(r8a_a8*P_K*KPase-r8a_d8*KPase_P_K)
r8b = compartment*r8b_k8*KPase_P_K
r9a = compartment*(r9a_a9*P_K*PP_KK-r9a_d9*PP_KK_P_K)
r9b = compartment*r9b_k9*PP_KK_P_K
```

```
r10a = compartment*(r10a_a10*PP_K*KPase-r10a_d10*KPase_PP_K)
r10b = compartment*r10b_k10*KPase_PP_K
J20 = J20_k*KK
J21 = J21_k*P_KK
J22 = J22_k*PP_KK

; Differential Equations:
E1' = - r1a + r1b
E2' = - r2a + r2b
KKK' = - r1a + r2b
P_KKK' = + r1b - r2a - r3a + r3b - r5a + r5b
KK' = - r3a + r4b - J20
P_KK' = + r3b - r4a - r5a + r6b - J21
PP_KK' = + r5b - r6a - r7a + r7b - r9a + r9b - J22
K' = - r7a + r8b
P_K' = + r7b - r8a - r9a + r10b
PP_K' = + r9b - r10a
KPase' = - r8a + r8b - r10a + r10b
KKPase' = - r4a + r4b - r6a + r6b
P_KKK_KK' = + r3a - r3b
PP_KK_K' = + r7a - r7b
KKPase_PP_KK' = + r6a - r6b
KPase_PP_K' = + r10a - r10b
E2_P_KKK' = + r2a - r2b
PP_KK_P_K' = + r9a - r9b
E1_KKK' = + r1a - r1b
KKPase_P_KK' = + r4a - r4b
P_KKK_P_KK' = + r5a - r5b
KPase_P_K' = + r8a - r8b
Cleaved_MAPKKs' = + J20 + J21 + J22
```

Oscillating Negative Feedback Model

```
; LF cleavage of MAPKK, MAPKK-P, and MAPK-PP (Kholodenko, 2000)

; Parameters for simulated experiment
method stiff            ;Rosenbrock stiff solver
starttime = 0
stoptime = 72000
dtmin = 0.0001          ;minimum (and initial) step size
dtmax=1                 ;maximum step size
tolerance=0.0001        ;error tolerance for stiff solver
dtout=0.1               ;communication interval (optional)

; Initial values of enzymes and assigned values of kinetic constants
init MAPK_PP = 10;
init Cleaved_MKK = 0;
init MKKK = 90;
init MKKK_P = 10;
init MKK = 280;
init MKK_P = 10;
init MKK_PP = 10;
init MAPK = 280;
init MAPK_P = 10;
```

```
uVol = 1;
J0_V1 = 2.5;
J0_Ki = 9;
J0_n = 1          ; n = 2 for cooperative inhibition by double phosphorylation of SOS by MAPK
J0_K1 = 10;
J1_V2 = 0.25;
J1_KK2 = 8;
J2_k3 = 0.025;
J2_KK3 = 15;
J3_k4 = 0.025;
J3_KK4 = 15;
J4_V5 = 0.75;
J4_KK5 = 15;
J5_V6 = 0.75;
J5_KK6 = 15;
J6_k7 = 0.025;
J6_KK7 = 15;
J7_k8 = 0.025;
J7_KK8 = 15;
J8_V9 = 0.5;
J8_KK9 = 15;
J9_V10 = 0.5;
J9_KK10 = 15;
J10_KK = 0.00015                ; kinetic constant (k) for LF cleavage of MAPKK
J11_KK_P = 0.00015              ; kinetic constant (k) for LF cleavage of MAPKK-P
J12_KK_PP = 0.00015             ; kinetic constant (k) for LF cleavage of MAPKK-PP

; Reaction Rates:
J0 = uVol*J0_V1*MKKK/((1+(MAPK_PP/J0_Ki)^(J0_n))*(J0_K1+MKKK))
J1 = uVol*J1_V2*MKKK_P/(J1_KK2+MKKK_P)
J2 = uVol*J2_k3*MKKK_P*MKK/(J2_KK3+MKK)
J3 = uVol*J3_k4*MKKK_P*MKK_P/(J3_KK4+MKK_P)
J4 = uVol*J4_V5*MKK_PP/(J4_KK5+MKK_PP)
J5 = uVol*J5_V6*MKK_P/(J5_KK6+MKK_P)
J6 = uVol*J6_k7*MKK_PP*MAPK/(J6_KK7+MAPK)
J7 = uVol*J7_k8*MKK_PP*MAPK_P/(J7_KK8+MAPK_P)
J8 = uVol*J8_V9*MAPK_PP/(J8_KK9+MAPK_PP)
J9 = uVol*J9_V10*MAPK_P/(J9_KK10+MAPK_P)
J10 = J10_KK*MKK                ; LF cleavage of MAPKK
J11 = J11_KK_P*MKK_P            ; LF cleavage of MAPKK-P
J12 = J12_KK_PP*MKK_PP          ; LF cleavage of MAPKK-PP

; Differential Equations:
MKKK' = - J0 + J1
MKK' = - J2 + J5 - J10
MKK_P' = + J2 - J3 + J4 - J5 - J11
MKK_PP' = + J3 - J4 - J12
MAPK' = - J6 + J9
MAPK_P' = + J6 - J7 + J8 - J9
MKKK_P' = + J0 - J1
MAPK_PP' = + J7 - J8
Cleaved_MKK' = + J10 + J11 + J12
```

Scaffold Proteins Model

```
; MAPK cascade with Scaffold protein, with LF cleavage of MAPKK, -P and -PP (non scaffold)
; (Levchenko and others, 2000)

;Parameters for simulated experiment
method stiff       ;Rosenbrock stiff solver
starttime = 0
stoptime = 54000
dtmin = 0.0001             ;minimum (and initial) step size
dtmax=2          ;maximum step size
tolerance=0.0001          ;error tolerance for stiff solver
dtout=1             ;communication interval (optional)

; Initial parameter values
init K_1_2 = 0;
init Cleaved_MAPKK = 0;
init MAPKP = 0.3;
init MEKP = 0.2;
init RAFK = 0.1;
init RAFP = 0.3;
init K_1_0 = 0.4;
init K_1_1 = 0;
init K_2_0 = 0.2;
init K_2_1 = 0;
init K_2_2 = 0;
init K_3_0 = 0.3;
init K_3_1 = 0;
init K_K_1_0_2_2 = 0;
init K_K_1_1_2_2 = 0;
init K_K_2_0_3_1 = 0;
init K_K_2_1_3_1 = 0;
init K_MAPKP_1_1 = 0;
init K_MAPKP_1_2 = 0;
init K_MEKP_2_1 = 0;
init K_MEKP_2_2 = 0;
init K_RAFK_3_0 = 0;
init K_RAFP_3_1 = 0;
init S_m1_m1_m1 = 0.1;
init S_m1_m1_0 = 0;
init S_m1_m1_1 = 0;
init S_m1_0_m1 = 0;
init S_m1_0_0 = 0;
init S_m1_0_1 = 0;
init S_m1_1_m1 = 0;
init S_m1_1_0 = 0;
init S_m1_1_1 = 0;
init S_m1_2_m1 = 0;
init S_m1_2_0 = 0;
init S_m1_2_1 = 0;
init S_0_m1_m1 = 0;
init S_0_m1_0 = 0;
init S_0_m1_1 = 0;
init S_0_0_m1 = 0;
```

```
init S_0_0_0 = 0;
init S_0_0_1 = 0;
init S_0_1_m1 = 0;
init S_0_1_0 = 0;
init S_0_1_1 = 0;
init S_0_2_m1 = 0;
init S_0_2_0 = 0;
init S_0_2_1 = 0;
init S_1_m1_m1 = 0;
init S_1_m1_0 = 0;
init S_1_m1_1 = 0;
init S_1_0_m1 = 0;
init S_1_0_0 = 0;
init S_1_0_1 = 0;
init S_1_1_m1 = 0;
init S_1_1_0 = 0;
init S_1_1_1 = 0;
init S_1_2_m1 = 0;
init S_1_2_0 = 0;
init S_1_2_1 = 0;
init S_2_m1_m1 = 0;
init S_2_m1_0 = 0;
init S_2_m1_1 = 0;
init S_2_0_m1 = 0;
init S_2_0_0 = 0;
init S_2_0_1 = 0;
init S_2_1_m1 = 0;
init S_2_1_0 = 0;
init S_2_1_1 = 0;
init S_2_2_m1 = 0;
init S_2_2_0 = 0;
init S_2_2_1 = 0;
init S_RAFK_m1_m1_0 = 0;
init S_RAFK_m1_0_0 = 0;
init S_RAFK_m1_1_0 = 0;
init S_RAFK_m1_2_0 = 0;
init S_RAFK_0_m1_0 = 0;
init S_RAFK_0_0_0 = 0;
init S_RAFK_0_1_0 = 0;
init S_RAFK_0_2_0 = 0;
init S_RAFK_1_m1_0 = 0;
init S_RAFK_1_0_0 = 0;
init S_RAFK_1_1_0 = 0;
init S_RAFK_1_2_0 = 0;
init S_RAFK_2_m1_0 = 0;
init S_RAFK_2_0_0 = 0;
init S_RAFK_2_1_0 = 0;
init S_RAFK_2_2_0 = 0;

J302_KK_k = 0.00059          ; LF cleavage of MAPKK
J301_KKP_k = 0.00059         ; LF cleavage of MAPKK-P
J303_KKPP_k = 0.00059        ; LF cleavage of MAPKK-PP
Cytoplasm = 1;
Reaction1_a1 = 1;
Reaction2_d1 = 0.4;
```

Reaction3_k1 = 0.1;
Reaction4_a2 = 0.5;
Reaction5_d2 = 0.5;
Reaction6_k2 = 0.1;
Reaction7_a3 = 3.3;
Reaction8_d3 = 0.42;
Reaction9_k3 = 0.1;
Reaction10_a4 = 10;
Reaction11_d4 = 0.8;
Reaction12_k4 = 0.1;
Reaction13_a5 = 3.3;
Reaction14_d5 = 0.4;
Reaction15_k5 = 0.1;
Reaction16_a6 = 10;
Reaction17_d6 = 0.8;
Reaction18_k6 = 0.1;
Reaction19_a7 = 20;
Reaction20_d7 = 0.6;
Reaction21_k7 = 0.1;
Reaction22_a8 = 5;
Reaction23_d8 = 0.4;
Reaction24_k8 = 0.1;
Reaction25_a9 = 20;
Reaction26_d9 = 0.6;
Reaction27_k9 = 0.1;
Reaction28_a10 = 5;
Reaction29_d10 = 0.4;
Reaction30_k10 = 0.1;
Reaction31_kon = 10;
Reaction32_koff = 0.5;
Reaction33_kon = 10;
Reaction34_koff = 0.5;
Reaction35_kon = 10;
Reaction36_koff = 0.5;
Reaction37_kon = 10;
Reaction38_koff = 0.5;
Reaction39_kon = 10;
Reaction40_koff = 0.5;
Reaction41_kon = 10;
Reaction42_koff = 0.5;
Reaction43_kon = 10;
Reaction44_koff = 0.5;
Reaction45_kon = 10;
Reaction46_koff = 0.5;
Reaction47_kon = 10;
Reaction48_koff = 0.5;
Reaction49_kon = 10;
Reaction50_koff = 0.5;
Reaction51_kon = 10;
Reaction52_koff = 0.5;
Reaction53_kon = 10;
Reaction54_koff = 0.5;
Reaction55_kpon = 0;
Reaction56_kpoff = 0.05;
Reaction57_kpon = 0;

```
Reaction58_kpoff = 0.05;
Reaction59_kpon = 0;
Reaction60_kpoff = 0.05;
Reaction61_kpon = 0;
Reaction62_kpoff = 0.05;
Reaction63_kpon = 0;
Reaction64_kpoff = 0.05;
Reaction65_kpon = 0;
Reaction66_kpoff = 0.05;
Reaction67_kpon = 0;
Reaction68_kpoff = 0.05;
Reaction69_kpon = 0;
Reaction70_kpoff = 0.05;
Reaction71_kpon = 0;
Reaction72_kpoff = 0.05;
Reaction73_kpon = 0;
Reaction74_kpoff = 0.05;
Reaction75_kpon = 0;
Reaction76_kpoff = 0.05;
Reaction77_kpon = 0;
Reaction78_kpoff = 0.05;
Reaction79_kpon = 0;
Reaction80_kpoff = 0.05;
Reaction81_kpon = 0;
Reaction82_kpoff = 0.05;
Reaction83_kpon = 0;
Reaction84_kpoff = 0.05;
Reaction85_kpon = 0;
Reaction86_kpoff = 0.05;
Reaction87_kpon = 0;
Reaction88_kpoff = 0.05;
Reaction89_kpon = 0;
Reaction90_kpoff = 0.05;
Reaction91_kpon = 0;
Reaction92_kpoff = 0.05;
Reaction93_kpon = 0;
Reaction94_kpoff = 0.05;
Reaction95_kpon = 0;
Reaction96_kpoff = 0.05;
Reaction97_kpon = 0;
Reaction98_kpoff = 0.05;
Reaction99_kpon = 0;
Reaction100_kpoff = 0.05;
Reaction101_kpon = 0;
Reaction102_kpoff = 0.05;
Reaction103_kon = 10;
Reaction104_koff = 0.5;
Reaction105_kon = 10;
Reaction106_koff = 0.5;
Reaction107_kon = 10;
Reaction108_koff = 0.5;
Reaction109_kpon = 0;
Reaction110_kpoff = 0.05;
Reaction111_kpon = 0;
Reaction112_kpoff = 0.05;
```

Reaction113_kpon = 0;
Reaction114_kpoff = 0.05;
Reaction115_kpon = 0;
Reaction116_kpoff = 0.05;
Reaction117_kpon = 0;
Reaction118_kpoff = 0.05;
Reaction119_kpon = 0;
Reaction120_kpoff = 0.05;
Reaction121_kon = 10;
Reaction122_koff = 0.5;
Reaction123_kon = 10;
Reaction124_koff = 0.5;
Reaction125_kon = 10;
Reaction126_koff = 0.5;
Reaction127_kpon = 0;
Reaction128_kpoff = 0.05;
Reaction129_kpon = 0;
Reaction130_kpoff = 0.05;
Reaction131_kpon = 0;
Reaction132_kpoff = 0.05;
Reaction133_kpon = 0;
Reaction134_kpoff = 0.05;
Reaction135_kpon = 0;
Reaction136_kpoff = 0.05;
Reaction137_kpon = 0;
Reaction138_kpoff = 0.05;
Reaction139_kon = 10;
Reaction140_koff = 0.5;
Reaction141_kon = 10;
Reaction142_koff = 0.5;
Reaction143_kon = 10;
Reaction144_koff = 0.5;
Reaction145_kpon = 0;
Reaction146_kpoff = 0.05;
Reaction147_kpon = 0;
Reaction148_kpoff = 0.05;
Reaction149_kpon = 0;
Reaction150_kpoff = 0.05;
Reaction151_kpon = 0;
Reaction152_kpoff = 0.05;
Reaction153_kpon = 0;
Reaction154_kpoff = 0.05;
Reaction155_kpon = 0;
Reaction156_kpoff = 0.05;
Reaction157_kon = 10;
Reaction158_koff = 0.5;
Reaction159_kon = 10;
Reaction160_koff = 0.5;
Reaction161_kon = 10;
Reaction162_koff = 0.5;
Reaction163_kpon = 0;
Reaction164_kpoff = 0.05;
Reaction165_kpon = 0;
Reaction166_kpoff = 0.05;
Reaction167_kpon = 0;

Reaction168_kpoff = 0.05;
Reaction169_kpon = 0;
Reaction170_kpoff = 0.05;
Reaction171_kpon = 0;
Reaction172_kpoff = 0.05;
Reaction173_kpon = 0;
Reaction174_kpoff = 0.05;
Reaction175_kon = 10;
Reaction176_koff = 0.5;
Reaction177_kpon = 0;
Reaction178_kpoff = 0.05;
Reaction179_kon = 10;
Reaction180_koff = 0.5;
Reaction181_kpon = 0;
Reaction182_kpoff = 0.05;
Reaction183_kon = 10;
Reaction184_koff = 0.5;
Reaction185_kpon = 0;
Reaction186_kpoff = 0.05;
Reaction187_kon = 10;
Reaction188_koff = 0.5;
Reaction189_kpon = 0;
Reaction190_kpoff = 0.05;
Reaction191_kon = 10;
Reaction192_koff = 0.5;
Reaction193_kpon = 0;
Reaction194_kpoff = 0.05;
Reaction195_kon = 10;
Reaction196_koff = 0.5;
Reaction197_kpon = 0;
Reaction198_kpoff = 0.05;
Reaction199_kon = 10;
Reaction200_koff = 0.5;
Reaction201_kpon = 0;
Reaction202_kpoff = 0.05;
Reaction203_kon = 10;
Reaction204_koff = 0.5;
Reaction205_kpon = 0;
Reaction206_kpoff = 0.05;
Reaction207_kon = 10;
Reaction208_koff = 0.5;
Reaction209_kpon = 0;
Reaction210_kpoff = 0.05;
Reaction211_kon = 10;
Reaction212_koff = 0.5;
Reaction213_kpon = 0;
Reaction214_kpoff = 0.05;
Reaction215_kon = 10;
Reaction216_koff = 0.5;
Reaction217_kpon = 0;
Reaction218_kpoff = 0.05;
Reaction219_kon = 10;
Reaction220_koff = 0.5;
Reaction221_kpon = 0;
Reaction222_kpoff = 0.05;

```
Reaction223_kon = 10;
Reaction224_koff = 0.5;
Reaction225_kpon = 0;
Reaction226_kpoff = 0.05;
Reaction227_kon = 10;
Reaction228_koff = 0.5;
Reaction229_kpon = 0;
Reaction230_kpoff = 0.05;
Reaction231_kon = 10;
Reaction232_koff = 0.5;
Reaction233_kpon = 0;
Reaction234_kpoff = 0.05;
Reaction235_kon = 10;
Reaction236_koff = 0.5;
Reaction237_kpon = 0;
Reaction238_kpoff = 0.05;
Reaction239_k7 = 0.1;
Reaction240_k7 = 0.1;
Reaction241_k7 = 0.1;
Reaction242_k9a = 0.1;
Reaction243_k9a = 0.1;
Reaction244_k9a = 0.1;
Reaction245_k3 = 0.1;
Reaction246_k5a = 0.1;
Reaction247_k3 = 0.1;
Reaction248_k5a = 0.1;
Reaction249_k3 = 0.1;
Reaction250_k5a = 0.1;
Reaction251_k3 = 0.1;
Reaction252_k5a = 0.1;
Reaction253_k1a = 100;
Reaction254_d1a = 0;
Reaction255_k1 = 0.1;
Reaction256_k1a = 100;
Reaction257_d1a = 0;
Reaction258_k1 = 0.1;
Reaction259_k1a = 100;
Reaction260_d1a = 0;
Reaction261_k1 = 0.1;
Reaction262_k1a = 100;
Reaction263_d1a = 0;
Reaction264_k1 = 0.1;
Reaction265_k1a = 100;
Reaction266_d1a = 0;
Reaction267_k1 = 0.1;
Reaction268_k1a = 100;
Reaction269_d1a = 0;
Reaction270_k1 = 0.1;
Reaction271_k1a = 100;
Reaction272_d1a = 0;
Reaction273_k1 = 0.1;
Reaction274_k1a = 100;
Reaction275_d1a = 0;
Reaction276_k1 = 0.1;
Reaction277_k1a = 100;
```

```
Reaction278_d1a = 0;
Reaction279_k1 = 0.1;
Reaction280_k1a = 100;
Reaction281_d1a = 0;
Reaction282_k1 = 0.1;
Reaction283_k1a = 100;
Reaction284_d1a = 0;
Reaction285_k1 = 0.1;
Reaction286_k1a = 100;
Reaction287_d1a = 0;
Reaction288_k1 = 0.1;
Reaction289_k1a = 100;
Reaction290_d1a = 0;
Reaction291_k1 = 0.1;
Reaction292_k1a = 100;
Reaction293_d1a = 0;
Reaction294_k1 = 0.1;
Reaction295_k1a = 100;
Reaction296_d1a = 0;
Reaction297_k1 = 0.1;
Reaction298_k1a = 100;
Reaction299_d1a = 0;
Reaction300_k1 = 0.1;

; Reaction Rates:
Reaction1 = Reaction1_a1*RAFK*K_3_0
Reaction2 = Reaction2_d1*K_RAFK_3_0
Reaction3 = Reaction3_k1*K_RAFK_3_0
Reaction4 = Reaction4_a2*RAFP*K_3_1
Reaction5 = Reaction5_d2*K_RAFP_3_1
Reaction6 = Reaction6_k2*K_RAFP_3_1
Reaction7 = Reaction7_a3*K_2_0*K_3_1
Reaction8 = Reaction8_d3*K_K_2_0_3_1
Reaction9 = Reaction9_k3*K_K_2_0_3_1
Reaction10 = Reaction10_a4*MEKP*K_2_1
Reaction11 = Reaction11_d4*K_MEKP_2_1
Reaction12 = Reaction12_k4*K_MEKP_2_1
Reaction13 = Reaction13_a5*K_2_1*K_3_1
Reaction14 = Reaction14_d5*K_K_2_1_3_1
Reaction15 = Reaction15_k5*K_K_2_1_3_1
Reaction16 = Reaction16_a6*MEKP*K_2_2
Reaction17 = Reaction17_d6*K_MEKP_2_2
Reaction18 = Reaction18_k6*K_MEKP_2_2
Reaction19 = Reaction19_a7*K_1_0*K_2_2
Reaction20 = Reaction20_d7*K_K_1_0_2_2
Reaction21 = Reaction21_k7*K_K_1_0_2_2
Reaction22 = Reaction22_a8*MAPKP*K_1_1
Reaction23 = Reaction23_d8*K_MAPKP_1_1
Reaction24 = Reaction24_k8*K_MAPKP_1_1
Reaction25 = Reaction25_a9*K_1_1*K_2_2
Reaction26 = Reaction26_d9*K_K_1_1_2_2
Reaction27 = Reaction27_k9*K_K_1_1_2_2
Reaction28 = Reaction28_a10*MAPKP*K_1_2
Reaction29 = Reaction29_d10*K_MAPKP_1_2
Reaction30 = Reaction30_k10*K_MAPKP_1_2
```

Reaction31 = Reaction31_kon*K_1_0*S_m1_m1_m1
Reaction32 = Reaction32_koff*S_0_m1_m1
Reaction33 = Reaction33_kon*K_1_0*S_m1_m1_0
Reaction34 = Reaction34_koff*S_0_m1_0
Reaction35 = Reaction35_kon*K_1_0*S_m1_m1_1
Reaction36 = Reaction36_koff*S_0_m1_1
Reaction37 = Reaction37_kon*K_1_0*S_m1_0_m1
Reaction38 = Reaction38_koff*S_0_0_m1
Reaction39 = Reaction39_kon*K_1_0*S_m1_0_0
Reaction40 = Reaction40_koff*S_0_0_0
Reaction41 = Reaction41_kon*K_1_0*S_m1_0_1
Reaction42 = Reaction42_koff*S_0_0_1
Reaction43 = Reaction43_kon*K_1_0*S_m1_1_m1
Reaction44 = Reaction44_koff*S_0_1_m1
Reaction45 = Reaction45_kon*K_1_0*S_m1_1_0
Reaction46 = Reaction46_koff*S_0_1_0
Reaction47 = Reaction47_kon*K_1_0*S_m1_1_1
Reaction48 = Reaction48_koff*S_0_1_1
Reaction49 = Reaction49_kon*K_1_0*S_m1_2_m1
Reaction50 = Reaction50_koff*S_0_2_m1
Reaction51 = Reaction51_kon*K_1_0*S_m1_2_0
Reaction52 = Reaction52_koff*S_0_2_0
Reaction53 = Reaction53_kon*K_1_0*S_m1_2_1
Reaction54 = Reaction54_koff*S_0_2_1
Reaction55 = Reaction55_kpon*K_1_1*S_m1_m1_m1
Reaction56 = Reaction56_kpoff*S_1_m1_m1
Reaction57 = Reaction57_kpon*K_1_1*S_m1_m1_0
Reaction58 = Reaction58_kpoff*S_1_m1_0
Reaction59 = Reaction59_kpon*K_1_1*S_m1_m1_1
Reaction60 = Reaction60_kpoff*S_1_m1_1
Reaction61 = Reaction61_kpon*K_1_1*S_m1_0_m1
Reaction62 = Reaction62_kpoff*S_1_0_m1
Reaction63 = Reaction63_kpon*K_1_1*S_m1_0_0
Reaction64 = Reaction64_kpoff*S_1_0_0
Reaction65 = Reaction65_kpon*K_1_1*S_m1_0_1
Reaction66 = Reaction66_kpoff*S_1_0_1
Reaction67 = Reaction67_kpon*K_1_1*S_m1_1_m1
Reaction68 = Reaction68_kpoff*S_1_1_m1
Reaction69 = Reaction69_kpon*K_1_1*S_m1_1_0
Reaction70 = Reaction70_kpoff*S_1_1_0
Reaction71 = Reaction71_kpon*K_1_1*S_m1_1_1
Reaction72 = Reaction72_kpoff*S_1_1_1
Reaction73 = Reaction73_kpon*K_1_1*S_m1_2_m1
Reaction74 = Reaction74_kpoff*S_1_2_m1
Reaction75 = Reaction75_kpon*K_1_1*S_m1_2_0
Reaction76 = Reaction76_kpoff*S_1_2_0
Reaction77 = Reaction77_kpon*K_1_1*S_m1_2_1
Reaction78 = Reaction78_kpoff*S_1_2_1
Reaction79 = Reaction79_kpon*K_1_2*S_m1_m1_m1
Reaction80 = Reaction80_kpoff*S_2_m1_m1
Reaction81 = Reaction81_kpon*K_1_2*S_m1_m1_0
Reaction82 = Reaction82_kpoff*S_2_m1_0
Reaction83 = Reaction83_kpon*K_1_2*S_m1_m1_1
Reaction84 = Reaction84_kpoff*S_2_m1_1
Reaction85 = Reaction85_kpon*K_1_2*S_m1_0_m1

Reaction86 = Reaction86_kpoff*S_2_0_m1
Reaction87 = Reaction87_kpon*K_1_2*S_m1_0_0
Reaction88 = Reaction88_kpoff*S_2_0_0
Reaction89 = Reaction89_kpon*K_1_2*S_m1_0_1
Reaction90 = Reaction90_kpoff*S_2_0_1
Reaction91 = Reaction91_kpon*K_1_2*S_m1_1_m1
Reaction92 = Reaction92_kpoff*S_2_1_m1
Reaction93 = Reaction93_kpon*K_1_2*S_m1_1_0
Reaction94 = Reaction94_kpoff*S_2_1_0
Reaction95 = Reaction95_kpon*K_1_2*S_m1_1_1
Reaction96 = Reaction96_kpoff*S_2_1_1
Reaction97 = Reaction97_kpon*K_1_2*S_m1_2_m1
Reaction98 = Reaction98_kpoff*S_2_2_m1
Reaction99 = Reaction99_kpon*K_1_2*S_m1_2_0
Reaction100 = Reaction100_kpoff*S_2_2_0
Reaction101 = Reaction101_kpon*K_1_2*S_m1_2_1
Reaction102 = Reaction102_kpoff*S_2_2_1
Reaction103 = Reaction103_kon*K_2_0*S_m1_m1_m1
Reaction104 = Reaction104_koff*S_m1_0_m1
Reaction105 = Reaction105_kon*K_2_0*S_m1_m1_0
Reaction106 = Reaction106_koff*S_m1_0_0
Reaction107 = Reaction107_kon*K_2_0*S_m1_m1_1
Reaction108 = Reaction108_koff*S_m1_0_1
Reaction109 = Reaction109_kpon*K_2_1*S_m1_m1_m1
Reaction110 = Reaction110_kpoff*S_m1_1_m1
Reaction111 = Reaction111_kpon*K_2_1*S_m1_m1_0
Reaction112 = Reaction112_kpoff*S_m1_1_0
Reaction113 = Reaction113_kpon*K_2_1*S_m1_m1_1
Reaction114 = Reaction114_kpoff*S_m1_1_1
Reaction115 = Reaction115_kpon*K_2_2*S_m1_m1_m1
Reaction116 = Reaction116_kpoff*S_m1_2_m1
Reaction117 = Reaction117_kpon*K_2_2*S_m1_m1_0
Reaction118 = Reaction118_kpoff*S_m1_2_0
Reaction119 = Reaction119_kpon*K_2_2*S_m1_m1_1
Reaction120 = Reaction120_kpoff*S_m1_2_1
Reaction121 = Reaction121_kon*K_2_0*S_0_m1_m1
Reaction122 = Reaction122_koff*S_0_0_m1
Reaction123 = Reaction123_kon*K_2_0*S_0_m1_0
Reaction124 = Reaction124_koff*S_0_0_0
Reaction125 = Reaction125_kon*K_2_0*S_0_m1_1
Reaction126 = Reaction126_koff*S_0_0_1
Reaction127 = Reaction127_kpon*K_2_1*S_0_m1_m1
Reaction128 = Reaction128_kpoff*S_0_1_m1
Reaction129 = Reaction129_kpon*K_2_1*S_0_m1_0
Reaction130 = Reaction130_kpoff*S_0_1_0
Reaction131 = Reaction131_kpon*K_2_1*S_0_m1_1
Reaction132 = Reaction132_kpoff*S_0_1_1
Reaction133 = Reaction133_kpon*K_2_2*S_0_m1_m1
Reaction134 = Reaction134_kpoff*S_0_2_m1
Reaction135 = Reaction135_kpon*K_2_2*S_0_m1_0
Reaction136 = Reaction136_kpoff*S_0_2_0
Reaction137 = Reaction137_kpon*K_2_2*S_0_m1_1
Reaction138 = Reaction138_kpoff*S_0_2_1
Reaction139 = Reaction139_kon*K_2_0*S_1_m1_m1
Reaction140 = Reaction140_koff*S_1_0_m1

Reaction141 = Reaction141_kon*K_2_0*S_1_m1_0
Reaction142 = Reaction142_koff*S_1_0_0
Reaction143 = Reaction143_kon*K_2_0*S_1_m1_1
Reaction144 = Reaction144_koff*S_1_0_1
Reaction145 = Reaction145_kpon*K_2_1*S_1_m1_m1
Reaction146 = Reaction146_kpoff*S_1_1_m1
Reaction147 = Reaction147_kpon*K_2_1*S_1_m1_0
Reaction148 = Reaction148_kpoff*S_1_1_0
Reaction149 = Reaction149_kpon*K_2_1*S_1_m1_1
Reaction150 = Reaction150_kpoff*S_1_1_1
Reaction151 = Reaction151_kpon*K_2_2*S_1_m1_m1
Reaction152 = Reaction152_kpoff*S_1_2_m1
Reaction153 = Reaction153_kpon*K_2_2*S_1_m1_0
Reaction154 = Reaction154_kpoff*S_1_2_0
Reaction155 = Reaction155_kpon*K_2_2*S_1_m1_1
Reaction156 = Reaction156_kpoff*S_1_2_1
Reaction157 = Reaction157_kon*K_2_0*S_2_m1_m1
Reaction158 = Reaction158_koff*S_2_0_m1
Reaction159 = Reaction159_kon*K_2_0*S_2_m1_0
Reaction160 = Reaction160_koff*S_2_0_0
Reaction161 = Reaction161_kon*K_2_0*S_2_m1_1
Reaction162 = Reaction162_koff*S_2_0_1
Reaction163 = Reaction163_kpon*K_2_1*S_2_m1_m1
Reaction164 = Reaction164_kpoff*S_2_1_m1
Reaction165 = Reaction165_kpon*K_2_1*S_2_m1_0
Reaction166 = Reaction166_kpoff*S_2_1_0
Reaction167 = Reaction167_kpon*K_2_1*S_2_m1_1
Reaction168 = Reaction168_kpoff*S_2_1_1
Reaction169 = Reaction169_kpon*K_2_2*S_2_m1_m1
Reaction170 = Reaction170_kpoff*S_2_2_m1
Reaction171 = Reaction171_kpon*K_2_2*S_2_m1_0
Reaction172 = Reaction172_kpoff*S_2_2_0
Reaction173 = Reaction173_kpon*K_2_2*S_2_m1_1
Reaction174 = Reaction174_kpoff*S_2_2_1
Reaction175 = Reaction175_kon*K_3_0*S_m1_m1_m1
Reaction176 = Reaction176_koff*S_m1_m1_0
Reaction177 = Reaction177_kpon*K_3_1*S_m1_m1_m1
Reaction178 = Reaction178_kpoff*S_m1_m1_1
Reaction179 = Reaction179_kon*K_3_0*S_m1_0_m1
Reaction180 = Reaction180_koff*S_m1_0_0
Reaction181 = Reaction181_kpon*K_3_1*S_m1_0_m1
Reaction182 = Reaction182_kpoff*S_m1_0_1
Reaction183 = Reaction183_kon*K_3_0*S_m1_1_m1
Reaction184 = Reaction184_koff*S_m1_1_0
Reaction185 = Reaction185_kpon*K_3_1*S_m1_1_m1
Reaction186 = Reaction186_kpoff*S_m1_1_1
Reaction187 = Reaction187_kon*K_3_0*S_m1_2_m1
Reaction188 = Reaction188_koff*S_m1_2_0
Reaction189 = Reaction189_kpon*K_3_1*S_m1_2_m1
Reaction190 = Reaction190_kpoff*S_m1_2_1
Reaction191 = Reaction191_kon*K_3_0*S_0_m1_m1
Reaction192 = Reaction192_koff*S_0_m1_0
Reaction193 = Reaction193_kpon*K_3_1*S_0_m1_m1
Reaction194 = Reaction194_kpoff*S_0_m1_1
Reaction195 = Reaction195_kon*K_3_0*S_0_0_m1

Reaction196 = Reaction196_koff*S_0_0_0
Reaction197 = Reaction197_kpon*K_3_1*S_0_0_m1
Reaction198 = Reaction198_kpoff*S_0_0_1
Reaction199 = Reaction199_kon*K_3_0*S_0_1_m1
Reaction200 = Reaction200_koff*S_0_1_0
Reaction201 = Reaction201_kpon*K_3_1*S_0_1_m1
Reaction202 = Reaction202_kpoff*S_0_1_1
Reaction203 = Reaction203_kon*K_3_0*S_0_2_m1
Reaction204 = Reaction204_koff*S_0_2_0
Reaction205 = Reaction205_kpon*K_3_1*S_0_2_m1
Reaction206 = Reaction206_kpoff*S_0_2_1
Reaction207 = Reaction207_kon*K_3_0*S_1_m1_m1
Reaction208 = Reaction208_koff*S_1_m1_0
Reaction209 = Reaction209_kpon*K_3_1*S_1_m1_m1
Reaction210 = Reaction210_kpoff*S_1_m1_1
Reaction211 = Reaction211_kon*K_3_0*S_1_0_m1
Reaction212 = Reaction212_koff*S_1_0_0
Reaction213 = Reaction213_kpon*K_3_1*S_1_0_m1
Reaction214 = Reaction214_kpoff*S_1_0_1
Reaction215 = Reaction215_kon*K_3_0*S_1_1_m1
Reaction216 = Reaction216_koff*S_1_1_0
Reaction217 = Reaction217_kpon*K_3_1*S_1_1_m1
Reaction218 = Reaction218_kpoff*S_1_1_1
Reaction219 = Reaction219_kon*K_3_0*S_1_2_m1
Reaction220 = Reaction220_koff*S_1_2_0
Reaction221 = Reaction221_kpon*K_3_1*S_1_2_m1
Reaction222 = Reaction222_kpoff*S_1_2_1
Reaction223 = Reaction223_kon*K_3_0*S_2_m1_m1
Reaction224 = Reaction224_koff*S_2_m1_0
Reaction225 = Reaction225_kpon*K_3_1*S_2_m1_m1
Reaction226 = Reaction226_kpoff*S_2_m1_1
Reaction227 = Reaction227_kon*K_3_0*S_2_0_m1
Reaction228 = Reaction228_koff*S_2_0_0
Reaction229 = Reaction229_kpon*K_3_1*S_2_0_m1
Reaction230 = Reaction230_kpoff*S_2_0_1
Reaction231 = Reaction231_kon*K_3_0*S_2_1_m1
Reaction232 = Reaction232_koff*S_2_1_0
Reaction233 = Reaction233_kpon*K_3_1*S_2_1_m1
Reaction234 = Reaction234_kpoff*S_2_1_1
Reaction235 = Reaction235_kon*K_3_0*S_2_2_m1
Reaction236 = Reaction236_koff*S_2_2_0
Reaction237 = Reaction237_kpon*K_3_1*S_2_2_m1
Reaction238 = Reaction238_kpoff*S_2_2_1
Reaction239 = Reaction239_k7*S_0_2_m1
Reaction240 = Reaction240_k7*S_0_2_0
Reaction241 = Reaction241_k7*S_0_2_1
Reaction242 = Reaction242_k9a*S_1_2_m1
Reaction243 = Reaction243_k9a*S_1_2_0
Reaction244 = Reaction244_k9a*S_1_2_1
Reaction245 = Reaction245_k3*S_m1_0_1
Reaction246 = Reaction246_k5a*S_m1_1_1
Reaction247 = Reaction247_k3*S_0_0_1
Reaction248 = Reaction248_k5a*S_0_1_1
Reaction249 = Reaction249_k3*S_1_0_1
Reaction250 = Reaction250_k5a*S_1_1_1

Reaction251 = Reaction251_k3*S_2_0_1
Reaction252 = Reaction252_k5a*S_2_1_1
Reaction253 = Reaction253_k1a*RAFK*S_m1_m1_0
Reaction254 = Reaction254_d1a*S_RAFK_m1_m1_0
Reaction255 = Reaction255_k1*S_RAFK_m1_m1_0
Reaction256 = Reaction256_k1a*RAFK*S_m1_0_0
Reaction257 = Reaction257_d1a*S_RAFK_m1_0_0
Reaction258 = Reaction258_k1*S_RAFK_m1_0_0
Reaction259 = Reaction259_k1a*RAFK*S_m1_1_0
Reaction260 = Reaction260_d1a*S_RAFK_m1_1_0
Reaction261 = Reaction261_k1*S_RAFK_m1_1_0
Reaction262 = Reaction262_k1a*RAFK*S_m1_2_0
Reaction263 = Reaction263_d1a*S_RAFK_m1_2_0
Reaction264 = Reaction264_k1*S_RAFK_m1_2_0
Reaction265 = Reaction265_k1a*RAFK*S_0_m1_0
Reaction266 = Reaction266_d1a*S_RAFK_0_m1_0
Reaction267 = Reaction267_k1*S_RAFK_0_m1_0
Reaction268 = Reaction268_k1a*RAFK*S_0_0_0
Reaction269 = Reaction269_d1a*S_RAFK_0_0_0
Reaction270 = Reaction270_k1*S_RAFK_0_0_0
Reaction271 = Reaction271_k1a*RAFK*S_0_1_0
Reaction272 = Reaction272_d1a*S_RAFK_0_1_0
Reaction273 = Reaction273_k1*S_RAFK_0_1_0
Reaction274 = Reaction274_k1a*RAFK*S_0_2_0
Reaction275 = Reaction275_d1a*S_RAFK_0_2_0
Reaction276 = Reaction276_k1*S_RAFK_0_2_0
Reaction277 = Reaction277_k1a*RAFK*S_1_m1_0
Reaction278 = Reaction278_d1a*S_RAFK_1_m1_0
Reaction279 = Reaction279_k1*S_RAFK_1_m1_0
Reaction280 = Reaction280_k1a*RAFK*S_1_0_0
Reaction281 = Reaction281_d1a*S_RAFK_1_0_0
Reaction282 = Reaction282_k1*S_RAFK_1_0_0
Reaction283 = Reaction283_k1a*RAFK*S_1_1_0
Reaction284 = Reaction284_d1a*S_RAFK_1_1_0
Reaction285 = Reaction285_k1*S_RAFK_1_1_0
Reaction286 = Reaction286_k1a*RAFK*S_1_2_0
Reaction287 = Reaction287_d1a*S_RAFK_1_2_0
Reaction288 = Reaction288_k1*S_RAFK_1_2_0
Reaction289 = Reaction289_k1a*RAFK*S_2_m1_0
Reaction290 = Reaction290_d1a*S_RAFK_2_m1_0
Reaction291 = Reaction291_k1*S_RAFK_2_m1_0
Reaction292 = Reaction292_k1a*RAFK*S_2_0_0
Reaction293 = Reaction293_d1a*S_RAFK_2_0_0
Reaction294 = Reaction294_k1*S_RAFK_2_0_0
Reaction295 = Reaction295_k1a*RAFK*S_2_1_0
Reaction296 = Reaction296_d1a*S_RAFK_2_1_0
Reaction297 = Reaction297_k1*S_RAFK_2_1_0
Reaction298 = Reaction298_k1a*RAFK*S_2_2_0
Reaction299 = Reaction299_d1a*S_RAFK_2_2_0
Reaction300 = Reaction300_k1*S_RAFK_2_2_0
Cleave_KKP = J301_KKP_k*K_2_1
Cleave_KK = J302_KK_k*K_2_0
Cleave_KKPP = J303_KKPP_k*K_2_2

; Differential Equations:
Cleaved_MAPKK' = + Cleave_KKP + Cleave_KK + Cleave_KKPP
MAPKP' = - Reaction22 + Reaction23 + Reaction24 - Reaction28 + Reaction29 + Reaction30
MEKP' = - Reaction10 + Reaction11 + Reaction12 - Reaction16 + Reaction17 + Reaction18
RAFK' = - Reaction1 + Reaction2 + Reaction3 - Reaction253 + Reaction254 + Reaction255 - Reaction256 + Reaction257 + Reaction258 - Reaction259 + Reaction260 + Reaction261 - Reaction262 + Reaction263 + Reaction264 - Reaction265 + Reaction266 + Reaction267 - Reaction268 + Reaction269 + Reaction270 - Reaction271 + Reaction272 + Reaction273 - Reaction274 + Reaction275 + Reaction276 - Reaction277 + Reaction278 + Reaction279 - Reaction280 + Reaction281 + Reaction282 - Reaction283 + Reaction284 + Reaction285 - Reaction286 + Reaction287 + Reaction288 - Reaction289 + Reaction290 + Reaction291 - Reaction292 + Reaction293 + Reaction294 - Reaction295 + Reaction296 + Reaction297 - Reaction298 + Reaction299 + Reaction300
RAFP' = - Reaction4 + Reaction5 + Reaction6
K_1_0' = - Reaction19 + Reaction20 + Reaction24 - Reaction31 + Reaction32 - Reaction33 + Reaction34 - Reaction35 + Reaction36 - Reaction37 + Reaction38 - Reaction39 + Reaction40 - Reaction41 + Reaction42 - Reaction43 + Reaction44 - Reaction45 + Reaction46 - Reaction47 + Reaction48 - Reaction49 + Reaction50 - Reaction51 + Reaction52 - Reaction53 + Reaction54
K_1_1' = + Reaction21 - Reaction22 + Reaction23 - Reaction25 + Reaction26 + Reaction30 - Reaction55 + Reaction56 - Reaction57 + Reaction58 - Reaction59 + Reaction60 - Reaction61 + Reaction62 - Reaction63 + Reaction64 - Reaction65 + Reaction66 - Reaction67 + Reaction68 - Reaction69 + Reaction70 - Reaction71 + Reaction72 - Reaction73 + Reaction74 - Reaction75 + Reaction76 - Reaction77 + Reaction78
K_1_2' = + Reaction27 - Reaction28 + Reaction29 - Reaction79 + Reaction80 - Reaction81 + Reaction82 - Reaction83 + Reaction84 - Reaction85 + Reaction86 - Reaction87 + Reaction88 - Reaction89 + Reaction90 - Reaction91 + Reaction92 - Reaction93 + Reaction94 - Reaction95 + Reaction96 - Reaction97 + Reaction98 - Reaction99 + Reaction100 - Reaction101 + Reaction102
K_2_0' = - Reaction7 + Reaction8 + Reaction12 - Reaction103 + Reaction104 - Reaction105 + Reaction106 - Reaction107 + Reaction108 - Reaction121 + Reaction122 - Reaction123 + Reaction124 - Reaction125 + Reaction126 - Reaction139 + Reaction140 - Reaction141 + Reaction142 - Reaction143 + Reaction144 - Reaction157 + Reaction158 - Reaction159 + Reaction160 - Reaction161 + Reaction162 - Cleave_KK
K_2_1' = + Reaction9 - Reaction10 + Reaction11 - Reaction13 + Reaction14 + Reaction18 - Reaction109 + Reaction110 - Reaction111 + Reaction112 - Reaction113 + Reaction114 - Reaction127 + Reaction128 - Reaction129 + Reaction130 - Reaction131 + Reaction132 - Reaction145 + Reaction146 - Reaction147 + Reaction148 - Reaction149 + Reaction150 - Reaction163 + Reaction164 - Reaction165 + Reaction166 - Reaction167 + Reaction168 - Cleave_KKP
K_2_2' = + Reaction15 - Reaction16 + Reaction17 - Reaction19 + Reaction20 + Reaction21 - Reaction25 + Reaction26 + Reaction27 - Reaction115 + Reaction116 - Reaction117 + Reaction118 - Reaction119 + Reaction120 - Reaction133 + Reaction134 - Reaction135 + Reaction136 - Reaction137 + Reaction138 - Reaction151 + Reaction152 - Reaction153 + Reaction154 - Reaction155 + Reaction156 - Reaction169 + Reaction170 - Reaction171 + Reaction172 - Reaction173 + Reaction174 - Cleave_KKPP
K_3_0' = - Reaction1 + Reaction2 + Reaction6 - Reaction175 + Reaction176 - Reaction179 + Reaction180 - Reaction183 + Reaction184 - Reaction187 + Reaction188 - Reaction191 + Reaction192 - Reaction195 + Reaction196 - Reaction199 + Reaction200 - Reaction203 + Reaction204 - Reaction207 + Reaction208 - Reaction211 + Reaction212 - Reaction215 + Reaction216 - Reaction219 + Reaction220 - Reaction223 + Reaction224 - Reaction227 + Reaction228 - Reaction231 + Reaction232 - Reaction235 + Reaction236
K_3_1' = + Reaction3 - Reaction4 + Reaction5 - Reaction7 + Reaction8 + Reaction9 - Reaction13 + Reaction14 + Reaction15 - Reaction177 + Reaction178 - Reaction181 + Reaction182 - Reaction185 + Reaction186 - Reaction189 + Reaction190 - Reaction193 + Reaction194 - Reaction197 + Reaction198 - Reaction201 + Reaction202 - Reaction205 + Reaction206 - Reaction209 + Reaction210 - Reaction213 + Reaction214 - Reaction217 + Reaction218 -

Reaction221 + Reaction222 - Reaction225 + Reaction226 - Reaction229 + Reaction230 - Reaction233 + Reaction234 - Reaction237 + Reaction238
K_K_1_0_2_2' = + Reaction19 - Reaction20 - Reaction21
K_K_1_1_2_2' = + Reaction25 - Reaction26 - Reaction27
K_K_2_0_3_1' = + Reaction7 - Reaction8 - Reaction9
K_K_2_1_3_1' = + Reaction13 - Reaction14 - Reaction15
K_MAPKP_1_1' = + Reaction22 - Reaction23 - Reaction24
K_MEKP_2_1' = + Reaction10 - Reaction11 - Reaction12
K_RAFK_3_0' = + Reaction1 - Reaction2 - Reaction3
S_m1_m1_m1' = - Reaction31 + Reaction32 - Reaction55 + Reaction56 - Reaction79 + Reaction80 - Reaction103 + Reaction104 - Reaction109 + Reaction110 - Reaction115 + Reaction116 - Reaction175 + Reaction176 - Reaction177 + Reaction178
S_m1_m1_0' = - Reaction33 + Reaction34 - Reaction57 + Reaction58 - Reaction81 + Reaction82 - Reaction105 + Reaction106 - Reaction111 + Reaction112 - Reaction117 + Reaction118 + Reaction175 - Reaction176 - Reaction253 + Reaction254
S_m1_m1_1' = - Reaction35 + Reaction36 - Reaction59 + Reaction60 - Reaction83 + Reaction84 - Reaction107 + Reaction108 - Reaction113 + Reaction114 - Reaction119 + Reaction120 + Reaction177 - Reaction178 + Reaction255
S_m1_0_m1' = - Reaction37 + Reaction38 - Reaction61 + Reaction62 - Reaction85 + Reaction86 + Reaction103 - Reaction104 - Reaction179 + Reaction180 - Reaction181 + Reaction182
S_m1_0_0' = - Reaction39 + Reaction40 - Reaction63 + Reaction64 - Reaction87 + Reaction88 + Reaction105 - Reaction106 + Reaction179 - Reaction180 - Reaction256 + Reaction257
S_m1_0_1' = - Reaction41 + Reaction42 - Reaction65 + Reaction66 - Reaction89 + Reaction90 + Reaction107 - Reaction108 + Reaction181 - Reaction182 - Reaction245 + Reaction258
S_m1_1_m1' = - Reaction43 + Reaction44 - Reaction67 + Reaction68 - Reaction91 + Reaction92 + Reaction109 - Reaction110 - Reaction183 + Reaction184 - Reaction185 + Reaction186
S_m1_1_0' = - Reaction45 + Reaction46 - Reaction69 + Reaction70 - Reaction93 + Reaction94 + Reaction111 - Reaction112 + Reaction183 - Reaction184 - Reaction259 + Reaction260
S_m1_1_1' = - Reaction47 + Reaction48 - Reaction71 + Reaction72 - Reaction95 + Reaction96 + Reaction113 - Reaction114 + Reaction185 - Reaction186 + Reaction245 - Reaction246 + Reaction261
S_m1_2_m1' = - Reaction49 + Reaction50 - Reaction73 + Reaction74 - Reaction97 + Reaction98 + Reaction115 - Reaction116 - Reaction187 + Reaction188 - Reaction189 + Reaction190
S_m1_2_0' = - Reaction51 + Reaction52 - Reaction75 + Reaction76 - Reaction99 + Reaction100 + Reaction117 - Reaction118 + Reaction187 - Reaction188 - Reaction262 + Reaction263
S_m1_2_1' = - Reaction53 + Reaction54 - Reaction77 + Reaction78 - Reaction101 + Reaction102 + Reaction119 - Reaction120 + Reaction189 - Reaction190 + Reaction246 + Reaction264
S_0_m1_m1' = + Reaction31 - Reaction32 - Reaction121 + Reaction122 - Reaction127 + Reaction128 - Reaction133 + Reaction134 - Reaction191 + Reaction192 - Reaction193 + Reaction194
S_0_m1_0' = + Reaction33 - Reaction34 - Reaction123 + Reaction124 - Reaction129 + Reaction130 - Reaction135 + Reaction136 + Reaction191 - Reaction192 - Reaction265 + Reaction266
S_0_m1_1' = + Reaction35 - Reaction36 - Reaction125 + Reaction126 - Reaction131 + Reaction132 - Reaction137 + Reaction138 + Reaction193 - Reaction194 + Reaction267
S_0_0_m1' = + Reaction37 - Reaction38 + Reaction121 - Reaction122 - Reaction195 + Reaction196 - Reaction197 + Reaction198
S_0_0_0' = + Reaction39 - Reaction40 + Reaction123 - Reaction124 + Reaction195 - Reaction196 - Reaction268 + Reaction269
S_0_0_1' = + Reaction41 - Reaction42 + Reaction125 - Reaction126 + Reaction197 - Reaction198 - Reaction247 + Reaction270
S_0_1_m1' = + Reaction43 - Reaction44 + Reaction127 - Reaction128 - Reaction199 + Reaction200 - Reaction201 + Reaction202
S_0_1_0' = + Reaction45 - Reaction46 + Reaction129 - Reaction130 + Reaction199 - Reaction200 - Reaction271 + Reaction272

S_0_1_1' = + Reaction47 - Reaction48 + Reaction131 - Reaction132 + Reaction201 - Reaction202 + Reaction247 - Reaction248 + Reaction273
S_0_2_m1' = + Reaction49 - Reaction50 + Reaction133 - Reaction134 - Reaction203 + Reaction204 - Reaction205 + Reaction206 - Reaction239
S_0_2_0' = + Reaction51 - Reaction52 + Reaction135 - Reaction136 + Reaction203 - Reaction204 - Reaction240 - Reaction274 + Reaction275
S_0_2_1' = + Reaction53 - Reaction54 + Reaction137 - Reaction138 + Reaction205 - Reaction206 - Reaction241 + Reaction248 + Reaction276
S_1_m1_m1' = + Reaction55 - Reaction56 - Reaction139 + Reaction140 - Reaction145 + Reaction146 - Reaction151 + Reaction152 - Reaction207 + Reaction208 - Reaction209 + Reaction210
S_1_m1_0' = + Reaction57 - Reaction58 - Reaction141 + Reaction142 - Reaction147 + Reaction148 - Reaction153 + Reaction154 + Reaction207 - Reaction208 - Reaction277 + Reaction278
S_1_m1_1' = + Reaction59 - Reaction60 - Reaction143 + Reaction144 - Reaction149 + Reaction150 - Reaction155 + Reaction156 + Reaction209 - Reaction210 + Reaction279
S_1_0_m1' = + Reaction61 - Reaction62 + Reaction139 - Reaction140 - Reaction211 + Reaction212 - Reaction213 + Reaction214
S_1_0_0' = + Reaction63 - Reaction64 + Reaction141 - Reaction142 + Reaction211 - Reaction212 - Reaction280 + Reaction281
S_1_0_1' = + Reaction65 - Reaction66 + Reaction143 - Reaction144 + Reaction213 - Reaction214 - Reaction249 + Reaction282
S_1_1_m1' = + Reaction67 - Reaction68 + Reaction145 - Reaction146 - Reaction215 + Reaction216 - Reaction217 + Reaction218
S_1_1_0' = + Reaction69 - Reaction70 + Reaction147 - Reaction148 + Reaction215 - Reaction216 - Reaction283 + Reaction284
S_1_1_1' = + Reaction71 - Reaction72 + Reaction149 - Reaction150 + Reaction217 - Reaction218 + Reaction249 - Reaction250 + Reaction285
S_1_2_m1' = + Reaction73 - Reaction74 + Reaction151 - Reaction152 - Reaction219 + Reaction220 - Reaction221 + Reaction222 + Reaction239 - Reaction242
S_1_2_0' = + Reaction75 - Reaction76 + Reaction153 - Reaction154 + Reaction219 - Reaction220 + Reaction240 - Reaction243 - Reaction286 + Reaction287
S_1_2_1' = + Reaction77 - Reaction78 + Reaction155 - Reaction156 + Reaction221 - Reaction222 + Reaction241 - Reaction244 + Reaction250 + Reaction288
S_2_m1_m1' = + Reaction79 - Reaction80 - Reaction157 + Reaction158 - Reaction163 + Reaction164 - Reaction169 + Reaction170 - Reaction223 + Reaction224 - Reaction225 + Reaction226
S_2_m1_0' = + Reaction81 - Reaction82 - Reaction159 + Reaction160 - Reaction165 + Reaction166 - Reaction171 + Reaction172 + Reaction223 - Reaction224 - Reaction289 + Reaction290
S_2_m1_1' = + Reaction83 - Reaction84 - Reaction161 + Reaction162 - Reaction167 + Reaction168 - Reaction173 + Reaction174 + Reaction225 - Reaction226 + Reaction291
S_2_0_m1' = + Reaction85 - Reaction86 + Reaction157 - Reaction158 - Reaction227 + Reaction228 - Reaction229 + Reaction230
S_2_0_0' = + Reaction87 - Reaction88 + Reaction159 - Reaction160 + Reaction227 - Reaction228 - Reaction292 + Reaction293
S_2_0_1' = + Reaction89 - Reaction90 + Reaction161 - Reaction162 + Reaction229 - Reaction230 - Reaction251 + Reaction294
S_2_1_m1' = + Reaction91 - Reaction92 + Reaction163 - Reaction164 - Reaction231 + Reaction232 - Reaction233 + Reaction234
S_2_1_0' = + Reaction93 - Reaction94 + Reaction165 - Reaction166 + Reaction231 - Reaction232 - Reaction295 + Reaction296
S_2_1_1' = + Reaction95 - Reaction96 + Reaction167 - Reaction168 + Reaction233 - Reaction234 + Reaction251 - Reaction252 + Reaction297

S_2_2_0' = + Reaction99 - Reaction100 + Reaction171 - Reaction172 + Reaction235 - Reaction236 + Reaction243 - Reaction298 + Reaction299
S_RAFK_m1_m1_0' = + Reaction253 - Reaction254 - Reaction255
S_RAFK_m1_0_0' = + Reaction256 - Reaction257 - Reaction258
S_RAFK_m1_1_0' = + Reaction259 - Reaction260 - Reaction261
S_RAFK_0_m1_0' = + Reaction265 - Reaction266 - Reaction267
S_RAFK_0_0_0' = + Reaction268 - Reaction269 - Reaction270
S_RAFK_0_1_0' = + Reaction271 - Reaction272 - Reaction273
S_RAFK_0_2_0' = + Reaction274 - Reaction275 - Reaction276
S_RAFK_1_m1_0' = + Reaction277 - Reaction278 - Reaction279
S_RAFK_1_0_0' = + Reaction280 - Reaction281 - Reaction282
S_RAFK_1_1_0' = + Reaction283 - Reaction284 - Reaction285
S_RAFK_1_2_0' = + Reaction286 - Reaction287 - Reaction288
S_RAFK_2_m1_0' = + Reaction289 - Reaction290 - Reaction291
S_RAFK_2_0_0' = + Reaction292 - Reaction293 - Reaction294
S_RAFK_2_1_0' = + Reaction295 - Reaction296 - Reaction297
S_RAFK_m1_2_0' = + Reaction262 - Reaction263 - Reaction264
K_MEKP_2_2' = + Reaction16 - Reaction17 - Reaction18
S_2_2_1' = + Reaction101 - Reaction102 + Reaction173 - Reaction174 + Reaction237 - Reaction238 + Reaction244 + Reaction252 + Reaction300
K_MAPKP_1_2' = + Reaction28 - Reaction29 - Reaction30
K_RAFP_3_1' = + Reaction4 - Reaction5 - Reaction6
S_2_2_m1' = + Reaction97 - Reaction98 + Reaction169 - Reaction170 - Reaction235 + Reaction236 - Reaction237 + Reaction238 + Reaction242
S_RAFK_2_2_0' = + Reaction298 - Reaction299 - Reaction300

Bibliography

Agrawal, Anshu, Jai Lingappa, Stephen H. Leppla, Sudhanshu Agrawal, Abdul Jabbar, Conrad Quinn, and Bali Pulendran. "Impairment of dendritic cells and adaptive immunity by anthrax lethal toxin," *Nature*, 424: 329-334 (17 July 2003).

American Heritage Stedman's Medical Dictionary (2nd Edition). Boston: Houghton Mifflin, 2004.

Anderson, Melvin E., Russell S. Thomas, Kevin W. Gaido, and Rory B. Conolly. "Dose–response modeling in reproductive toxicology in the systems biology era," *Reproductive Toxicology*, 19: 327-337 (2005).

Apic, Gordana, Tijana Ignjatovic, Scott Boyer, and Robert B. Russell. "Illuminating drug discovery with biological pathways," *FEBS Letters*, 579: 1872-1877 (2005).

Baldari, Cosima T., Fiorella Tonello, Silvia Rossi Paccani, and Cesare Montecucco. "Anthrax toxins: a paradigm of bacterial immune suppression," *TRENDS in Immunology*, 27: 434-440 (September 2006).

Banks, David J., Moshe Barnajian, Francisco J. Maldonado-Arocho, Ana M. Sanchez, Kenneth A. Bradley. "Anthrax toxin receptor 2 mediates *Bacillus anthracis* killing of macrophages following spore challenge," *Cellular Microbiology*, 7: 1173–1185 (2005).

Bardwell, A. Jane, Mahsa Abdollahi annd Lee Bardwell. "Anthrax lethal factor-cleavage products of MAPK (mitogen-activated protein kinase) kinases exhibit reduced binding to their cognate MAPKs," *The Biochemical Journal*, 378: 569–577 (2004).

"BIOMD0000000009 - Huang1996_MAPK_ultrasens." Huang and Ferrell (1996) ultrasensitivity MAPK cascade model in SBML at EMBL-EBI BioModels Database. n.pag. http://www.ebi.ac.uk/compneur-srv/biomodels-main/publ-model.do?mid=BIOMD0000000009. 13 July 2007.

"BIOMD0000000010 - Kholodenko2000_MAPK_feedback." Kholodenko (2000) oscillating, negative-feedback MAPK cascade model in SBML at EMBL-EBI BioModels Database. n.pag. http://www.ebi.ac.uk/compneur-srv/biomodels-main/publ-model.do?mid=BIOMD0000000010. 12 July 2007.

"BIOMD0000000014 - Levchenko2000_MAPK_Scaffold." Levchenko and others (2000) MAPK cascade model with scaffold proteins in SBML at EMBL-EBI BioModels Database. n.pag. http://www.ebi.ac.uk/compneur-srv/biomodels-main/publ-model.do?mid=BIOMD0000000014. 1 August 2007.

Bonni, Azad, Anne Brunet, Anne E. West, Sandeep Robert Datta, Mari A. Takasu, Michael E. Greenberg. "Cell survival Promoted by the Ras-MAPK Signaling Pathway by Transcription-Dependent and -Independent Mechanisms," *Science*, 286: 1358-1362 (12 November 1999).

Chakrabarty, Kaushik, Wenxin Wu, J. Leland Booth, Elizabeth S. Duggan, K. Mark Coggeshall, and Jordan P. Metcalf. "*Bacillus anthracis* Spores Stimulate Cytokine and Chemokine Innate Immune Responses in Human Alveolar Macrophages through Multiple Mitogen-Activated Protein Kinase Pathways," *Infection and Immunity*, 74(8): 4430-4438 (August 2006).

Chen, Peili, Ji Li, Janice Barnes, Gertrude C. Kokkonen, John C. Lee, and Yusen Liu. "Restraint of Proinflammatory Cytokine Biosynthesis by Mitogen-Activated Protein Kinase Phosphatase-1 in Lipopolysaccharide-Stimulated Macrophages," *The Journal of Immunology*, 169: 6408-6416 (December 2002).

Cho, Carolyn R., Mark Labow, Mischa Reinhardt, Jan van Oostrum, and Manual C. Peitcsh. "The application of systems biology to drug discovery," *Current Opinion in Chemical Biology*, 19: 294-302 (2006).

Cho, K.-H. and O. Wolkenhauer. "Analysis and modeling of signal transduction pathways in systems biology," *Biochemical Society Transactions*, 31: 1503-1509 (2003).

Chopra, Arun P., Sherrie A. Boone, Xudong Liang, and Nicholas S. Duesbery. "Anthrax Lethal Factor Proteolysis and Inactivation of MAPK Kinase," *The Journal of Biological Chemistry*, 278: 9402-9406 (14 March 2003).

Cleret, Aurélie, Anne Quesnel-Hellmann, Alexandra Vallon-Eberhard, Bernard Verrier, Steffen Jung, Dominique Vidal, Jacques Mathieu, and Jean-Nicolas Tournier. "Lung Dendritic Cells Rapidly Mediate Anthrax Spore Entry through the Pulmonary Route," *The Journal of Immunology*, 178: 7994-8001 (2007).

Comer, Jason E., Ashok K. Chopra, Johnny W. Peterson, and Rolf Konig. "Direct Inhibition of T-Lymphocyte Activation by Anthrax Toxins in Vivo," *Infection and Immunity*, 73: 8275-8281 (December 2005).

Cooper, Geoffrey M. *The Cell: A Molecular Approach* (2nd edition). Washington DC: ASM Press, 2000.

Cronin, Audrey Kurth. *Report for Congress: Terrorist Motivations for Chemical and Biological Weapons Use: Placing the Threat in Context.* Congressional Research Service (CRS) Report RL31831. (http://www.au.af.mil/au/awc/awcgate/crs/rl31831.pdf) Washington: GPO (28 March 2003).

Cui, Qinghua, Yun Ma, Maria Jaramillo, Hamza Bari1, Arif Awan, Song Yang, Simo Zhang, Lixue Liu, Meng Lu, Maureen O'Connor-McCourt, Enrico O Purisima1, and Edwin Wan. "A map of human cancer signaling," *Molecular Systems Biology*, 3 (article number 152): 1-13 (2007).

Davidov, Eugen J., Joanne M. Holland, Edward W. Marple, and Stephen Naylor. "Advancing drug discovery through systems biology," *Drug Discovery Today*, 8: 175-183 (4 February 2003).

Derbes, Vincent J. "De Mussis and the Great Plague of 1348: A Forgotten Episode of Bacteriological Warfare," *JAMA*, 196: 179-182 (4 April 1966).

Dörger, Martina and Fritz Krombach. "Response of Alveolar Macrophages to Inhaled Particulates," *European Surgical Research*, 34:47–52 (2002).

Dorland, W.A. Newman. *Dorland's Illustrated Medical Dictionary* (29th Edition). Philadelphia: W.B. Saunders Company, 2000.

Downward, Julian. "The ins and outs of signaling," *Nature*, 411: 759-762 (14 June 2001).

Driks, Adam. "The dynamic Spore," *PNAS*, 100: 3007-3009 (2003).

Duesbery, N.S. and G.F. Vande Woude. "Anthrax lethal factor causes proteolytic inactivation of mitogen-activated protein kinase kinase," *Journal of Applied Microbiology*, 87: 289-293 (1999).

Engel, Paul C. *Enzyme Kinetics: The Steady-State Approach*. London: Chapman and Hall, 1977.

Fang, Hui, Ruth Cordoba-Rodriguez, Carla S.R. Lankford, and David M. Frucht. "Anthrax Lethal Toxin Blocks MAPK Kinase-Dependent IL-2 production in CD4+ T Cells," *The Journal of Immunology*, 174: 4966-4971 (April 2005).

Fang, Hui, Lixin Xu, Trina Y. Chen, Julianne M. Cyr, and David M. Frucht. "Anthrax Lethal Toxin Has Direct and Potent Inhibitory Effects on B Cell Proliferation and Immunoglobulin Production," *The Journal of Immunology*, 176: 6155-6161 (May 2006).

Ferrell, James E., Jr. and Eric M. Machleder. "The Biochemical Basis of an All-or-None Cell Fate Switch in Xenopus Oocytes," *Science*, 280: 895-898 (8 May 1998).

Forst, Christian V. "Host-pathogen systems biology," *Drug Discovery Today*, 11: 220-227 (March 2006).

Franke, Raimo, Melanie Müller, Nicole Wundrack, Ernst-Dieter Gilles, Steffen Klamt, Thilo Kähne1, and Michael Naumann. "Host-pathogen systems biology: Logical modelling of hepatocyte growth factor and *Helicobacter pylori* induced c-Met signal transduction," *BMC Systems Biology*, 2: 4-30 (2008).

Fraunholz, Martin J. "Systems biology in malaria research," *TRENDS in Parasitology*, 21: 393-395 (September 2005).

Friedlander, Arthur M., Rakesh Bhatnagar, Stephen H. Leppla, Larry Johnson, and Yogendra Singh. "Characterization of Macrophage Sensitivity and Resistance to Anthrax Lethal Toxin," *Infection and Immunity*, 61: 245-252 (January 1993).

Guidi-Rontani, Chantal, Martine Wever-Levy, Elisabeth Labruyère, and Michèle Mock. "Germination of *Bacillus anthracis* spores within alveolar macrophages," *Molecular Microbiology*, 31: 9-17 (1999).

Guidi-Rontani, Chantal, Martine Levy, Helene Ohayon, and Michèle Mock. "Fate of germinated *Bacillus anthracis* spores in primary murine macrophages," *Molecular Microbiology*, 42: 931-938 (2001).

Guidi-Rontani, Chantal. "The alveolar macrophage: the Trojan horse of *Bacillus anthracis*," *TRENDS in Microbiology*, 10: 405-409 (September 2002).

Goldbeter, Albert and Daniel E. Koshland, Jr. "An amplified sensitivity arising from covalent modification in biological systems," *PNAS*, 78: 6840–6844 (1981).

Goldbeter, Albert and Daniel E. Koshland, Jr. "Ultrasensitivity in Biochemical Systems Controlled by Covalent Modification: Interplay Between Zero-Order And Multistep Effects," *The Journal of Biological Chemistry*, 259: 14441–14447 (1984).

Gutting, B.W., K.S. Gaske, A.S. Schilling, A.F. Slaterbeck, L. Sobota, R.S. Mackie, and T.L. Buhr. "Differential susceptibility of macrophage cell lines to *Bacillus anthracis*-Vollum 1B," *Toxicology in Vitro*, 19: 221-229 (2005).

Hanna, Philip C., Deborah Acosta, and R. John Collier. "On the role of macrophages in anthrax," *PNAS*, 90: 10198-10201 (November 1993).

Hart, Derek N.J. "Dendritic Cells: Unique Leukocyte Populations Which Control the Primary Immune Response," *Blood*, 90: 3245-3287 (1 November 1997).

Herlaar, Ellen and Zarin Brown. "p38 MAPK signalling cascades in inflammatory disease," *Molecular Medicine Today*, 5: 439-447 (October 1999).

Heyman, David L. *Control of Communicable Diseases Manual* (18th edition). Washington: American Public Health Association, 2004.

Holt, Patrick G., Jane Oliver, Natalie Bilyk, Christine McMenamin, Paul G. McMenamin, Georg Kraal, and Theo Thepen. "Downregulation of the Antigen Presenting Cell Function(s) of Pulmonary Dendritic Cells In Vivo by Resident Alveolar Macrophages," *The Journal of Experimental Medicine*, 177: 397-407 (1993).

Huang, Chi-Ying and James E. Ferrell, Jr. "Ultrasensitivity in the mitogen-activated protein kinase cascade," *PNAS*, 93: 10078-10083 (September 1996).

Inglesby, Thomas V., Donald A Henderson, John G. Bartlett, Michael S. Ascher, Edward Eittzen, Arthur M. Fiedlander, Jerome Hauer, Joseph McDade, Michael T. Osterholm, Tara O'Tole, Gerald Parker, Trish M. Perl, Philip K. Russell, Kevin Tonat. "Anthrax as a Biological Weapon: Medical and Public Health Management," *JAMA*, 281: 1735-1745 (12 May 1999).

Jakubzick, Claudia, Frank Tacke, Jaime Llodra, Nico van Rooijen, and Gwendalyn J. Randolph. "Modulation of Dendritic Cell Trafficking to and from the Airways," *The Journal of Immunology*, 176: 3578 (2006)

Janes, Kevin A., John G. Albeck, Suzanne Gaudet, Peter K. Sorger, Douglas A. Lauffenburger, and Michael B. Yaffe. "A Systems Model of Signaling Identifies a Molecular Basis Set for Cytokine-Induced Apoptosis," *Science*, 310: 1646-1653 (9 December 2005).

Janeway, Charles A., Paul Travers, Mark Walport, and Mark Shlomchik. *Immunobiology* (5th edition). New York: Garland Publishing, 2001.

Jarvis, Bruce W., Tajie H. Harris, Nilofer Qureshi, and Gary A. Splitter. "Rough Lipopolysaccharide from *Brucella abortus* and *Escherichia coli* Differentially Activates the Same Mitogen-Activated Protein Kinase Signaling Pathways for Tumor Necrosis Factor Alpha in RAW 264.7 Macrophage-Like Cells," *Infection and Immunity*, 70: 7165-7168 (December 2002).

Junghae, Muthoni and John G. Raynes. "Activation of p38 Mitogen-Activated Protein Kinase Attenuates *Leishmania donovani* Infection in Macrophages," *Infection and Immunity*, 70: 5026-5035 (September 2002).

Kefaloyianni, Erene, Eleni Gourgou, Vanessa Ferle, Efstathios Kotsakis, Catherine Gaitanaki, and Isisdoros Beis. "Acute thermal stress and various heavy metals induce tissue-specific pro- or anti-apoptotic events *via* the p38-MAPK signal transduction pathway in *Mytilus galloprovincialis* (Lam.)," *The Journal of Experimental Biology*, 208: 4427-4436 (2005).

Kholodenko, Boris N. "Negative feedback and ultrasensitivity can bring about oscillations in the mitogen-activated protein kinase cascades," *European Journal of Biochemistry*, 267: 1583-1588 (2000).

Klaassen, Curis D. and John B Watkins III. *Casarett & Doull's Essentials of Toxicology*. New York: McGraw Hill, 2003.

Kobayashi, Scott D., Kevin R. Braughton, Adeline R. Whitney, Jovanka M. Voyich, Tom G Schwan, James M. Musser, and Frank R DeLeo. "Bacterial pathogens modulate an apoptosis differentiation program in human neutrophils," *PNAS*, 100: 10948-10953 (16 September 2003).

Koo, Han-Mo, Matt VanBrocklin, Mary Jane McWilliams, Stephan H. Leppla, Nicholas S. Duesbery, and George F. Vande Woude. "Apoptosis and melangenesis in human melanoma cells induced by anthrax lethal factor inactivation of mitogen-activated protein kinase kinase," *PNAS*, 99: 3052-3057 (5 March 2002).

Kraatz, James, Laurel Clair, Jorge L. Rodriguez, and Michael A. West. "Macrophage TNF Secretion in Endotoxin Tolerance: Role of SAPK, p38, and MAPK," *Journal of Surgical Research*, 83: 158-164 (1999).

Krishna Rao, K. Murali. "MAP kinase activation in macrophages," *Journal of Leukocyte Biology*, 69: 3-10 (January 2001).

Leppla, Stephen H. "Anthrax toxin edema factor: A bacterial adenylate cyclase that increases cyclic AMP concentrations in eukaryotic cells," *PNAS*, 79:3162-3166 (May 1982).

Levchenko, Andre, Jehoshua Bruck, and Paul W. Sternberg. "Scaffold proteins may biphasically affect the levels of mitogen-activated protein kinase signaling and reduce its threshold properties," *PNAS*, 97: 5818–5823 (23 May 2000).

Liu, Hongbin, Nicholas H. Bergman, Brendan Thomason, Shamira Shallom, Alyson Hazen, Joseph Crossno, David A. Rasko, Jacques Ravel, Timothy D. Read, Scott N. Peterson, John Yates III, and Philip C. Hanna. "Formation and Composition of the *Bacillus anthracis* Endospore," *Journal of Bacteriology*, 186: 164–178 (January 2004).

Lodish, Harvey, Arnold Berk, Lawrence S. Zipursky, Paul Matsudaira, David Baltimore, and James Darnell. *Molecular Cell Biology* (4th edition). New York: W. H. Freeman, 2000.

Mancuso, Giuseppe, Angelina Midiri, Concetta Beninati, Giovanna Piraino, Andrea Valenti, Giacomo Nicocia, Diana Teti, James Cook, and Giuseppe Teti. "Mitogen-Activated Protein Kinases and NF-κB Are Involved in TNF-α Responses to Group B Streptococci," *The Journal of Immunology*, 169: 1401-1409 (August 2002).

Musser, James M. and Frank R. DeLeo. "Toward a Genome-Wide Systems Biology Analysis of Host-Pathogen Interactions in Group A *Streptococcus*," *American Journal of Pathology*, 167: 1461-1472 (December 2005).

Nagele, P. "Misuse of standard error of the mean (SEM) when reporting variability of a sample. A critical evaluation of four anaesthesia journals," *British Journal of Anaesthesia*, 90: 514-516 (2001).

Nicholson, Wayne L., Nobuo Munakata, Gera Horneck, Henry J. Melosh, and Peter Setlow. "Resistance of *Bacillus* Endospores to Extreme Terrestrial and Extraterrestrial Environments," *Microbiology and Molecular Biology Reviews*, 64: 548-572 (September 2000).

Nick, Jerry A., Scott K. Young, Kevin K. Brown, Natalie J. Avdi, Patrick G. Arndt, Benjamin T. Suratt, Michael S. Janes, Peter M. Henson, and G. Scott Worthen. "Role of p38 Mitogen-Activated Protein Kinase in a Murine Model of Pulmonary Inflammation," *The Journal of Immunology*, 164: 2151-2159 (February 2000).

Office of Technology Assessment (OTA), U.S. Congress. *Proliferation of Weapons of Mass Destruction: Assessing the Risk*. OTA-ISC-559. Washington: GPO, August 1993.

Paccani, Silvia Rossi, Fiorella Tonello, Raffaella Ghittoni, Mariarita Natale, Lucia Muraro,Mario Milco D'Elios, Wei-Jen Tang, Cesare Montecucco, and Cosima T. Baldari. "Anthrax toxins suppress T lymphocyte activation by disrupting antigen receptor signaling," *The Journal of Experimental Medicine*, 201: 325-331 (2005).

Park, Jin Mo, Florian R. Greten, Zhi-Wei Li, and Michael Karin. "Macrophage Apoptosis by Anthrax Lethal Factor Through p38 MAP Kinase Inhibition," *Science*, 297: 2048-2051 (2002).

Pearson, Gray, Fred Robinson, Tara Beers Gibson, Bing-E Xu, Mahesh Karandikar, Kevin Berman, and Melanie H. Cobb. "Mitogen-Activated Protein (MAP) Kinase Pathways: Regulation and Physiological Functions," *Endocrine Reviews*, 22: 153-183 (2001).

Pellizzari, Rossella, Chantal Guidi-Rontani, Gaetano Vitale, Michèle Mock, and Cesare Montecucco. "Anthrax lethal factor cleaves MKK3 in macrophages and inhibits the LPS/IFNgamma-induced release of NO and TNF-alpha," *FEBS Letters*, 462:199-204 (26 Nov 1999).

Pezard, Corinne, Patrick Berche and Michèle Mock. "Contribution of Individual Toxin Components to Virulence of *Bacillus anthracis*," *Infection and Immunity*, 59: 3472-3477 (October 1991).

Robinson, P.J, J.M. Gearhart, G.A. Andrews, T. Nichols, I. Baumel, and B.W. Gutting. "Biologically-based Modeling of the Toxigenic Phase of Anthrax Infection: Modulation of Map Kinase Signaling Pathway," *Proceedings of 5th Annual ASM Biodefense and Emerging Diseases Research Meeting*, Washington D.C., 27 February – 2 March 2007.

Rotz, Lisa D., Ali S. Khan, Scott R. Lillibridge, Stephen M. Ostroff, and James M. Hughes. "Public Health Assessment of Potential Biological Terrorism Agents," *Emerging Infectious Diseases*, 8: 225-230 (February 2002).

Roux, Philippe P. and John Blenis. "ERK and p38 MAPK-Activated Protein Kinases: a Family of Protein Kinases with Diverse Biological Functions," *Microbiology and Molecular Biology Reviews*, 68(2): 320–344 (June 2004).

Sauro, Herbert M. and Boris N. Kholodenko. "Quantitative analysis of signaling networks," *Progress in Biophysics & Molecular Biology*, 86: 5–43 (2004).

Sharma, Shiv K. and Thomas J. Carew. "The Roles of MAPK Cascades in Synaptic Plasticity and Memory in *Aplysia*: Facilitatory Effects and Inhibitory Constraints," *Learning & Memory*, 11: 373-378 (2004).

Shea, Dana A. *Terrorism: Background on Chemical, Biological, and Toxin Weapons and Options for Lessening Their Impact.* Congressional Research Service (CRS) Report RL31669. (http://www.au.af.mil/au/awc/awcgate/crs/rl31669.pdf) Washington: GPO (1 December 2004).

Singh, Yogendra, Kurt R. Klimpel, Seema Goel, Prabodha K. Swain, and Stephen H. Leppla. "Oligomerization of Anthrax Toxin Protective Antigen and Binding of Lethal Factor during Endocytic Uptake into Mammalian Cells," *Infection and Immunity*, 67: 1853-1859 (April 1999).

Smith, Kelly D. and Hamid Bolouri. "Dissecting innate immune responses with the tools of systems biology," *Current Opinion in Immunology*, 17:49-54 (2005).

Tegnèr, Jesper, Roland Nilsson, Vladimir B. Bajic, Johan Björkegren, and Timothy Ravasi. "Systems biology of innate immunity," *Cellular Immunology*, 244: 105-109 (2006).

Tournier, Jean-Nicolas, Anne Quesnel-Hellmann, Jacques Mathieu, Cesare Montecucco, Wei-Jen Tang, Michèle Mock, Dominique R. Vidal, and Pierrre L. Goossens. "Anthrax Edema Toxin Cooperates with Lethal Toxin to Impair Cytokine Secretion during Infection of Dendritic Cells," *The Journal of Immunology*, 174: 4934-4941 (April 2005).

U.S. Army Medical Research Institute of Infectious Disease. *USAMRIID's Medical Management of Biological Casualties Handbook* (6th edition). Ft Detrick: USAMRIID, April 2005.

van Aken, Jan and Edward Hammond. "Genetic engineering and biological weapons," *EMBO Reports*, 4:S57-S60 (2003).

Vitale, Gaetano, Rossella Pellizzari, Chiara Recchi, Giorgio Napolitani, Michèle Mock and Cesare Montecucco. "Anthrax Lethal Factor Cleaves the N-Terminus of MAPKKs and Induces Tyrosine/Threonine Phosphorylation of MAPKs in Cultured Macrophages," *Biochemical and Biophysical Research Communications*, 248: 706-711 (30 July 1998).

Vitale, Gaetano, Bernardi L, Giorgio Napolitani, Michèle Mock, and Cesare Montecucco. "Susceptibility of mitogen-activated protein kinase kinase family members to proteolysis by anthrax lethal factor," The Biochemical Journal, 352: 739-45 (15 December 2000).

Wheelis, Mark. "Biological Warfare at the 1346 Siege of Caffa," *Emerging Infectious Diseases*, 8: 971-975 (September 2002).

You, Lingchong. "Toward Computational System Biology," *Cell Biochemistry and Biophysics*, 40: 167-184 (2004).

Zhang, Yue, Adrian T. Ting, Kenneth B. Marcu, and James B. Bliska. "Inhibition of MAPK and NF-κB Pathways Is Necessary for Rapid Apoptosis in Macrophages Infected with *Yersinia*," *The Journal of Immunology*, 174: 7939-7949 (June 2005).

Zhu, Jianzhong, Gowdahilla Krishnegowda, and D. Channe Gowda. "Induction of Proinflammatory Responses in Macrophages by the Glycosylphosphatidylinositols of *Plasmodium falciparum*: The Requirement of Extracellular Signal-Regulated Kinase, p38, c-Jun N-Terminal Kinase and NF-κB Pathways for the Expression of Proinflammatory Cytokines and Nitric Oxide," *The Journal of Biological Chemistry*, 280: 8617-8627 (4 March 2005).

Zhu, Wei, Jocelyn S. Downey, Jun Gu, Franco Di Padova, Hermann Gram, and Jiahuai Han. "Regulation of TNF Expression by Multiple Mitogen-Activated Protein Kinase Pathways," *The Journal of Immunology*, 164: 6349-6358 (June 2000).

Vita

Captain Daniel J. Schneider graduated from Beavercreek High School in Beavercreek, Ohio. He entered undergraduate studies at The Ohio State University in Columbus, Ohio where he graduated with a Bachelor of Science degree in Chemical Engineering in June 2000. Upon graduation, he received a direct commission into the Biomedical Science Corps of the United States Air Force, and in August 2000 he was assigned to the 22d Aeromedical Dental Squadron, McConnell Air Force Base (AFB), Kansas as a Bioenvironmental Engineer. In July 2003, he was assigned to the 48th Aerospace Medicine Squadron, Royal Air Force (RAF) Lakenheath, England. Capt Schneider was the chief of environmental protection and the Chemical, Biological, Radiological, and Nuclear Medical Defense Officer for two main operating bases and ten geographically separated units (GSUs) in England, Norway and Iceland. He also directed occupational health programs for the GSUs. In August 2006, he entered the Graduate Industrial Hygiene program of the Graduate School of Engineering and Management, Air Force Institute of Technology, Wright-Patterson AFB, Ohio. Upon graduation, he will be anticipates being assigned to the Air Force Institute for Operational Health, Brooks City-Base, Texas.

REPORT DOCUMENTATION PAGE

Form Approved
OMB No. 074-0188

1. REPORT DATE *(DD-MM-YYYY)*	**2. REPORT TYPE**	**3. DATES COVERED** *(From – To)*
27-03-2008	Master's Thesis	Sep 2006 – Mar 2008

4. TITLE AND SUBTITLE

Three Models of Anthrax Toxin Effects on the MAP-Kinase Pathway and Macrophage Survival

5a. CONTRACT NUMBER

5b. GRANT NUMBER

5c. PROGRAM ELEMENT NUMBER

6. AUTHOR(S)

Schneider, Daniel J., Captain

5d. PROJECT NUMBER
None

5e. TASK NUMBER

5f. WORK UNIT NUMBER

7. PERFORMING ORGANIZATION NAMES(S) AND ADDRESS(S)
Air Force Institute of Technology
Graduate School of Engineering and Management (AFIT/EN)
2950 Hobson Way
WPAFB OH 45433-7765

8. PERFORMING ORGANIZATION REPORT NUMBER

AFIT/GIH/ENV/08-M02

9. SPONSORING/MONITORING AGENCY NAME(S) AND ADDRESS(ES)
Dr. Peter Robinson
AFRL/RHPB (AFMC)
2729 R St., Bldg. 837
WPAFB, OH 45433-5707
Phone: 937-904-9502
E-mail: peter.robinson@wpafb.af.mil

10. SPONSOR/MONITOR'S ACRONYM(S)

11. SPONSOR/MONITOR'S REPORT NUMBER(S)

12. DISTRIBUTION/AVAILABILITY STATEMENT
APPROVED FOR PUBLIC RELEASE; DISTRIBUTION UNLIMITED.

13. SUPPLEMENTARY NOTES

14. ABSTRACT
Lethal factor (LF), a component of anthrax toxin, is the primary virulence factor that allows Bacillus anthracis to evade the immune response by blocking the activation of mitogen-activated protein kinase (MAPK) enzymes. This research modifies three published MAPK models to reflect this signal inhibition and to estimate a first-order reaction rate by fitting the models to published viability data for two macrophage cell lines cultured with the LF-producing Bacillus anthracis-Vollum1B strain. One model appears to be ill-suited for this purpose because not all relevant MAPK components could be integrated into the inhibition equations. Despite different underlying parameters and values, the remaining two models display consistent behavior, due to the highly conserved signal pathway structure, and provide approximately equal rate constants and measures of the relative sensitivity between cell lines. The results demonstrate model robustness and an ability to guide experimental design toward quantifying the LF reaction rate and estimating the sensitivity of human alveolar macrophages. The models serve as a first step toward an inhalation dose-response model and, by providing a measure of differential susceptibility, can lend increased confidence in extrapolation between cell types in vitro or between species in vivo.

15. SUBJECT TERMS
Anthrax; bacterial diseases; toxins and antitoxins; biological agents; biological warfare; mass destruction weapons; molecular biology; mathematical models

16. SECURITY CLASSIFICATION OF:			**17. LIMITATION OF ABSTRACT**	**18. NUMBER OF PAGES**	**19a. NAME OF RESPONSIBLE PERSON**
REPORT	**ABSTRACT**	**c. THIS PAGE**			Jeremy M. Slagley, Major
U	**U**	**U**	**UU**	122	**19b. TELEPHONE NUMBER** *(Include area code)* (937) 255-3636 x4511 ; jslagley@afit.edu

Standard Form 298 (Rev: 8-98)
Prescribed by ANSI Std. Z39-18